AD-A114 420 EG AND G WASHINGTON ANALYTICAL SERVICES CENTER INC R--ETC F/G 15/5
A METHODOLOGY FOR THE EVALUATION OF ALTERNATIVE OFFSHORE CONTAI--ETC(U)
APR 82 J D BIRD N00014-78-C-0787
UNCLASSIFIED WASC-TR-D200-0002 NL

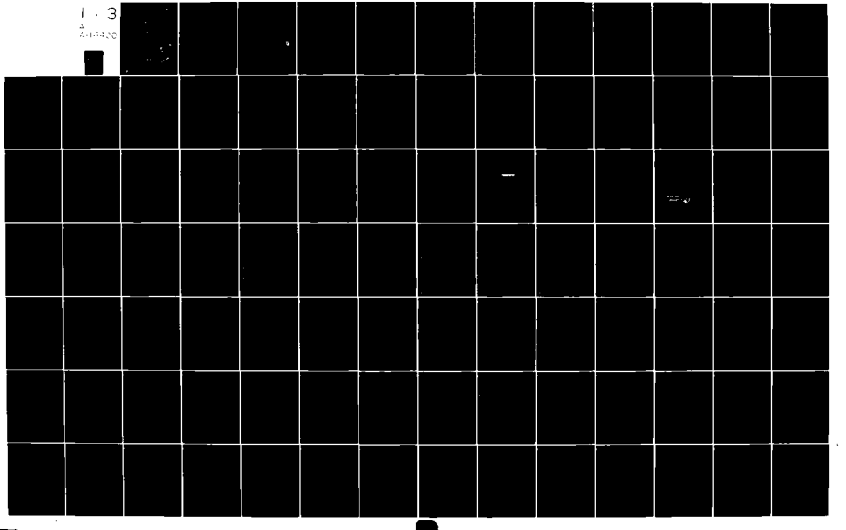

WASC TR D200-0002
APRIL 1982

A METHODOLOGY FOR THE EVALUATION OF ALTERNATIVE OFFSHORE CONTAINER DISCHARGE SYSTEMS

FINAL REPORT

Prepared For

OFFICE OF NAVAL RESEARCH
800 NORTH QUINCY STREET
ARLINGTON, VIRGINIA 22217

UNDER CONTRACT
N00014-78-C-0787

Prepared By
J. DEXTER BIRD, III

EG&G WASHINGTON ANALYTICAL SERVICES CENTER, INC.
2150 FIELDS ROAD
ROCKVILLE, MARYLAND 20850

82 05 12 063

UNCLASSIFIED

SECURITY CLASSIFICATION OF THIS PAGE (When Data Entered)

REPORT DOCUMENTATION PAGE	READ INSTRUCTIONS BEFORE COMPLETING FORM
1. REPORT NUMBER: WASC TR D200-0002	2. GOVT ACCESSION NO.: AD-A114 420
3. RECIPIENT'S CATALOG NUMBER	
4. TITLE (and Subtitle): A Methodology for the Evaluation of Alternative Offshore Container Discharge Systems	5. TYPE OF REPORT & PERIOD COVERED: Final 1979-81
6. PERFORMING ORG. REPORT NUMBER	
7. AUTHOR(s): J. Dexter Bird, III	8. CONTRACT OR GRANT NUMBER(s): N 00014-78-C-0787
9. PERFORMING ORGANIZATION NAME AND ADDRESS: EG&G WASHINGTON ANALYTICAL SERVICES CENTER, INC. 2150 Fields Road, Rockville, MD 20850	10. PROGRAM ELEMENT, PROJECT, TASK AREA & WORK UNIT NUMBERS
11. CONTROLLING OFFICE NAME AND ADDRESS: Office of Naval Research, Code 232 800 North Quincy Street, Arlington, VA 22217	12. REPORT DATE: April, 1982
	13. NUMBER OF PAGES: 209
14. MONITORING AGENCY NAME & ADDRESS (if different from Controlling Office): Mr. C. C. Stevens, FAC 032B Naval Facilities Engineering Command 200 Stovall Street, Rm. 12S45 Arlington, VA 22332	15. SECURITY CLASS. (of this report): UNCLASSIFIED
	15a. DECLASSIFICATION/DOWNGRADING SCHEDULE: n/a

16. DISTRIBUTION STATEMENT (of this Report)

Distribution of this Document is Unlimited

17. DISTRIBUTION STATEMENT (of the abstract entered in Block 20, if different from Report)

-

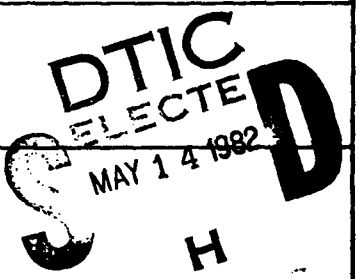

18. SUPPLEMENTARY NOTES

-

19. KEY WORDS (Continue on reverse side if necessary and identify by block number)

Container Offloading and Transfer System (COTS)
Temporary Container Discharge Facility (TCDF)
Tethered Float Breakwater
Motion Compensation (MOCOMP)
Rider Block Tagline System (RBTS)

20. ABSTRACT (Continue on reverse side if necessary and identify by block number)

An analytical model and methodology are developed for the evaluation of alternative offshore container discharge systems. The study utilizes a computer program for a sensitivity analysis and tradeoff evaluations of various technical options, including breakwater systems and motion mitigating crane systems. Preferred mixes of options are presented. The computer model is compared with actual test results. Validity of the computer program cannot be confirmed, but good utility potential is indicated.

DD FORM 1 JAN 73 1473 EDITION OF 1 NOV 65 IS OBSOLETE

UNCLASSIFIED

SECURITY CLASSIFICATION OF THIS PAGE (When Data Entered)

WASC TR D200-0002
APRIL 1982

A METHODOLOGY FOR THE EVALUATION OF ALTERNATIVE OFFSHORE CONTAINER DISCHARGE SYSTEMS

FINAL REPORT

Prepared For

OFFICE OF NAVAL RESEARCH
800 NORTH QUINCY STREET
ARLINGTON, VIRGINIA 22217

UNDER CONTRACT
N00014-78-C-0787

Prepared By
J. DEXTER BIRD, III

EG&G WASHINGTON ANALYTICAL SERVICES CENTER, INC.
2150 FIELDS ROAD
ROCKVILLE, MARYLAND 20850

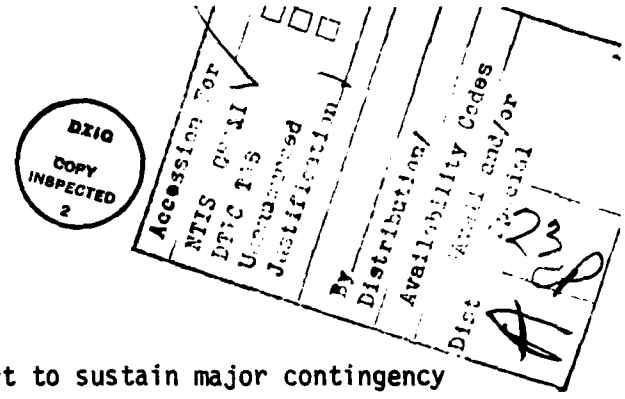

PREFACE

DOD planning for the logistics support to sustain major contingency operations, including amphibious assault operations for Logistics-Over-the-Shore (LOTS) evolutions, relies extensively on the utilization of U.S. Flag commercial shipping. Since the mid 1960's commercial shipping has been steadily shifting towards containerships, Roll-on/Roll-off (RO-RO) ships and barge ships (e.g., LASH, SEABEE). By 1985 as much as 85% of U.S. Flag sealift capacity may be in container capable ships -- mainly non-selfsustaining (NSS) containerships. Such ships cannot operate without extensive port facilities. Amphibious assault and/or LOTS operations are usually conducted over undeveloped beaches and expeditious response times preclude conventional port development. Handling of containers in this environment presents a serious problem. The problem, as defined above, is addressed in the overall DOD Over-the-Shore Discharge of Cargo (OSDOC) efforts involving developments by the Army, Navy and Marine Corps. Guiding policy is documented in the "DOD Project Master Plan for Surface Container Supported Distribuiton System" and the OASD I&L system definition paper "Over-the-Shore Discharge of Cargo (OSDOC) System."

In response to the DOD Master Plan, Navy Operational Requirement (OR-YSL03) has been prepared for an integrated Container Offloading and Transfer System (COTS) for discharging container capable ships in the absence of port facilities. The COTS Navy Development Concept Paper (NDCP) No. YSL03 was promulgated July 1975 and the Navy Material Command tasked with development. The Naval Facilities Engineering Command has been assigned as Principal Development Activity (PDA) with the Naval Sea Systems Command assisting.

The COTS advanced development program includes the ship unloading subsystem, the ship-to-shore subsystem and common system elements. The ship unloading subsystem includes: (a) the development of Temporary Container Discharge Facilities (TCDF) employing merchant ships and/or barges with add-on cranes and support equipment to offload non-selfsustaining (NSS) containerships alongside; (b) the development of Crane on Deck (COD) techniques and equipment for direct placement of cranes on the decks of NSS containerships to render them selfsustaining in an expedient manner; (c) the development of equipment and techniques to offload RO-RO ships offshore and (d) the development of interface equipment and techniques to enable ship discharge by helicopters (either existing or projected in other development programs). The ship-to-shore subsystem includes the development of elevated causeways to allow cargo handling over the surfline and development of self-propelled causeways to transport cargo from ships to the shoreside interface. The commonality subsystem includes: (a) the development of wave attenuating Tethered Float Breakwaters (TFB) to provide protection to COTS operating elements; (b) the development of special cranes and/or crane systems to compensate for container motion experienced during afloat handling; (c) the development of transportability interface items to enable essential outsize COTS equipment transport on merchant ships -- particularly bargeships, and (d) the development of system integration components such as moorings, fendering, communications and services.

This report addresses the progress and accomplishments associated with the development of a methodology for the modeling and analysis of the complex interactions among the elements of the ship unloading subsystem. Finally, a limited sample of actual test data is used to validate the "COTS" computer program developed for this study.

ACKNOWLEDGMENT

This research was funded by the office of Naval Research under contract N00014-78-C-0787.

EG&G wishes to express its appreciation to Mr. Milon E. Essoglou and Mr. Clifton C. Stevens of the Naval Facilities Engineering Command for their support and interest throughout this effort. EG&G also wishes to express its gratitude to Dr. Richard Seymour of the Scripps Institution of Oceanography for his assistance in formulating models of the tethered float breakwater and to Mr. Duane Davis of the Civil Engineering Laboratory for providing input data for and assistance in running the RELMO computer program.

The author wishes to express special appreciation to Dr. Ira Jacobson and other members of the faculty of the University of Virginia, School of Engineering and Applied Science for their encouragement and suggestions. The main body of this research was submitted to the University of Virginia in partial fulfillment of the requirements for the degree of Doctor of Philosophy in Systems Engineering.

Messrs. Lawrence A. Kahn and Charles F. Rushing, employees of EG&G, assisted the author in modifying the preliminary report to include subsequent actual test data for this final report.

TABLE OF CONTENTS

TABLE OF CONTENTS (Cont'd)

LIST OF FIGURES

LIST OF FIGURES (Cont'd)

LIST OF TABLES

LIST OF SYMBOLS

A	=	constant
B	=	constant
C, C_1, C_2	=	viscious damping
CT	=	cycle time
$ETR(\omega)$	=	energy transmission ratio of a breakwater
F	=	force
g	=	acceleration of gravity, 32.2 ft/sec^2 (9.8 m/sec^2)
$G(s)$	=	series compensation transfer function
H_s	=	significant wave height
HP_s	=	significant horsepower
j	=	$\sqrt{-1}$
K	=	feedback gain
k, k_1, k_2	=	stiffness of crane structure
ℓ	=	pendulum length
M	=	mass
R	=	radius of operation of a crane
s	=	Laplace operator
$S(\omega)$	=	single sided power density spectrum
t	=	time
T_ℓ	=	average lost time over lighter
T_m	=	minimum practical offload time
T_s	=	average lost time over ship
u	=	wind speed
u_h	=	horizontal input motions

u_v = vertical input motions

V_s = significant hoisting velocity

W = weight

x = horizontal displacement in longitudinal direction of ship

y = horizontal displacement in transverse direction of ship

z = vertical displacement

α = constants

β = constants

ζ = damping ratio

η = efficiency factor

θ = pitch angle of floating vessel or pendulation angle

ϕ = roll angle of floating vessel

ψ = yaw angle of floating vessel

σ = standard deviation

τ = time constant

ω = circular frequency (rad/sec)

ω_c = breakwater cutoff frequency

ω_{n_h} = natural frequency of hydraulic system

ω_{n_c} = natural frequency of crane structure

ω_{n_p} = natural frequency of pendulation

LIST OF ACRONYMS

COD	=	Crane on Deck
COTS	=	Container Offloading and Transfer System
DOD	=	Department of Defense
ETR	=	Energy Transmission Ratio
LCM8	=	Landing Craft, Mechanized (Mark VIII)
LOTS	=	Logistics Over the Shore
MAF	=	Marine Amphibious Force
MSC	=	Military Sealift Command
NAVFAC	=	Naval Facilities Engineering Command
OSDOC	=	Over the Shore Discharge of Cargo
RAO	=	Response Amplitude Operator
RBTS	=	Rider Block Tagline System
STOL	=	Short Take-off and Landing
TCDF	=	Temporary Container Discharge Facility
TFB	=	Tethered Float Breakwater

ABSTRACT

A strong trend in the commercial shipping industry is toward containerization of cargo, a system that utilizes specialized ships and extensive port facilities. With dwindling numbers of auxiliary ships, the military is forced to place increased reliance upon these commercial shipping assets. Since military operations are often conducted over unimproved beaches, an integrated container handling system is required to support a broad spectrum of supply operations in the absence of improved port facilities.

The Navy's Container Offloading and Transfer System (COTS) is under development to meet this need. Cranes mounted on floating platforms will be used to lift the containers from the cells of ships and place them into lighterage for transport ashore. When this operation is conducted in the presence of significant wave activity, a combination of breakwaters to shelter the floating vessels and/or motion compensating capability of the cranes may be required.

A methodology is developed herein for the evaluation of these container handling systems. The wave activity is treated as a random forcing function. The dynamics and interactions of the system elements are described by appropriate differential equations and the system measures of effectiveness are described in terms of the responses of the dynamic elements and the overall system configuration. The computer model is compared with actual test results.

SECTION I

INTRODUCTION

1.1 BACKGROUND

The purpose of this study is to provide a methodology for the evaluation of alternative container offloading system configurations in support of a variety of military amphibious assault operations. This system includes the interface between the ships involved, their dynamics, the offloading dynamics, and the dynamics of other control devices used.

The success of any sustained military amphibious assault operation is highly dependent upon the effectiveness of the supporting logistics resupply activities. In the event of a military contingency involving the landing of a Marine Amphibious Force (MAF) of approximately 50,000 men on an unimproved beach, the resupply pipeline will need to be in full operation within the first two weeks (approximately two weeks of supplies go ashore with the MAF).[1] Department of Defense (DOD) level planning for the logistic support necessary to sustain contingency sealift operations relies heavily upon the utilization of U.S. Flag commercial shipping assets to augment the dwindling number of Navy and Military Sealift Command (MSC) breakbulk ships.[2] In the last decade, the dominant trend in commercial shipping has been toward high speed, non-self-sustaining container ships, and by 1985, as much as 85% of the U.S. Flag sealift capabilities may be in these container capable ships.[3]

The containership, however, requires extensive well-developed port facilities including deep draft berths and large industrial gantry cranes. The response time and general nature of amphibious assault operations preclude the construction of such port facilities in their support as they are usually conducted over undeveloped beaches.[4] An integrated and balanced cargo handling system is required for discharging container-capable ships in support of a broad spectrum of military contingency supply operations in the absence of improved port facilities. The system could also find peacetime applications for emergency relief operations following international disasters such as floods or earthquakes.

The Naval Facilities Engineering Command (NAVFAC) has been tasked as the Principal Development Activity for the Container Offloading and Transfer System (COTS).[5] This involves the development of the required technology, and identification and procurement of the hardware necessary for the offloading of containers from ships to lighters (smaller landing craft and amphibious or air cushion vehicles) in an unprotected, offshore environment. Current development efforts are directed at the application of some form of crane to extract the containers from the cells and place them into the lighterage. It is desirable, from the standpoint of economy and availability, to utilize standard, commercially available, mobile, construction cranes for this purpose. However, recent tests have indicated that these cranes, designed to operate on land, suffer degraded performance when employed in unprotected, offshore environments.[6,7]

This environment is characterized by a variety of natural factors such as wind, rain, salt spray, and wave activity. Wind and rain, also experienced by shoreside facilities, do not pose major hurdles except in extreme cases. These occur with such small likelihoods that operations can be terminated temporarily with little effect on the overall system productivity. Much work has been done in the protection of machinery from the harsh marine environment. Significant wave activity, however, occurs with such regularity in offshore environments that it cannot be dismissed lightly. The random wave activity at sea results in irregular motions of the ships, crane platforms, and lighterage.

These wave induced motions of the floating crane platform are transmitted through the crane to the container. Large relative displacements between the container and the adjacent vessels make cargo transfer both difficult and dangerous. Lateral motions near the natural frequency of the suspended load are amplified. The resulting pendulation may introduce high side loads, and thus bending, on the crane boom, a structural member designed primarily for compression. These effects become significantly more pronounced as the sea conditions worsen.

A variety of diverse alternative technologies have been proposed to ameliorate the adverse effects of sea induced motions. These include the use of larger capacity cranes to withstand the extra loads, structural modifications or add-on features to existing cranes to improve their capabilities, and deployment of larger quantities of ships and cranes to offset the loss of productivity resulting from

their degraded performance. More sophisticated approaches include the development of automatic, motion compensating cranes and readily deployable floating breakwaters.

The motion compensating crane, as the name implies, is equipped with a means of sensing the sea induced motions and automatically raising and lowering the load to minimize their adverse effects. Oil exploration, particularly in the rough North Sea, has brought about recent commercial interest in the development of this technology. A variety of techniques have been proposed including below the hook devices,[8] hydraulic cylinder cable tensioners,[9] and servo-controlled winches with control strategies ranging from simple acceleration feedback[10] to complex adaptive controllers approximating trajectories derived from application of the optimal, quadratic, linear regulator results.[11]

Breakwaters, on the other hand, attack the problem at the source. Breakwaters attenuate the wave energy before it reaches the cargo handling elements. Fixed breakwaters have been used for many years for harbor protection and beach erosion control.[12] Floating breakwaters have been built for use in deep water applications such as protecting offshore oil terminals.[13,14] Whether operating on the principle of energy reflection or dissipation, they tend to be large, massive structures. Current development efforts are directed at improving the effectiveness of floating breakwaters that are easily transportable and deployable.[3]

In addition to the above technologies, a variety of basic system configurations have been proposed[2,3] including the Crane on Deck (COD)

and the Temporary Container Discharge Facility (TCDF). The COD approach suggests that mobile cranes can be placed on the deck of the container ships to give them self-offloading capability. The TCDF approach envisions a dedicated platform, either a ship or a large barge, that can be equipped with the necessary cranes and personnel to remain in the objective area and act as an offshore floating pier.

Because of the diverse nature of the technologies that affect the system design and performance, the complex nature of the interactions between the various system elements, and the large number of possible system configurations, there has been no quantitative means of comparing and evaluating alternative system design candidates.

1.2 PROBLEM DESCRIPTION

The problems faced by designers of the Container Offloading and Transfer System (COTS) can be divided into two major areas. The first is the description of the complex interactions between the system elements and how these interactions affect the system measures of effectiveness. The second is the determination of the optimal allocation of available resources to maximize the overall system performance.

The COTS problem is not unique, but a member of a larger, more general class of problems. Many complex systems of dynamic elements are driven by random inputs where system performance is measured in terms of descriptive statistics of the system's response. In designing to required performance criteria, a tradeoff may exist between reduction of the undesirable aspects of the random input or modification of the dynamic characteristics of the system itself.

Other examples of such systems include high speed rail transportation systems and short take-off and landing (STOL) air terminal design. In the case of rail transportation, the tradeoff might be between the costs of straightening the rails to various tolerances versus implementation of anticipatory control suspension hardware on the trains themselves. Performance criteria might be mean square linear acceleration or noise level experienced by the passengers. In the case of STOL air terminals, the costs of wind screens may be traded off against more sophisticated control strategies for the aircraft[15] where expected touchdown accuracy might be the index of performance.

The COTS design problem is similarly organized. The random input from the sea can be reduced by the addition of breakwaters. On the other hand, a variety of system configurations and crane designs that ameliorate the adverse effects of this input are available. Overall cargo handling productivity and system cost are governed by the design of the system as a whole.

1.3 OBJECTIVE

The objective of this effort is to develop a methodology by which alternative Container Offloading and Transfer Systems (COTS) can be compared and evaluated with respect to their productivity and cost. This will include the development of an analytical model to predict the system cost and performance in terms of descriptive parameters of the system elements. With this model, optimization studies will be conducted on certain parameters of interest. Sensitivity analyses can

be performed on the optimal solutions with respect to system parameters and constraints to help identify profitable areas for further research and development.

1.4 SYSTEM ELEMENTS

The Container Offloading and Transfer System (COTS) is composed of eight basic elements - sea state, breakwater, crane platform, container ship, lighterage, crane, cargo, and personnel. These are described briefly in Table 1.1 along with typical parameters commonly used in their quantification. These elements are also arranged in an interaction matrix (Figure 1.1), providing a visual representation of the kinds of relationships that must be identified in order to effectively model the system.

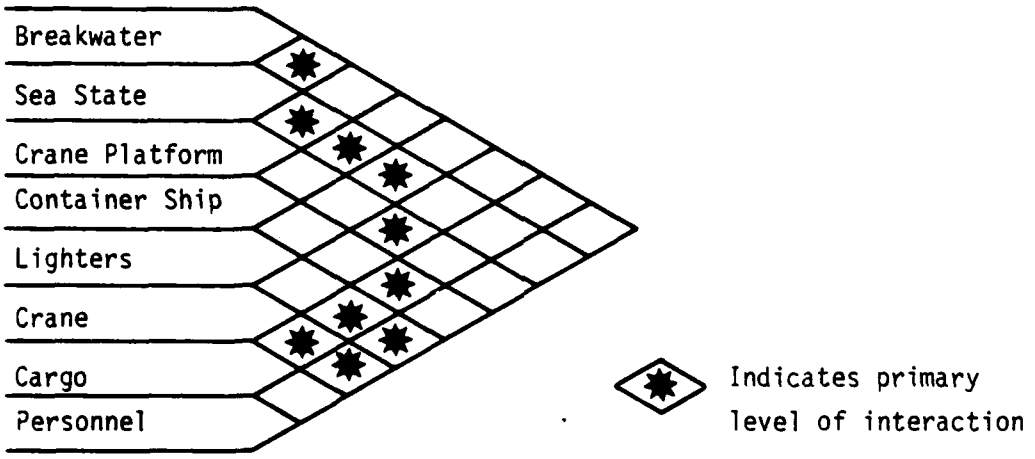

Figure 1.1. COTS Interaction Matrix

TABLE 1.1 DESCRIPTION OF SYSTEM ELEMENTS

SYSTEM ELEMENTS	BRIEF DESCRIPTION	TYPICAL PARAMETERS
Sea State	Measure of wave activity	Significant wave height power density spectrum
Breakwater	Wave attenuating device	Transmission coefficients, length
Crane Platform	Floating vessel on which the crane is placed	Length, breadth, draft, weight, hull design
Container Ship	Large oceangoing vessels for transporting containerized cargo	Length, breadth, draft, weight, hull design
Lighterage	Small floating vessels used for transporting personnel and logistics from ships to shore	Length, breadth, draft, weight, hull design
Crane	Mechanical structure for lifting and moving heavy loads	Lift capacity, reach, horsepower, stiffness, design
Cargo	Supplies to be handled by the system	Weight, dimensions, impact resistance
Personnel	Collection of individuals necessary to operate the system	Training, motivation

With the system bounded to include these basic elements, it is worthwhile to consider the environment in which the system will operate and the influence it may exert on the system elements. Such factors as weather conditions other than wave activity, personnel training and motivation, availability of lighterage, and the like must be considered. These may vary greatly from one scenario to another, but for the purpose of this study, nominal conditions, based on past Department of Defense (DOD) experience, will be assumed.[7]

1.5 MEASURES OF EFFECTIVENESS

There are a number of system measures of effectiveness that reflect DOD goals and objectives. They include cost, productivity, transportability, reliability, response time, personnel requirements, and safety. Of these, cost and productivity are the more easily quantifiable. Further, the others can be represented in terms of these two. For example, a Temporary Container Discharge Facility (TCDF), consisting of a crane mounted on a barge, can be towed at a maximum speed of five knots.[3] It could, however, be loaded onto a SEABEE ship (a commercial vessel designed to carry large barges) and transported at 20 knots to the objective area.[3,16] Because there is a limited number of these ships, space on them would be worth a premium during a military contingency, but a dollar value can be placed on its use. This would provide a basis to assign a cost to this option for evaluation purposes. Based upon this line of reasoning, cost and productivity are chosen as useful parameters for the purpose of alternative evaluations.

1.6 SYSTEM SYNTHESIS

In addition to the descriptive parameters of the system elements, system configuration information is needed to describe the dynamic interactions of the system elements. System configuration includes information relating to system operation, arrangement of the elements, the mooring plan, and the like.

In order to insure the broad capability of a model to evaluate a variety of COTS alternatives, other miscellaneous inputs may be required such as fixed cost information or baseline productivity data that are particular to the configurations under investigation.

The basic structure of the model is shown in Figure 1.2. The model is divided into two major areas - system dynamics and system evaluation. The system dynamics model addresses the system interactions that can be described by the appropriate application of physical laws of nature. This includes the calculation of transmitted wave activity, ship and platform motions, crane structural requirements, and control system response. The system evaluation model, however, is less well defined. It includes the estimation of component costs and system productivity based upon outputs from the system dynamics model. The relationships necessary for system evaluation will be developed empirically, extrapolated from existing data, and structured in a manner that appears most reasonable to experts familiar with the Container Offloading and Transfer System (COTS).

A system synthesis flow chart (Figure 1.3) shows the interactions between the various system elements and the contributions to the system measures of effectiveness. It provides a visual representation of the

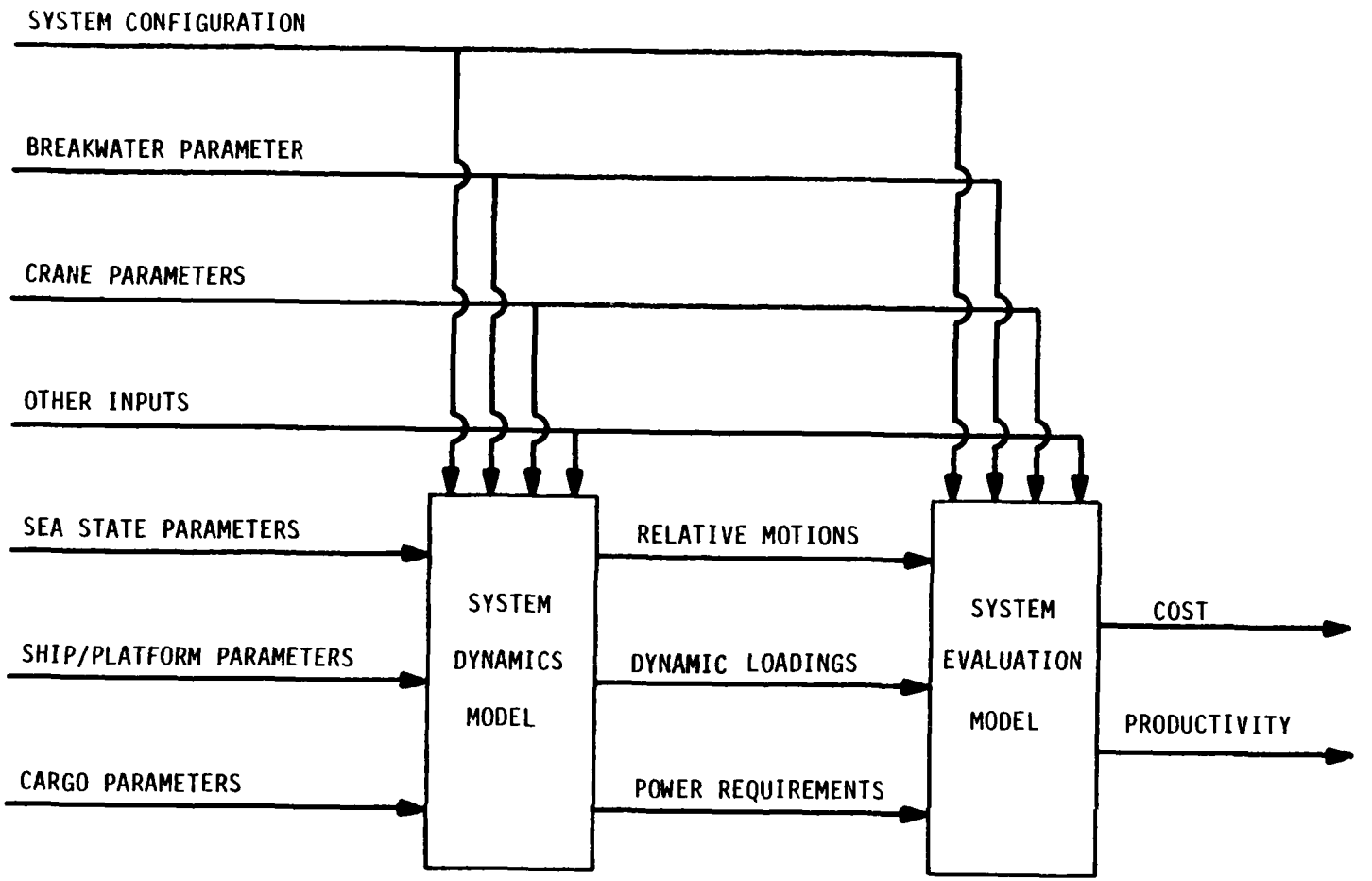

Figure 1.2. Basic Structure of the COTS Model

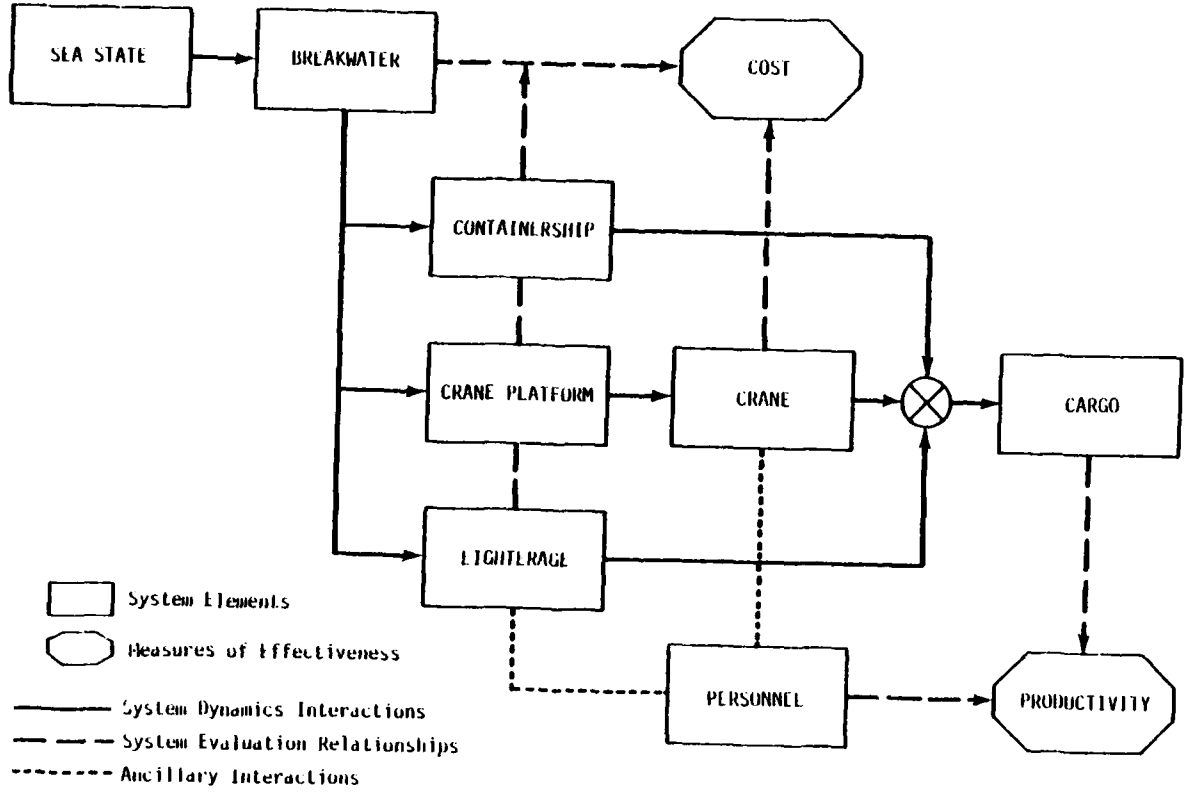

Figure 1.3. System Synthesis Flow Chart

relationship between the system dynamics model and the system evaluation model. The ancillary interactions between personnel, lighterage, and cranes are also shown, although they will be implicitly included in the empirical relationships for productivity.

SECTION II

METHODOLOGY

2.1 APPROACH

In developing the models necessary to effectively describe the system interactions, a number of simplifying assumptions are made. This is done in accordance with conventional engineering practice in order to enhance the mathematical tractability of the problem and to make use of a wide body of powerful analytical techniques. The advantages, consequences, and limitations of these assumptions are addressed.

The system dynamics are described by differential equations that are assumed to be linear or linearizable about an operating point. The coefficients of these equations are constant. Although few, if any, physically realizable systems can be exactly described by linear differential equations with constant coefficients, many can be approximated in this manner over limited operating ranges.

An important characteristic of linear systems is frequency preservation. A sinusoidal input of a given frequency results in a sinusoidal output at the same frequency, in which only amplitude and phase are modified.[17,18] For this reason, a useful characterization of linear systems is by their frequency response operators or transfer functions. These transfer functions can be obtained by Laplace transformation of the governing differential equations or by experimental methods on the hardware itself.

The governing differential equations that describe the motion of the sea surface can also be simplified. The fluid is assumed to be inviscid, the Bernoulli equation is linearized, the boundary conditions of the free surface are satisfied at its mean value and not along the wave profile, and the pressure at the surface is assumed to be constant.[19] This results in a sinusoidal motion of the sea surface. The variation in the level of the sea surface at any point results from the summation of contributions from many relatively unrelated disturbances. This collection of sinusoids of varying amplitudes and phase angles is assumed to be an ergodic, Gaussian random process. Statistical analysis of actual wave records indicates that, after elimination of the linear trends, the Gaussian assumption is quite reasonable.[20]

This linearized, Gaussian model of a seaway is limited by the fact that it is not valid for high or extreme sea conditions. The linearization introduces errors into the profile of the higher waves. In a strictly Gaussian process, extremely high waves, although improbable, would be possible, but waves are limited in height by breaking.

For the purpose of the COTS modeling, these do not represent objectionable limitations. The operational requirements of moderate sea conditions are well within the capabilities of the linearized models. Under extreme sea or storm conditions where this model is less reliable, the container handling operations would not be conducted.

The advantage of the linearized Gaussian model is that a wide body of powerful mathematical tools are available for the analysis of systems with these forcing functions. A zero mean random process of this type can be completely described by its power density spectrum. This is a measure of the energy density of the random process as a function of frequency. This is obtained by taking the Fourier transform of the auto correlation function or may be determined by experimentally measuring, filtering, and squaring a time history of the process. A narrowband random process is one with a peaked power density spectrum, indicating that the majority of its energy is concentrated in a narrow frequency range.

It has been shown that a linear system, subjected to a Gaussian random input, has a Gaussian output.[17,21] Lord Rayleigh demonstrated that the peaks of a narrow band, Gaussian process are distributed according to a Rayleigh probability density function.[17,22] The power density spectrum of the output, $S_o(\omega)$, of a linear system can be calculated from the power density spectrum of the input, $S_i(\omega)$, and the system's complex transfer function, $H(j\omega)$, by the relationship:

$$S_o(\omega) = H(j\omega)\, H^*(j\omega)\, S_i(\omega),$$ [17,21]

where the asterisk indicates the complex conjugate.

The standard deviation, and therefore a complete description of the Gaussian distribution of a zero mean random process, can be calculated from its power density spectrum.

$$\sigma^2 = \int_0^\infty S(\omega)\, d\omega, \quad (17,21)$$

where σ is the standard deviation and $S(\omega)$ is the single-sided power density spectrum.

The system dynamics model is based on the above analytical techniques. The various system elements or groups of elements are described by their power density spectra. The standard deviations of some of the outputs will be used by the system evaluation model in order to calculate expected values of those outputs that affect the cost and productivity of the system.

2.2 SYSTEM PARAMETERS

In light of the above assumptions, it is useful to examine the system elements and the types of parameters that are descriptive of their role in the system.

2.2.1 Sea State Parameters

The sea state has been discussed above. It will be considered as a narrowband, Gaussian, random process. Sea state will be described by its power density spectrum. The sea is a continuously changing source of activity driven by wind velocity, duration, fetch, bottom contour, and the like. Because of the complex nature of the wave generation process, the power density spectrum changes with time. Oceanographers have examined the growth of wave spectra as the seas develop under a variety of conditions. For a given set of wind conditions, a steady state wave spectrum is reached, beyond which no further increase in

energy is observed. This is called a fully developed sea. Mariners, on the other hand, have a relatively simple, although operationally effective method of describing the wave activity associated with sea states. This is significant wave height, defined as the average of the one third largest waves as measured from their peak to trough. For the purposes of the COTS modeling, an analytical form of the power density spectrum of a fully developed sea that can be defined in terms of significant wave heights will be used.

2.2.2 Breakwater Parameters

There are two basic types of breakwater - fixed and floating. Most fixed breakwaters provide a rigid, full depth barrier to the progress of the waves. Floating breakwaters provide a movable, partial barrier and operate by a combination of energy reflection and dissipation. Figure 2.1 shows several breakwater configurations.

With the great variety in the designs of breakwaters, parameters descriptive of the physical characteristics would be difficult to handle effectively in the model. Since the primary interaction of the breakwater is with the sea state, parameters associated with the transmitted wave height would be most useful. A casual examination of typical floating breakwater wave transmission coefficients suggests that breakwaters have frequency characteristics similar to those of low pass filters. The longer wave length, lower frequency waves are transmitted with very little attenuation. The shorter, higher frequency waves, however, are significantly reduced. This motivates a description of breakwater transmission coefficients as a function of cut off frequency and

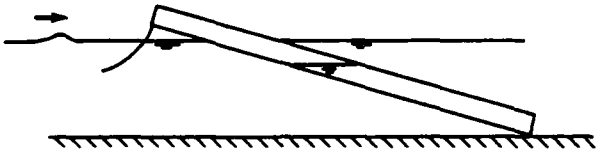

FLOODED-PONTOON BARRIER

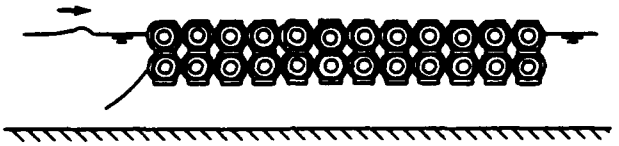

BOLTED ASSEMBLY OF TIRE CASINGS

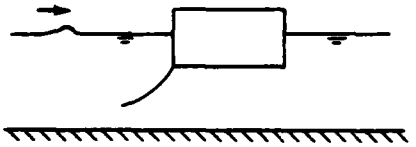

RECTANGULAR-PRISM PONTOON

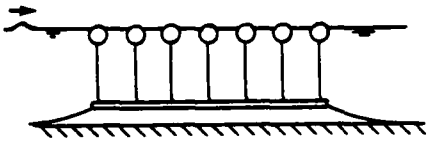

TETHERED FLOAT BREAKWATER

FLOATING BREAKWATERS

MOUND OF NATURAL MATERIAL

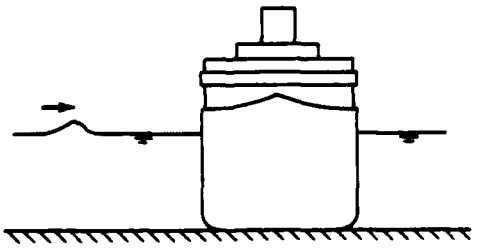

SUNKEN SHIP

FIXED BREAKWATERS

Figure 2.1. Typical Breakwater Configurations

high frequency attenuation.

The Tethered Float Breakwater (TFB) is currently under development at the Naval Ocean Systems Center and Scripps Institution of Oceanography[23] for possible COTS applications. A comparison of transmission coefficients and cost for several alternative TFB designs indicate that cost may also be approximated by a function of the parameters that define the transmission coefficient.

2.2.3 Ship, Lighterage, and Platform Parameters

The Container Offloading and Transfer System includes three different types of floating vessels - the crane platform, the containership, and the lighterage. All of these contribute to the cargo handling problem by virtue of their response to the sea state. The motions of the crane platform result in amplified motions of the suspended cargo, inducing dynamic loads in the crane structure. Relative motions between the other ships and the cargo result in degraded cargo handling productivity.

A floating vessel, assumed to be rigid, has six degrees of freedom - heave, surge, sway, roll, pitch, and yaw. The ratio of the amplitude of the response of a ship to the amplitude of the incident waves as a function of frequency is called the response amplitude operator (RAO). It has been shown that these RAO's are linear operators for wall-sided ships oscillating in light to moderate seas.[24,25,26] The RAO's for the six degrees of freedom of a ship may be calculated experimentally by recording the response of a scale model in a wave tank.[27] Analytical techniques have been developed to calculate the

RAO's through solution of linearized differential equations.[26,28] The information necessary to describe the ship includes length, breadth, draft, hull design, weight, moments of inertia, natural roll period, water depth, and direction of the incident waves.

2.2.4 Crane Parameters

2.2.4.1 Conventional Cranes

A crane is a mechanical device designed to hoist and move a load in a controlled manner. Cranes come in a variety of shapes and sizes (Figures 2.2). They can be divided into two major types - those with traveling beams such as overhead bridge and gantry cranes and those with revolving jibs such as mobile construction cranes and shipboard cargo handling cranes. Gantry cranes have been employed effectively on-board ships for the offloading of containerized cargo. These cranes, however, are specially designed for each ship and crane rails must be provided on the deck of the ship. Only a limited number of container ships are equipped with these features[29] and they may not be readily available on short notice. The response of a COTS to a military requirement precludes the use of such cranes. Mobile construction cranes of the revolving boom type have sufficient lift and reach capabilities to meet the COTS requirements and are readily available from the commercial construction industry.[30,31] It has been determined that these cranes represent viable candidates for the COTS crane application. It is desirable to analyze their capabilities in the commercially available state, with minor modifications such as power taglines or a Rider Block Tagline System (RBTS), and with major

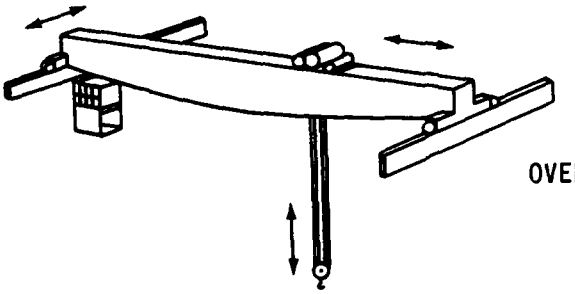

OVERHEAD BRIDGE CRANE

GANTRY CRANE

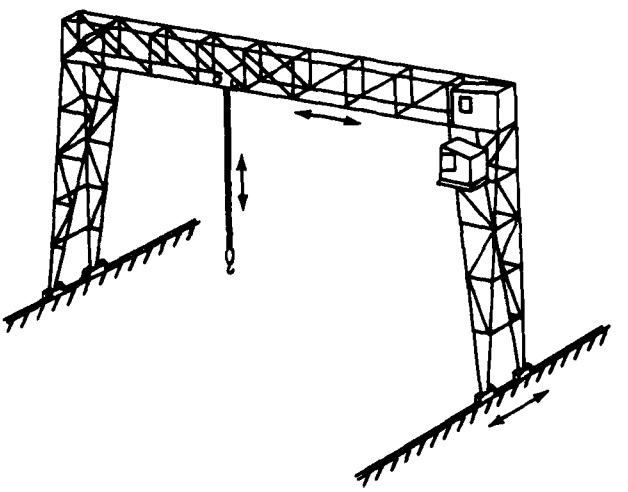

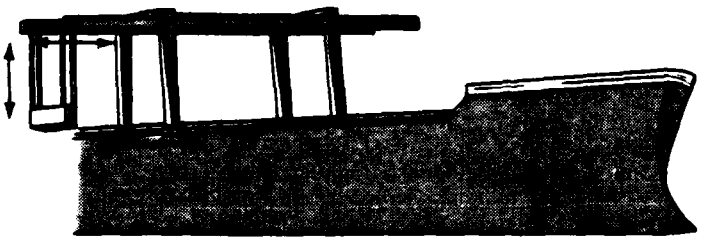

SHIPBOARD CONTAINER CRANE

Figure 2.2.a. Traveling Beam Cranes

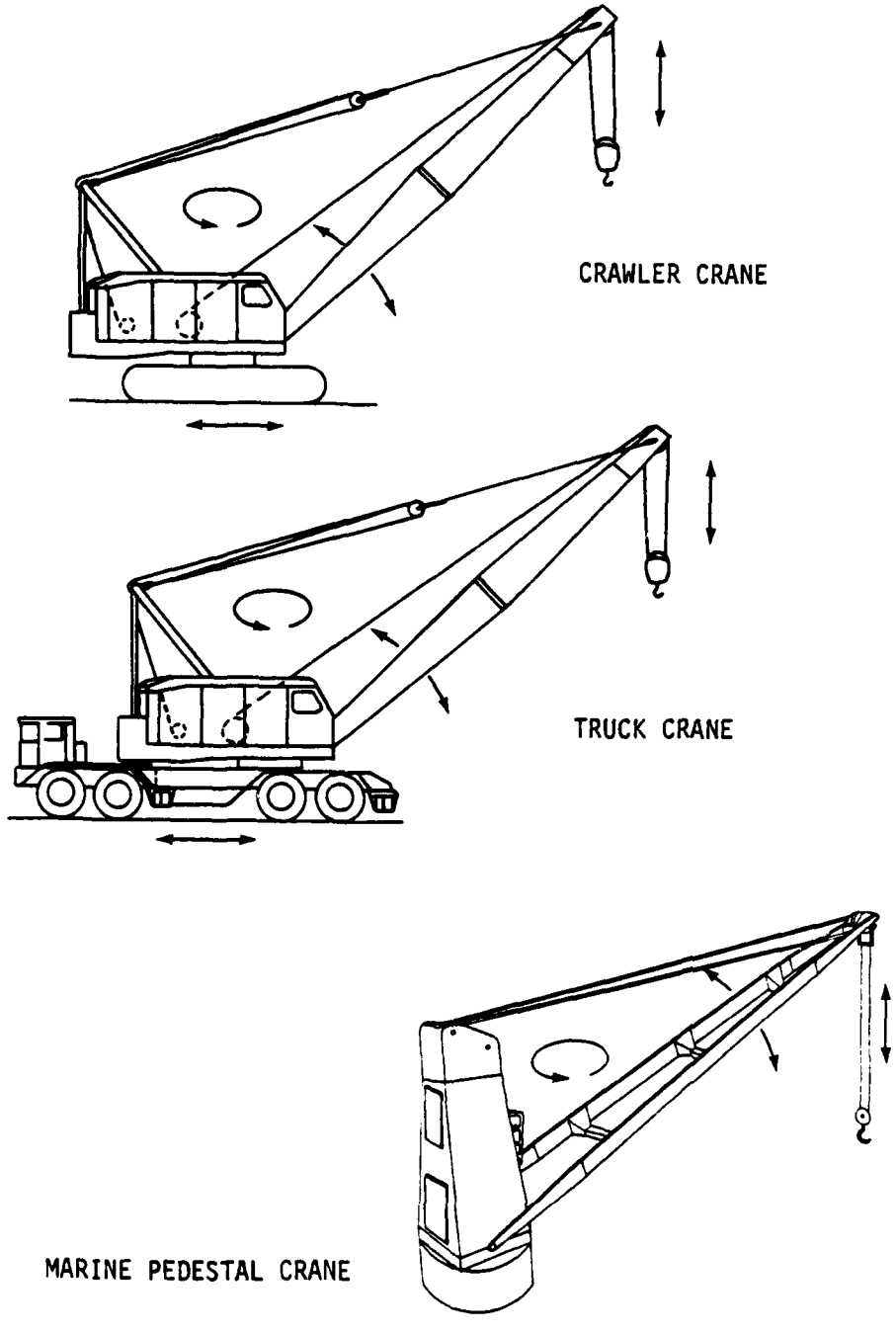

Figure 2.2.b. Revolving Jib Cranes

modifications such as automatic vertical motion compensation.

The primary parameters that describe COTS cranes are their type, lift capacity, and reach capability. Mobile construction cranes are basically of two major types - truck mounted and crawler mounted, although special modifications like the Ringer[32] and the Skyhorse[33] are available on certain cranes to greatly increase their lift - reach capability.

The position of a load being handled by a revolving jib crane is controlled by a) raising and lowering the hook, called hoisting, b) changing the vertical angle of the boom, called luffing, and c) rotating the crane structure about its vertical axis, called slewing. Lift capacity is the load that the crane can safely handle. Reach is the radius at which it can handle the load.

Typical lift - reach characteristics of a commercially available crawler crane are displayed in Figure 2.3. It can be seen that the lifting capacity is significantly reduced as the operating radius is increased, where overturning of the crane becomes the primary limiting factor.

Other characteristics of a crane that influence the system performance are the crane's operating speeds, the vertical stiffness of the crane structure, and its pendulation characteristics. The maximum crane operating speeds place a practical limit on the maximum container offloading rate. The combination of the vertical stiffness of the crane structure and the mass of the lifted load constitutes a dynamic system that may amplify the effective load on the crane at certain

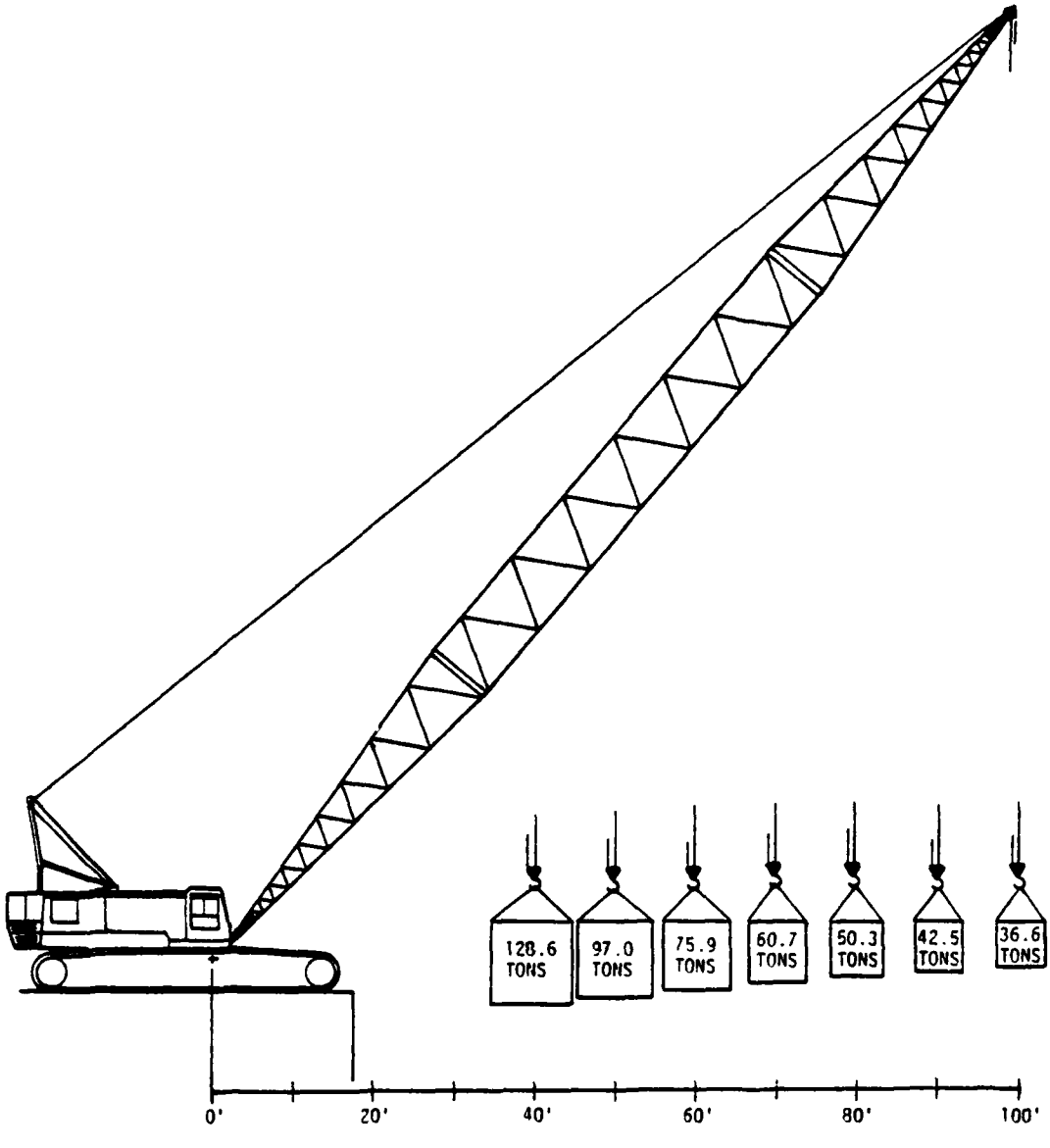

Figure 2.3. Typical Lift-Reach Characteristics of a Standard Crawler Crane

frequencies and contribute to the maximum impact loads experienced during lift off of the containers from the deck.[34,35,36] The natural period of the pendulus load suspended from the boom tip is a function of the length of the pendulum. This lightly damped system can be excited by the motions of the crane platform. The resulting pendulation if unrestrained, may introduce excessive sideloads on the crane boom, a structural member designed primarily for axial compression. Development efforts have been directed at reducing this effect. Hydraulically powered taglines reeved from winches near the boom base to the load have been employed to introduce damping,[37] and the Rider Block Tagline System (RBTS) has been developed to reduce the adverse effects of pendulation.[38]

2.2.4.2 Rider Block Tagline System

The Rider Block Tagline System, shown in Figure 2.4, consists of a rider block, outriggers, tagline, and a rider block line supplementing the conventional, commercial crane's hardware. The load lines pass over sheaves in the rider block. The horizontal and vertical positions of the rider block are controlled by the operator with the taglines and the rider block line, respectively. This allows the operator to control the pendulation length and load position simultaneously. Figure 2.5 shows the rider block in greater detail. It is fully articulated so that it can conform to the line of action of each wire.

Actuation of the taglines or the rider block line results in a nonlinear response of the load that may require a degree of operator/signalman proficiency to insure a smooth operation. Figure 2.6 depicts the

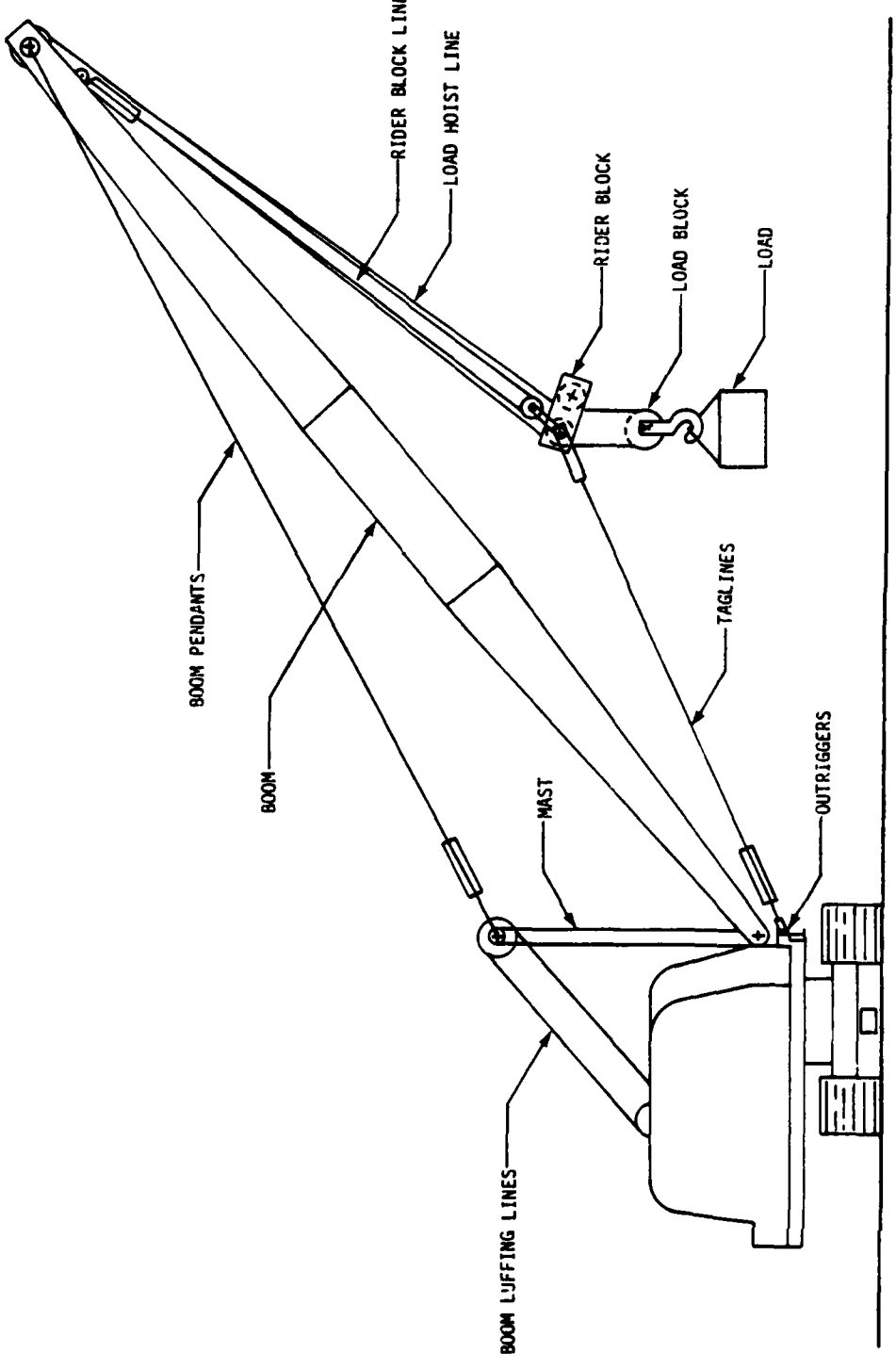

Figure 2.4. Bucyrus Erie 38B with Rider Block Tagline System

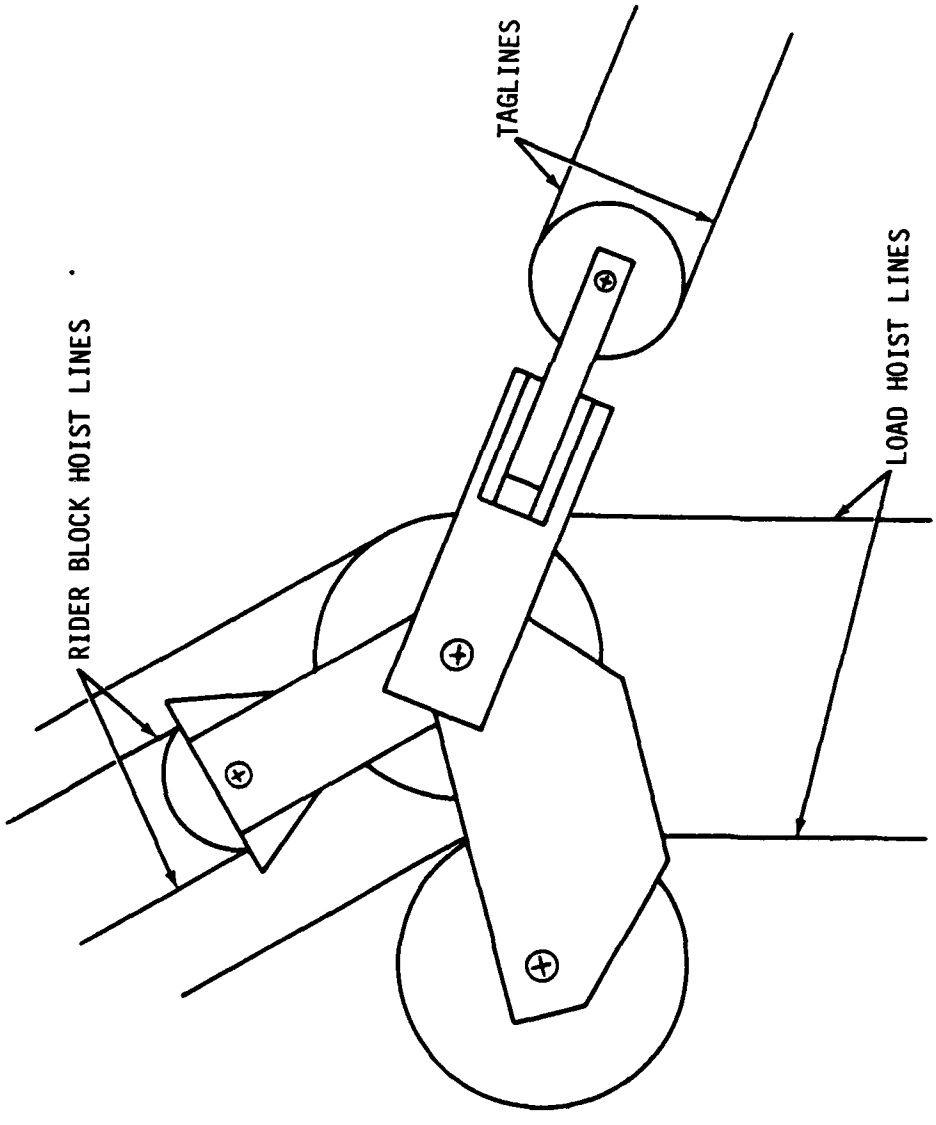

Figure 2.5. Rider Block Components

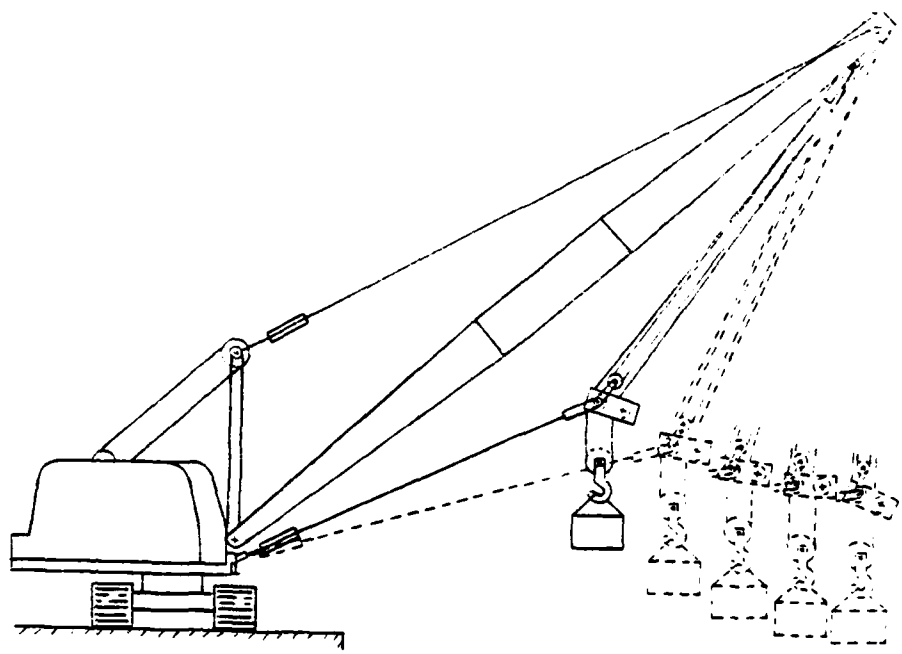

TAGLINE CONTROL

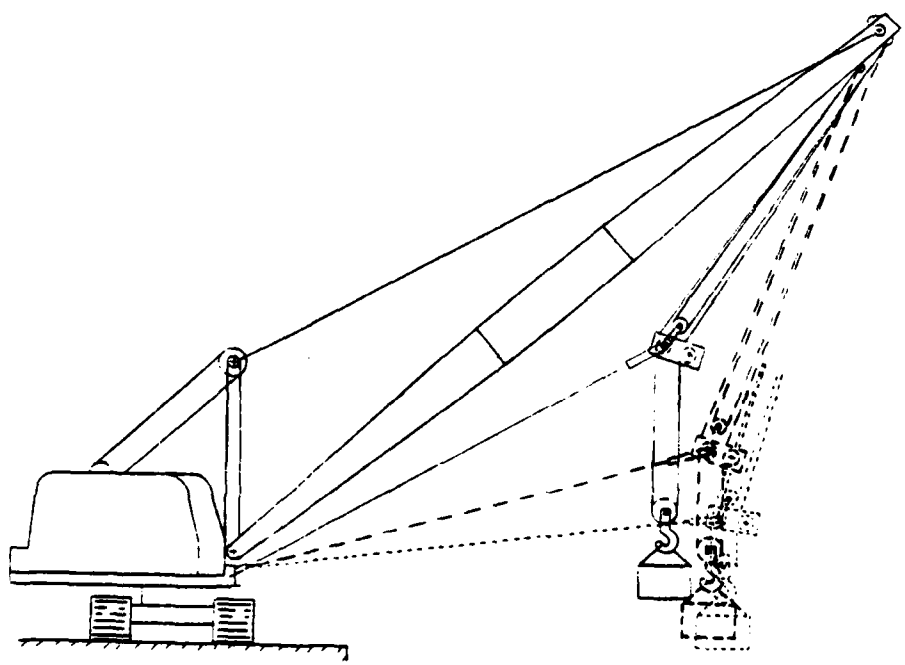

RIDER BLOCK LINE CONTROL

Figure 2.6. Load Response to Tagline and Rider Block Line Control

nature of this response for equal increments of tagline and rider block line position.

The principal advantage of the RBTS is that it redirects the forces caused by pendulation and ship roll from sideloading of the boom into differential tagline tensions. The RBTS also reduces the effective length of the pendulum, providing a more controllable load handling operation.

2.2.4.3 Motion Compensating Cranes

Motion compensating cranes represent an extension of conventional crane technology by incorporating motion sensing and automatic control circuitry with the hoisting machinery to reduce the relative motion between the cargo and the lighterage or containership. Development of an effective motion compensating crane include sensing hardware, a control strategy, and a means of implementing the control.

A number of reports have addressed the problem of sensing the relative motion between ships at sea.[39,40] Solutions include:

a) Accelerometers mounted in the load block, crane boom tip, and on the deck of the adjacent ship.

b) Laser or radar units mounted on the container spreader bar directed downward.

c) A system of triangulating, angle sensing, taut wires from the crane platform to the load and the adjacent ship.

d) A cable reel mounted on the container spreader with a line that can be hand held by a cargo handler on or

temporarily attached to the adjacent craft to provide a direct measure of relative vertical displacement.

The first control strategies examined in detail were those that synchronized the load with the deck of the ship on which it was to be placed.[41;42] They included variations of acceleration, velocity, and position feedback systems, but all involved consumption of large amounts of horsepower, resulting in massive hoist machinery designs. Like most servo systems, the bandwidth of the response is reduced as the masses of the moving parts increase. The necessary horsepower could be obtained from diesel engines, but applying it at the winch drum in a controlled manner is a more formidable problem.

Several methods have been proposed including:[41,43]

a) Variable pressure clutch and brake systems.

b) Electric motor and generator systems of the Ward Leonard type.

c) Hydraulic motors driven by variable displacement pumps.

The clutch - brake system is responsive but has severe wear problems over extended periods of time. The electric motor - generator systems have time constants that are highly dependent on the effective inertia of the system, and for the COTS loads, are not sufficiently responsive. The hydraulic systems are commercially available, are easily adaptable to diesel drives, and have adequate response characteristics that are relatively insensitive to load.

Adaptive control strategies have been examined to reduce the horse-

power requirements.[11] The objective is to land the cargo near the crest of a wave where the relative velocities will be small, and therefore, the synchronization energy minimized. This work, however, is still in the theoretical stages, and practical implementation of the strategy in the presence of structural resonances and human operator interfaces, has yet to be demonstrated.

An alternative motion compensating strategy that is within the range of current commercial capabilities will be considered here. It is the platform stabilized motion compensating crane. As the crane platform rolls and heaves, the load experiences random vertical displacements in inertial space. A control system based on velocity feedback could be employed to hoist or lower the load line in order to reduce this motion. This technique is examined in greater detail in Appendix A.2. Such a system can be represented by transfer functions and analyzed and stabilized by classical control theory techniques. The transfer function between the vertical motion of the crane boom and the load has the characteristics of a high pass filter. That is, low frequency excursions of the crane boom can be compensated, but the higher frequency motions would be transmitted to the load with very little attenuation. The low frequency attenuation and the bandwidth of the system can be directly converted into horsepower and hardware requirements for any given sea conditions. This can be reflected in the system cost, and the reduction in relative motion of the cargo can be translated into increased productivity.

2.3 MODEL SYNTHESIS

With all of the relevant dynamic characteristics of the elements described by transfer functions (Energy Transmission Ratio (ETR), Response Amplitude Operator (RAO), and the like), the input - output characteristics of the dynamic model can be determined. The dynamic model is a single input - multiple output system. The single input is the wave activity or sea state described in terms of its power density spectrum.

By the appropriate arrangement of the transfer functions of the dynamic elements, the power density spectra of the desired outputs can be calculated. These include:

a) the transmitted sea state,

b) the motions of the vessels,

c) the dynamic loadings on the crane,

d) the relative displacement between the cargo and adjacent ships, and

e) the hoist line velocities of the motion compensating machinery.

These are all spectra of Gaussian random processes, whose variance is the integral from zero to infinity of its spectrum. The square root of the variance is the standard deviation. It can be shown that the significant amplitude, defined as the average of the one-third highest excursions of the random process, is approximately equal to twice the standard deviation.[22] The average of the 1/1000th highest excursions, often used as a measure of the maximum value, equals 3.7 times the

standard deviation.[10, 42] The significant and maximum values of the system responses can be calculated by the above method and supplied to the system evaluation model.

The system evaluation model will calculate a cost and productivity for the total system using the nominal cost input data, breakwater cost estimates based on size and frequency characteristics, crane cost estimates based on crane dynamic loadings and horsepower requirements, nominal crane characteristics, and significant relative displacements between the load and the adjacent vessels.

Figure 2.7 is an expanded system synthesis flow chart showing the block diagram of the system dynamics transfer functions and the flow of information to the system evaluation models.

2.4 EVALUATION TECHNIQUES

The COTS model can be used in a variety of ways. The most direct is in the evaluation of alternative COTS configurations. In this mode, the alternative systems are completely described by the user and the model would evaluate the cost and productivity of each alternative.

Another use might be to generate productivity versus sea state curves for certain alternative designs. This information could be used to reevaluate the sea state/productivity requirements currently placed on the system or used in conjunction with sea state probability information to predict expected container offloading capabilities over extended periods of time.

Tradeoff studies between competing technologies can also be conducted with this model. The primary tradeoff in this COTS analysis is

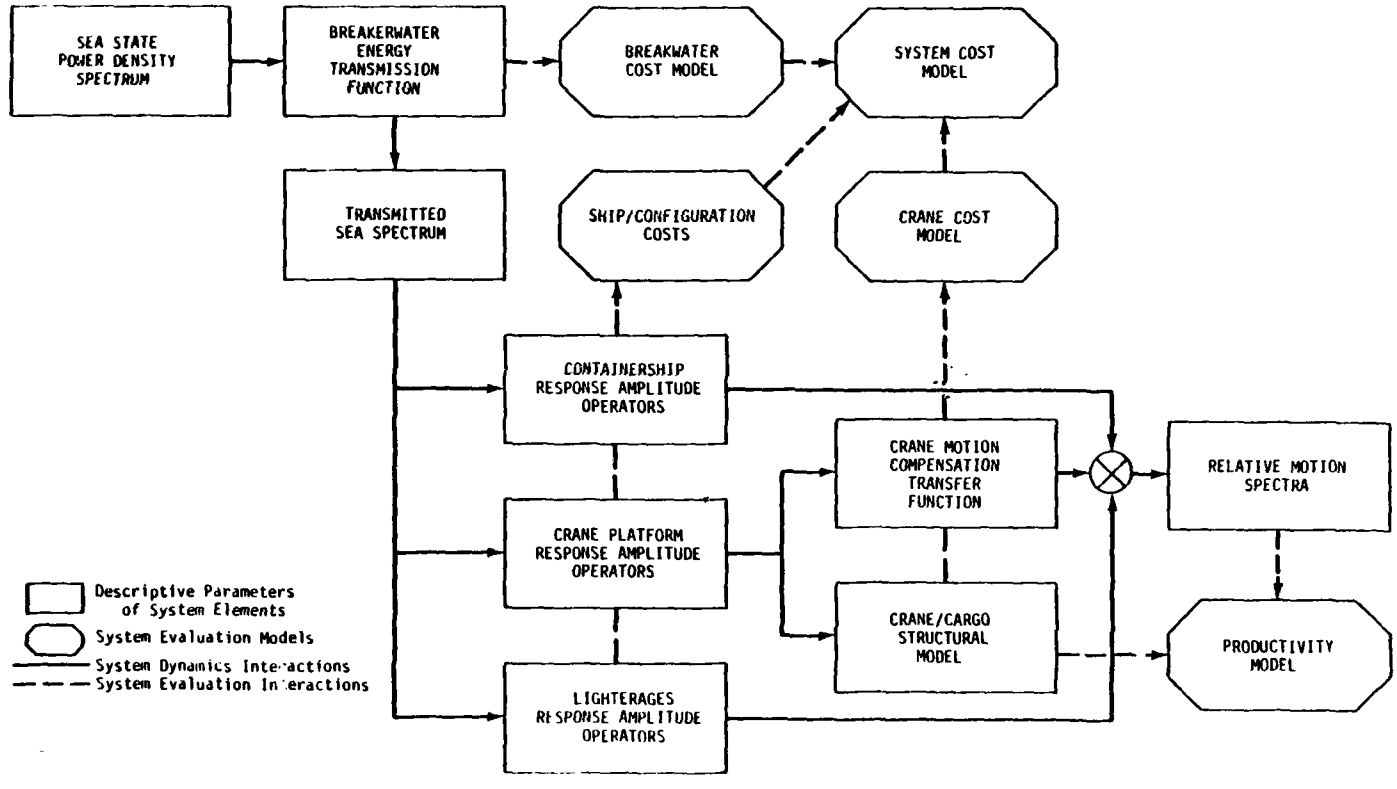

Figure 2.7. Expanded System Synthesis Flow Chart

between motion compensating cranes and breakwaters as a means of improving the productivity of the system. The breakwater affects the cargo motion as a low pass filter while the motion compensating crane appears as a high pass filter. The costs of both breakwaters and motion compensating cranes increase rapidly as their bandwidths are broadened to include the majority of the sea induced cargo and ship motions. It is, therefore, reasonable to investigate whether or not there is some optimum, intermediate design of breakwaters and motion compensating cranes that will provide a required level of productivity at minimum cost. A steepest descent algorithm with numerical partial deviations of cost and productivity with respect to descriptive parameters of the crane and breakwater design or a parameter search technique could be employed in the solution of this minimum cost tradeoff problem.

The model would also be useful in conducting a sensitivity analysis of a particular configuration's cost and productivity to all of the descriptive parameters of the system elements by evaluating partial derivatives as described above. The sensitivity of the optimal solution can also be compared to the coefficients of the empirically derived system evaluation models in order to identify any areas where additional data may be required to improve the confidence in some of the models.

In summary, this model can be a versatile tool for a variety of system analysis techniques, depending upon the needs of the user. Examples of several of these will be presented in the section on applications.

SECTION III

MODELING

3.1 GENERAL

In this section, the characteristics of the dynamic elements will be described by their appropriate differential equations or transfer functions in terms of the most descriptive and useful input and output parameters. The system evaluation models used in determining the measures of effectiveness will be described as algebraic combinations of significant statistics of the dynamic models and other system configurations and baseline input data.

Some of the cost models will be developed in conjunction with the system dynamics models in order to preserve continuity in the presentation. These will be referenced in the development of total system cost.

3.2 DYNAMIC ELEMENTS

Of the eight basic system elements identified in Section I, seven of these elements - sea state, breakwater, crane platform, container ship, lighterage, crane, and cargo - have dynamic characteristics that influence the system performance. The transfer functions of the breakwater and the floating vessel can be derived independently of the other system dynamics because there are no predominant cross coupling effects. The crane and cargo, however, will be analyzed as a single entity because the dynamic interaction between the stiffness of the crane and

the mass of the cargo contributes strongly to the frequency characteristics of the system.

3.2.1 Sea State

As discussed earlier, a reasonable and useful representation of the sea state is its power density spectrum. A number of researchers have developed analytical expressions for sea spectra to approximate actual wave records.[44] For the purpose of this study, any spectrum that approximates the type of seas that are representative of the COTS environment would be adequate. Many researchers accept the Pierson-Moscowitz spectrum for fully developed sea as correct, and recent studies by the Naval Coastal Systems Center have determined that it is representative of the majority of the potential COTS environments.[45] It is defined as[46]

$$S(\omega) = (\alpha g^2/\omega^5) \exp(-\beta\, \omega_o^4/\omega^4)$$

for values of from zero to infinity, where

$\alpha = 8.10 \times 10^{-3}$

$\beta = .74$

g = acceleration of gravity

$\omega_o = g/u$

u = wind speed

Any set of g, u, and ω can be used with consistent units. The acceleration of gravity, g, is taken to be 32.2 ft/sec^2, then the spectrum

$$S(\omega) = (8.4/\omega^5) \exp(^{-795,530}/u^4\omega^4).$$

Since the significant wave height,

$$H_s = 4.0 \sqrt{\int_0^\infty S(\omega) d\omega} \quad ,$$

the wind speed, u, can be expressed in terms of the significant wave height, H_s, and the spectrum can be written:

$$S(\omega) = (8.4/\omega^5) \exp\left(-33.6/H_s^2\omega^4\right),$$

where H_s is in feet.

The sea state power density spectrum can now be completely defined by the significant wave height, H_s. This provides an effective descriptive parameter for sea state with a strong physical connotation for the user. The Pierson-Moscowitz sea spectra for two values of significant wave height are shown in Figure 3.1.

3.2.2 Breakwater

As discussed earlier, there are a variety of designs of breakwaters. The tethered float breakwater (TFB), shown in Figure 3.2, was chosen as a viable candidate for this study because there have been a number of theoretical analyses of its performance,[23,47] wave tank model tests,[48] engineering design and deployment studies,[49] and a full scale prototype test is currently being conducted outside San Diego Bay.[50] It should be emphasized that the COTS model is not restricted to the use of the TFB models. Any breakwater design whose energy transmission ratio can be calculated, measured, or estimated can be input to the model.

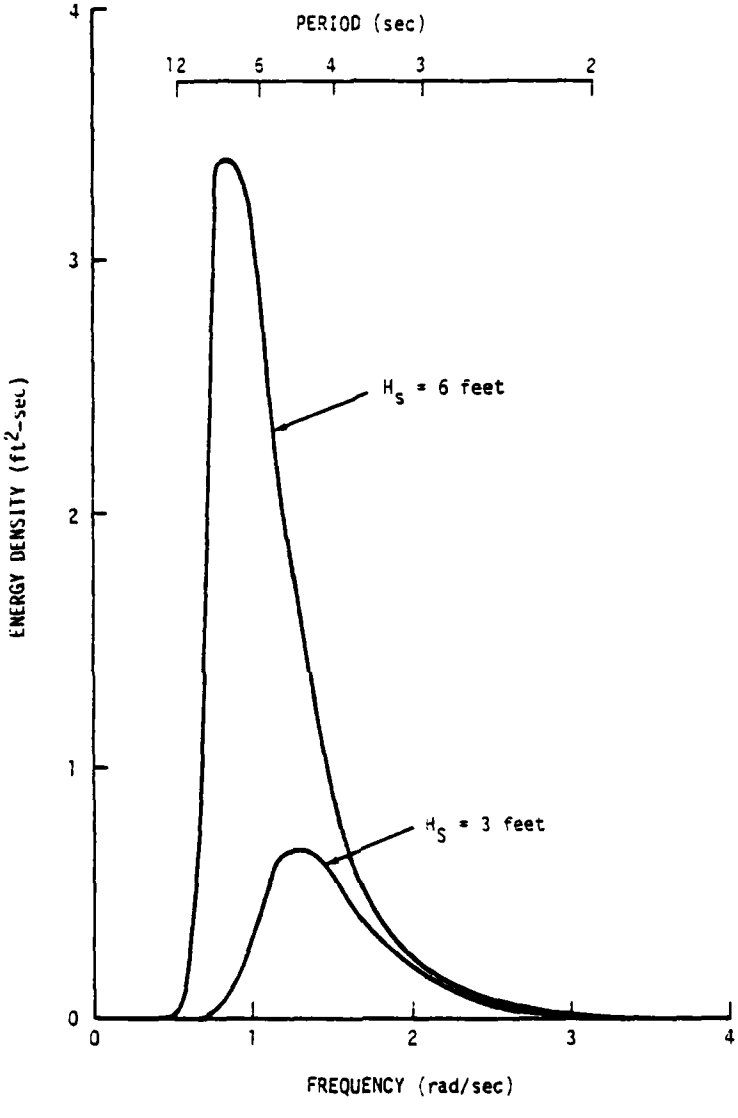

Figure 3.1. Pierson-Moscowitz Sea Spectra

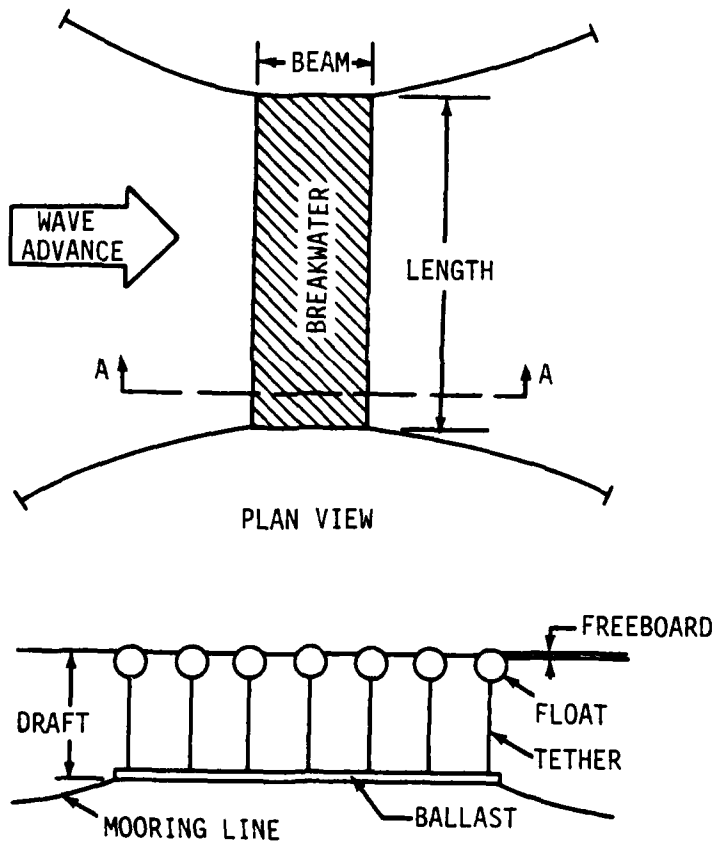

Figure 3.2. Tethered Float Breakwater

The theoretical energy tranmission ratios (ETR) as a function of frequency obtained from Scripps Institute of Oceanography, (Appendix C) characteristically appear as shown below.

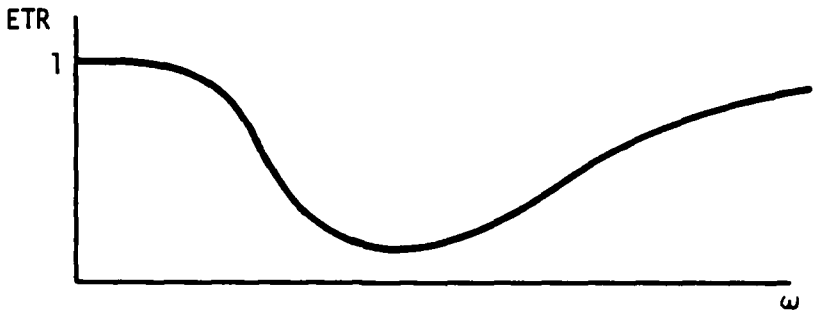

The tail of the curve would indicate that high frequency energy is transmitted as well as low; however, in practice, these frequencies are well above any significant energy found in the sea and well above the response characteristics of the floating vessels. For this reason, in practical applications, the TFB's energy transmission ratio (ETR) can be modeled as a simple low pass filter, described by a cutoff frequency, ω_c, and a high frequency attenuation, α.

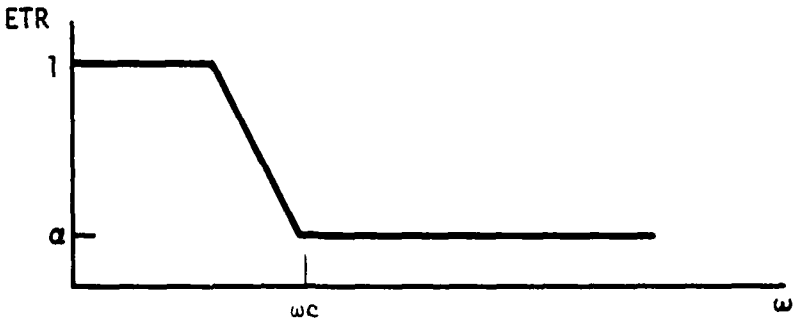

Of the designs reviewed (Appendix C), nine were chosen with high frequency attenuations in the neighborhood of .05. These were recommended by Scripps as being the most promising designs. The negative slopes of the curves beyond the cutoff frequency are also approximately equal. Cutoff frequency ranges from 1.0 to 2.0 rad/sec, with construction costs ranging from $5250 to $300 per foot respectively. A log-log plot of cost versus cutoff frequency is shown in Figure 3.3, indicating that a power function provides a reasonable representation of this relationship.

The analytical forms of ETR and breakwater cost (Appendix C) to be used in the model are:

$$ETR(\omega) = \begin{cases} 1.0 & ; \ \omega \leq \omega_1 \\ 1.0 - 2.07\ (\omega\ \omega_1) & ; \ \omega_1 < \omega \leq \omega_c \\ .05 & ; \ \omega_c < \omega \end{cases},$$

where $\omega_1 = \omega_c - .459$,

and

$$COST\ (\omega_c) = 5.4\ \left(\frac{2\ \pi}{\omega_c}\right)^{3.8} \quad \frac{dollars}{ft}$$

3.2.3 Floating Elements

A vessel oscillating in a fluid medium under the influence of random waves is a relatively complex phenomenon that is difficult to accurately describe and predict by analytical means. The vessel is subjected to a variety of forces. There are forces due to the inertial effects of the water that moves in harmony with the oscillating vessel.

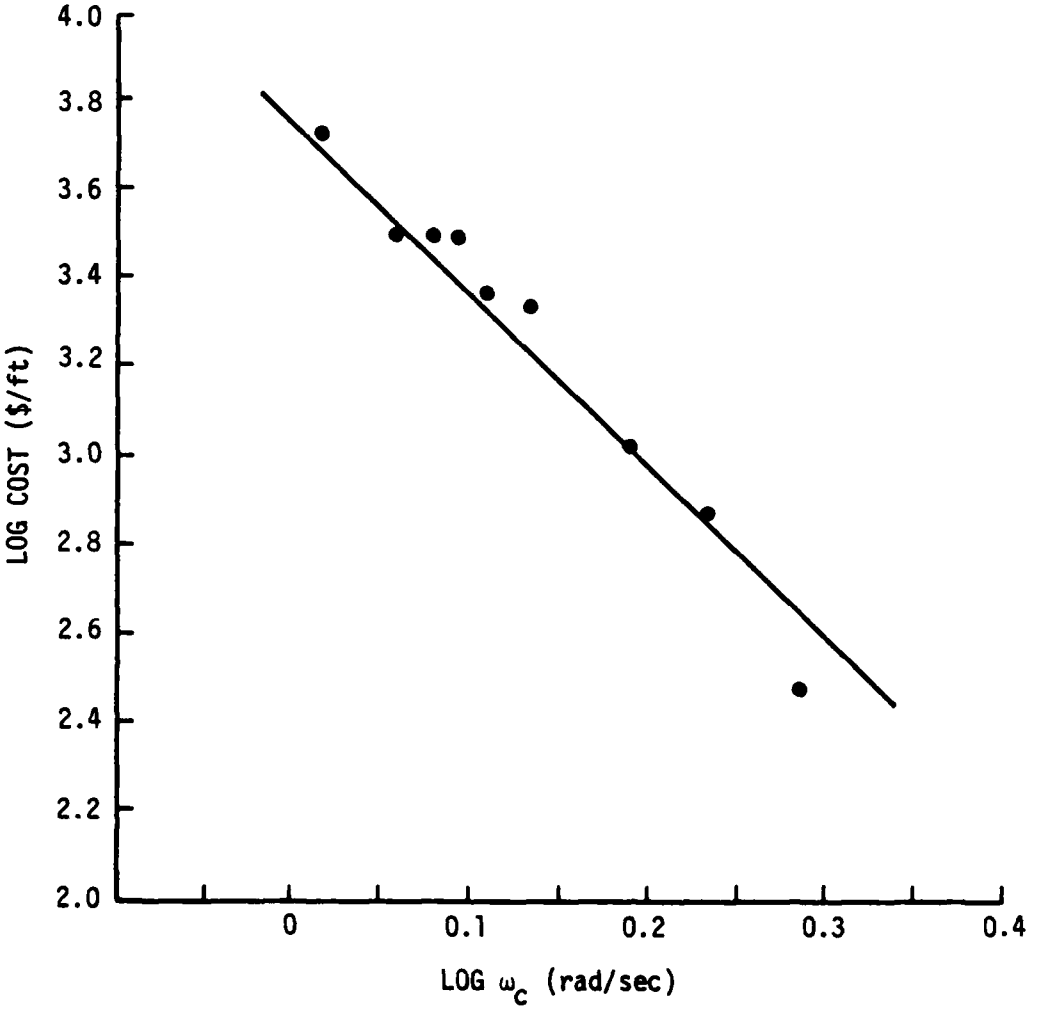

Figure 3.3. Log-Log Plot of TFB Cost Versus Cutoff Frequency

This effect is referred to as the added mass. There are damping forces that remove energy from the vessel through secondary wave generation and viscous effects. There are hydrostatic restoring forces of the water pressure acting on the hull of the ship, and there are forces resulting from the action of the incident waves. Consider the equation of motion for vertical heave:

$$M\ddot{z} = F_a + F_d + F_h + F_w$$

where z = vertical displacement

M = mass of the ship

F_a = added mass inertial forces

F_d = damping forces

F_h = hydrostatic restoring forces

F_w = wave forces.

In general, these forces are not expressible as linear functions of z and its derivatives. Observations, however, indicate that wall-sided vessels in moderate sea conditions exhibit linear response characteristics.[24,25,26] The dynamic character of a vessel is often expressed in terms of its response amplitude operators (RAO) for its six degrees of freedom - heave, surge, sway, putch, roll, and yaw. An RAO is defined as the ratio of the amplitude of the response (either translational or angular) to the amplitude of the incident waves as a function of

frequency. A ships's RAO's can be determined experimentally by placing a scale model in a wave tank and recording the ship's responses to known input wave conditions.

Analytical methods have been developed to determine ship RAO's. The most completely developed and frequently used technique is known as strip theory.[25,26] The complex, three-dimensional, fluid flow problem of a six-degree-of-freedom, oscillating ship is approximated by a summation of several simpler two-dimensional problems. The ship (Figure 3.4) is divided into a number of transverse slices, each represented by a two-dimensional cylinder. The hydrostatic and dynamic forces are calculated for each slice independently and then integrated along the length of the vessel to obtain the total effects of the forces and moments. This technique has been implemented in the RELMO computer program developed at the Navy's Civil Engineering Laboratory.[28]

The RELMO program was originally developed to predict the relative motions between points on two ships. In order to do this, it solves for the six RAO's simultaneously. The RAO's are complex functions of frequency, and therefore, contain phase as well as amplitude information. The program will be used to obtain these complex RAO's for the floating elements in the analysis. The input data format for this program is given in Appendix D.

3.2.4 Crane/Cargo

By virtue of their strong interaction, the crane and cargo models cannot be developed independently. The crane is subjected to a variety

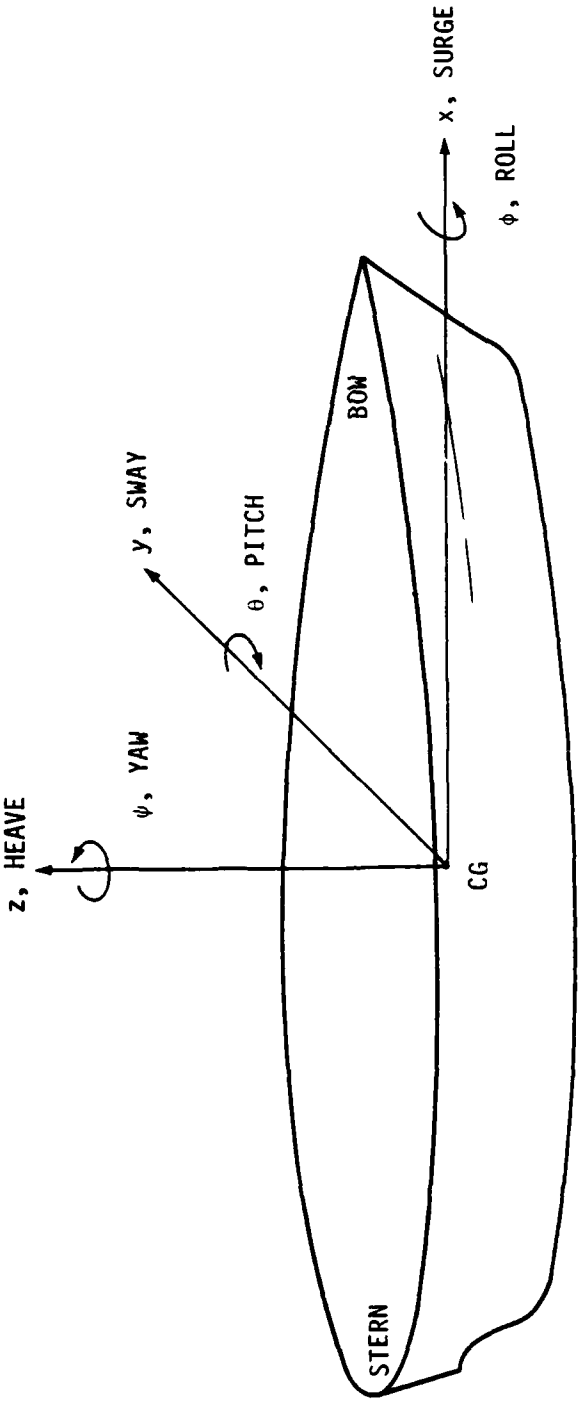

Figure 3.4. Ship Coordinate System

of forces during the offloading process. These include the static weight of the container, acceleration forces - some of which are amplified by the structural resonance of the crane/cargo system, and pendulation loads which appear primarily as side loads on the crane boom. The required radius of operation of the crane will depend on the dimensions of the ships involved and the system configuration. A simplified dynamic model of the crane/cargo system is shown below.

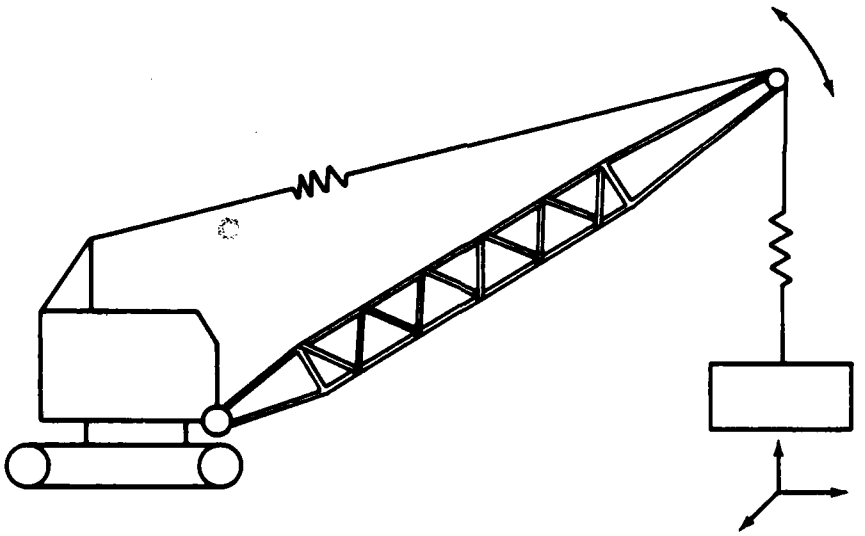

The equations of motion for its degrees of freedom are coupled. Linearization and simplification of the equations results in two models that describe the important characteristics of the system, a vertical stiffness model and a pendulation model,

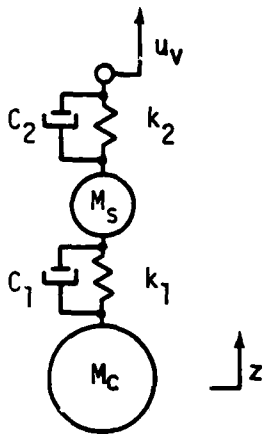

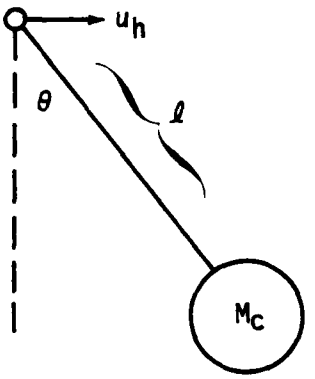

where M_c = mass of cargo and hook blocks

k_1 = stiffness of hoist cable

C_1 = damping of hoist cable

M_s = effective mass of moving crane structure

k_2 = equivalent stiffness of crane structure

C_2 = damping of crane structure

ℓ = pendulation length of load line

u_v = vertical input motions

u_h = horizontal input motions

θ = pendulation angle

z = vertical displacement of the load

All physical systems have mechanisms of energy dissipation, such as sliding friction, viscous damping, structural damping, and the like. Although these various damping mechanisms are represented by somewhat different mathematical descriptions, for very lightly damped systems such as a crane, the linear approximation of equivalent viscous damping is a reasonable representation of reality.[51]

Since $k_1 > k_2$ and $M_s < M_c$ for the crawler cranes under consideration, the vertical stiffness model can be further simplified,[36]

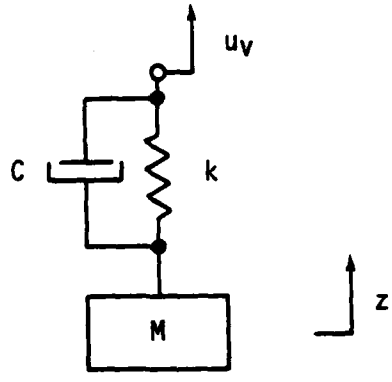

where M = equivalent suspended mass

k = total vertical stiffness

C = equivalent linear damping coefficient

u_v = vertical displacement of the boom tip if the crane were a rigid body

z = vertical displacement of the cargo.

The input motions, u(t), induced by the crane platform motions are related to the cargo motion z(t) by the differential equation,

$$M\ddot{z} + C\dot{z} + kz = C\dot{u}_v + ku_v$$

The transfer function, resulting from the Laplace transformation is:

$$\frac{z(s)}{u_v(s)} = \frac{Cs + k}{Ms^2 + Cs + k}$$

The dynamic load on the crane resulting from the suspended mass and its acceleration is expressed by,

$$F = M\ddot{z} .$$

When this expression is combined with the transfer function, $z(s)/u_v(s)$, the transfer function between $u_v(s)$ and $F(s)$ is found to be

$$\frac{F(s)}{u_v(s)} = \frac{s^2M\,(Cs + k)}{Ms^2 + Cs + k} .$$

When this force, F, is added to the weight of the container, W, the result is a force approximating the vertical component actually experienced by the crane.

A similar analogy can be made for the pendulation model.

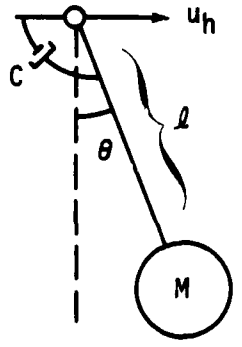

$$\ddot{Mx} + \frac{C}{\ell}\dot{x} + \frac{Mg}{\ell}x = \frac{C}{\ell}\dot{u}_h + \frac{Mg}{\ell}u_h ,$$

leads to

$$\frac{\theta(s)}{u_h(s)} = \frac{1}{\ell}\left(\frac{s^2}{s^2 + 2\zeta\omega_{n_p}s + \omega_{n_p}^2}\right),$$

where

$$\omega_{n_p} = \sqrt{g/\ell} = \text{natural frequency of pendulation,}$$

$$\zeta = \frac{C}{2M\sqrt{g/\ell}} = \text{damping ratio.}$$

The side load at the point of suspension can be approximated by:

$$\text{Side Load} = Mg \sin(\theta).$$

For conventional boom cranes, manufacturers recommend that this load should not exceed a fixed percentage of the rated vertical load, usually 2%.[52] For cranes equipped with a rider block tagline system, this figure can be increased to as much as 7%.[53]

The vertical stiffness and damping coefficients required for the above models can be easily measured on the cranes of interest. These models constitute the crane/cargo structural models shown in the system synthesis flow chart. The output of these models is an equivalent load imposed on the crane by virtue of its operation in the dynamic environment. This load along with the maximum reach requirements of the

system configuration define the crane cost by the formula

$$\text{Crane Cost (in \$1000.00)} = \frac{W\,R}{(7356 - 25.72\,R)}$$

where W = Load in lbs.

R = Radius of operation in ft.

This relationship is developed in Appendix A.1.

The motion compensation model is also described in detail in Appendix A.2. It appears as an intermediate system between the input motion, $u_v(t)$, and the vertical structural model.

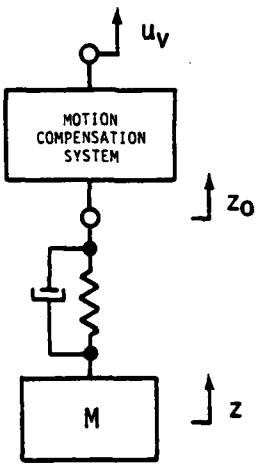

The transfer function for this motion compensation system, developed in Appendix A.2 is,

$$\frac{z_o(s)}{u_v(s)} = \frac{(1 + \tau s)(1 + \frac{2\zeta s}{\omega_{n_h}} + \frac{s^2}{\omega_{n_h}^2})}{(1 + \tau s)(1 + \frac{2\zeta s}{\omega_{n_h}} + \frac{s^2}{\omega_{n_h}^2}) + KG(s)},$$

where τ = hydraulic pump swashplate time constant $\approx$ .3 sec.

ω_{n_h} = hydraulic pump/motor system resonance $\approx$ 10 rad/sec.

ζ = damping ratio $\approx$ .5

K = system feedback gain

G(s) = series compensation.

The system feedback gain, K, is a design parameter that affects both the performance and the cost of implementation of the motion compensation system. The low frequency motion attenuation is approximately equal to $\frac{1}{K+1}$. Increasing K reduces the low frequency motions of the load and increases the effective bandwidth of the system, however, this also increases the horsepower consumption of the system and makes stabilization more difficult. The difference between the input and output velocities is the hoisting velocity that must be supplied to the system. The significant value of this hoist line velocity can be calculated by the spectral analysis techniques described earlier. The transfer function between the hoist line velocity and the input motion, also developed in Appendix A.2, is:

$$\frac{V(s)}{u_v(s)} = \frac{sKG(s)}{(1 + \tau s)\left(1 + \frac{2\zeta s}{\omega_{n_h}} + \frac{s^2}{\omega_{n_h}^2}\right) + K\,G(s)} .$$

The system horsepower can be calculated by,

$$HP_s = \frac{W\,V_s}{550}$$

where HP_s = significant horsepower

W = weight of cargo in lbs

V_s = significant hoist speed in ft./sec.

A motion compensation cost model of the form,

Motion Compensation Cost = A + B HP_s results,

where A = fixed cost of major motion compensating hardware components and installation on crane.

B = variable cost associated with required horsepower.

These cost factors are addressed in further detail in Appendix A.2.

Because effective crane operation at sea requires the continuous positioning of a pendulus load, a simple, idealized, positioning problem (shown below) is examined in detail in Appendix B.1.

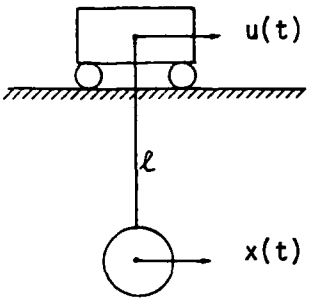

$$x(0) = \dot{x}(0) = \ddot{x}(0) = 0$$

$$u(0) = 0$$

$$u(t_f) = x(t_f) = x_f$$

$$\dot{x}(t_f) = \ddot{x}(t_f) = 0$$

$$|\dot{u}(t)| \leq V_{max}$$

Find t_f, such that t_f is minimum over all u(t).

It is shown that the minimum time required to transfer a pendulum from rest to a nearby position at rest is approximately proportional to the square root of the pendulum length. This relationship will be used in

the development of analytical expressions for system productivity in Appendix B.2.

3.3 MEASURES OF EFFECTIVENESS

The system evaluation model uses input data in conjunction with the outputs from the system dynamics model to generate estimates of system cost and productivity. The following sections describe how the models of the various system elements are combined to produce the values for these system measures of effectiveness.

3.3.1 Cost

The total system cost is the sum of the costs of the various subsystems. This includes the breakwater cost, basic crane cost, additional crane costs associated with the riderblock or motion compensating hardware, and the system configuration cost.

The breakwater cost model has been described along with the breakwater dynamic model in Section 3.2.2. The output of the breakwater cost model is cost per unit length in dollars per foot. This must be multiplied by the length of breakwater required for the particular configuration under consideration to obtain the total, installed, breakwater cost. This cost is based on domestic material costs and civilian labor rates in effect during 1977.

The basic crane and motion compensation cost models have been given in Section 3.2.4 along with the crane dynamic models. The load used in the equation is the larger of either the vertical dynamic load or the effective pendulation load. The vertical dynamic load is the static weight of the cargo plus the maximum expected vertical inertial load.

The effective pendulation load is the maximum expected side load divided by the allowable percent side load for the particular crane under consideration, (.02 for standard cranes and .07 for cranes equipped with a rider block).

The cost of the Rider Block Tagline System (RBTS) is assumed to be $25,000 plus one tenth of the basic crane cost. This figure was obtained from the costs of a prototype RBTS that was installed on a small crane and a full scale RBTS that is currently being manufactured for a much larger crane.

The motion compensation cost is assumed to be a fixed cost of $250,000 plus $400 per horsepower required by the motion compensation system[2] (Appendix C).

The system configuration cost represents all other fixed costs that are associated with the basic system configuration. These include the costs of ships, moorings, and other hardware as well as the indirect costs, if applicable, of transportability, availability, and reliability that are further descriptive of the configuration. This information is assumed to be a constant for a particular configuration.

3.3.2 Productivity

Productivity can be defined as the number of containers offloaded in a given period of time, containers per hour or containers per day being the most commonly used. It is a somewhat less well defined parameter than system cost. There has been very little work done in developing functional relationships between other system parameters and productivity with the exception of one report that used linear

regression techniques to fit the times required to perform various portions of the offload cycle to relative vertical displacement.[54]

The offload cycle time is difficult to define analytically because it is a function of so many variables, many of which are not readily quantifiable. A list of the most important of these include:

a. Operator Proficiency
b. System Configuration
c. Sea State
d. Vertical Relative Motion
e. Lateral Relative Motion
f. Maximum Crane Speeds
g. Pendulum Length
h. Weight of the Cargo
i. Load Placement Accuracy Requirements
j. Communication to the Crane Operator
k. Weather Conditions other than Wave Action

Only two military exercises have been conducted in which any significant amount of productivity data was collected. These were the Over-the-Shore Discharge of Cargo II (OSDOC II) exercises[7] conducted in October of 1972 and the Logistics-Over-the-Shore (LOTS) exercises[16] conducted in August of 1977. During OSDOC II, container handling operations were performed in sea states 1 and 2. Data were taken for a variety of configurations. It was observed that cranes with shorter booms were more productive than cranes with longer booms. The longer booms resulted in longer pendulums in most cases. In both exercises,

the significant time losses during a cycle were in positioning of the load over the ship or the lighter. These observations lead to the hypothesis of a cycle time model of the form:

$$CT = T_m + T_s + T_\ell ,$$

where CT = Total Cycle Time

T_m = Minimum practical time to move a container in complete calm.

T_s = Average time lost over the ship.

T_ℓ = Average time lost over the lighter.

After the OSDOC II exercises, several observers, knowledgable in the field of marine operations and Naval material handling, extrapolated the data to generate estimates of offload cycle times for sea states 1 through 4.[55] The minimum time, T_m,[56] was subtracted from these estimates to obtain the total lost time. A review of the data indicated that the time lost over the ship, T_s, was approximately 70% greater than the time lost over the lighter, T_ℓ.[7]

These lost times were hypothesized to have a form:

$$T = A\sigma^{\alpha}\ell^{\beta}$$

where

A = constant

σ = relative vertical displacement between the cargo and the ship or lighter

ℓ = pendulum length

$\alpha\&\beta$ = exponents

Vertical displacement is not the only motion that affects the container transfer rate, but a high correlation has been shown to exist between the two[54] and the other motions tend to increase along with vertical displacement.

The pendulum length is closely related to the controlability of the load. Each container positioning operation is actually the result of a finite number of small repositionings and minor adjustments. The number required increases with the amount of relative motion. It is assumed that an experienced crane operator might perform these positioning tasks in some suboptimal manner that is approximately proportional to the optimal solution as derived in Appendix B.1. Therefore, the exponent, B, in the lost time expressions is chosen to be 1/2.

A typical container offloading configuration was chosen and the relative vertical displacements were obtained from the RELMO computer program for the various sea states. This information is plotted against the lost time data in Appendix B.2 to obtain the remaining variables in the lost time expressions. The resulting expressions are:

$$T_s = .82\sigma_s \ell_s^{\frac{1}{2}}$$

and

$$T_\ell = .3\sigma_\ell^2 \ell_\ell^{\frac{1}{2}} .$$

The system productivity is measured in containers per 20 hour day. Four hours are allowed each day for maintenance of the equipment. Therefore,

$$OLR = \frac{1200n}{CT}$$

where,

OLR = offload rate

n = efficiency factor.

The efficiency factor accounts for the time lost moving hatch-covers, repositioning the cranes, mooring the lighters and the like. Preliminary indications from the LOTS test indicate that this efficiency factor was approximately 65%.[16]

3.4 COMPUTER PROGRAM

A computer program has been written (Appendix E) to implement the models that have been developed. It is written in Fortran and makes extensive use of the subroutine structure to permit the substitution of alternative models for the various system elements and to facilitate the reconstruction of the output for a variety of applications.

The ship response operators are calculated by a separate program and stored on tape or disk files. This data is called and read by the main program at the beginning of each run. This is done because the evaluation of the response amplitude operators for the six degrees of freedom of a floating vessel is significantly more expensive than running the remainder of the system dynamics and system evaluation models.

The subroutine names and their functions in the main program are:

RAOG - reads RAO's for the required number of vessels.

PIERMOS - Calculates PIERSON-MOSCOWITZ Sea Spectrum
for given significant wave height

TFB - calculates Energy Transmission Ratio and cost
for Tethered Float Breakwater

CRANE - calculates structural and pendulation transfer
functions for crane

MOCOMP - calculates motion compensation transfer
function

CRCOST - calculates total crane cost

PROD - calculates system productivity in offload rate

INTEG - calculates area under a power density spectrum

EVAL - combines the input data with the other subroutines to
generate total crane cost, breakwater cost, total
system cost, and offload rate.

Input data can be provided through two namelists - CONFIG and VARIAB. The system configuration data contained in CONFIG includes:

XCG - Relative position of the ship and lighter with respect
YCG to the crane platform

XR - Points of interest on the ship and the
YR lighter
ZR

CFCOST - Fixed configuration cost

BWL - Breakwater length

MCO - Motion compensation option

0 = standard crane

1 = rider block tagline system

2 = rider block with motion compensation

NC - Number of Cranes

PMT - Practical minimum cycle time

EFF - Efficiency factor

The other variables that are contained in VARIAB are:

WC - Container Weight

VS - Vertical Stiffness of Crane Structures

FK - Motion compensation feedback gain

BCF - Breakwater cutoff frequency

H13 - Significant wave height

The program has been run on a commercial time sharing system (Control Data Corporation's Cyber 174). The program can be compiled and 180 variations of a basic system configuration can be evaluated for approximately $24.00. The RAO's for the six degrees of freedom of a floating vessel can be calculated and stored on a file for approximately $30.00.

SECTION IV
APPLICATIONS

4.1 GENERAL.

The COTS computer model developed in the preceding sections can be used in a variety of ways. In this section, a number of potential applications will be demonstrated using the model. This is followed by two actual applications using test data. A comparative analysis between the model and the actual test data then is presented.

4.2 THEORETICAL DEMONSTRATIONS

For the purpose of demonstrating potential applications of the model, an example system configuration will be investigated. It is shown in Figure 4.1. The crane platform is a C7 class container ship, heavily loaded for a lower roll resonance providing better stability in the dynamic ocean environment. The container ship is a C4 class, moderately loaded, simulating a partially unloaded vessel. The lighter is an LCM-8, a fairly light landing craft capable of carrying one container at a time.

The ships are in quartering seas. That is, the direction of the waves is 135° counter clockwise, measured from the stern of the vessels.

The center of gravity of the crane platform is used as a reference for the definition of the system configuration. The center of gravity of the container ship and the lighter is located with respect to the right handed coordinate system whose origin is the center of gravity of the crane platform. The center of rotation of the crane is also located with respect to this coordinate system. The X axis faces forward along the longitudinal axis of the ship. The X-Y plane is parallel to the horizon, with the Z axis pointing vertically upward. The X and Y coordinates of the container ship are 0 and -110 feet (0,-33.5m)

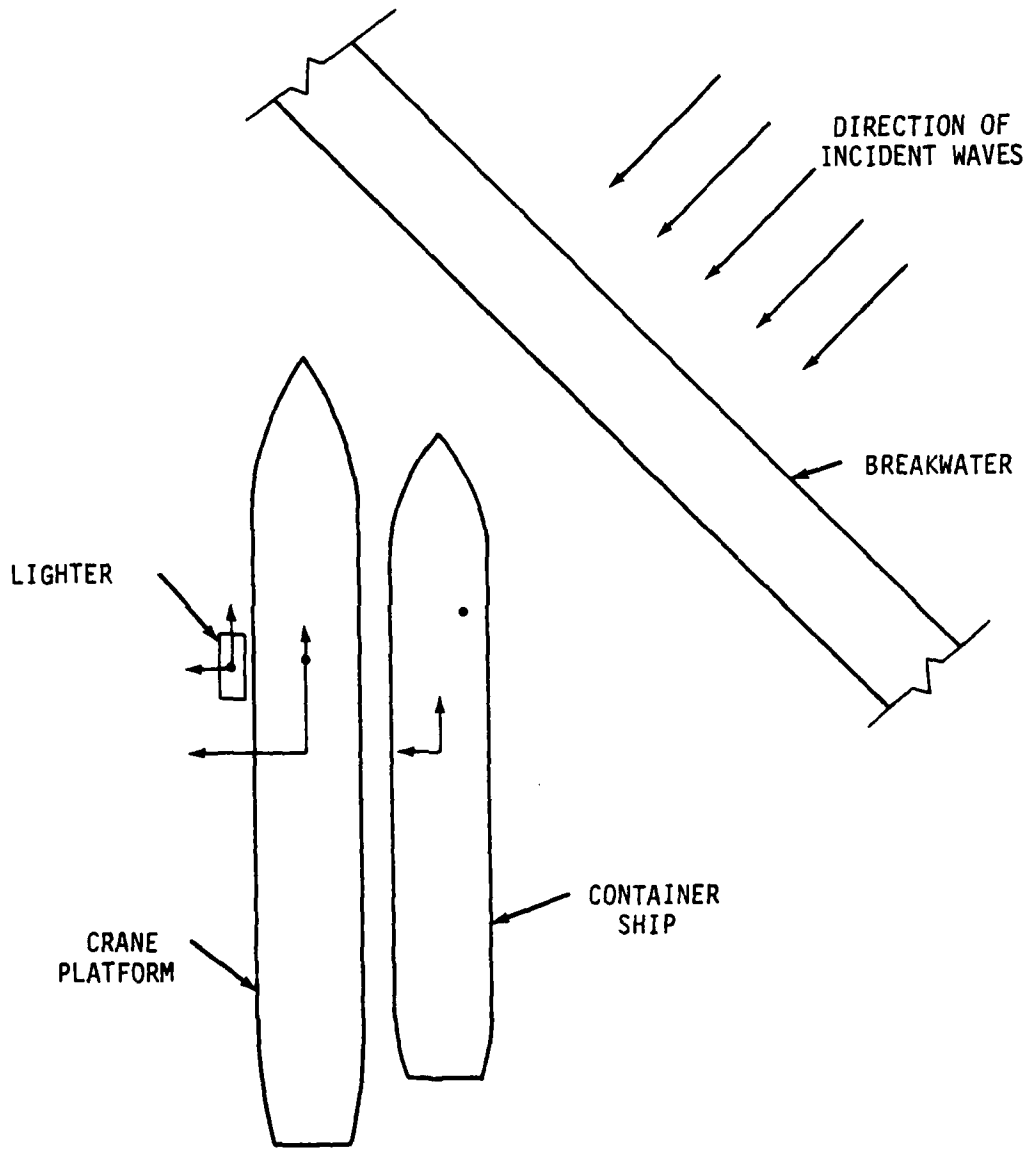

Figure 4.1. An Example COTS Configuration

respectively. The coordinates of the lighter are 60 and 70 feet (18.3, 21.3 m). The center of rotation of the crane is at 80 and 0 feet (24.4, 0 m). The reference point of the containership and the lighter used in the estimation of reach and motion requirements is defined from secondary coordinate systems whose origins are at the center of gravity of the respective vessels. The X and Y coordinates of the points of the container ship and the lighter are 120 and -20 feet (36.6, 6.1 m) and 0 and 0 feet (0, 0 m) respectively.

The other input variables used to describe this configuration are:

Fixed Cost (CFCOST) = $1,000,000

Breakwater Length (BWL) = 1200 feet (365.8 m)

Motion Compensation Option (MCO) = 0 = (standard crane)

Number of Cranes (NC) = 1

Practical Minimum Time (PMT) = 4.0 minutes

Efficiency (EFF) = 0.65

Container Weight (WC) = 40,000 lbs (18,144 kg)

Vertical Stiffness (VS) = 3500 lbs/in (395 N/m)

Motion Compensation Gain (FK) = 0

Breakwater Cutoff Frequency (BCF) = 4.0 rad/sec

Significant Wave Height (H13) = 6.0 feet (1.83 m)

These data along with the configuration coordinates and the response amplitude operators for the three vessels constitute the initial input data for the program. These variables can be altered within the program in order to evaluate a variety of alternative system variations.

4.2.1 EFFECT OF SEA STATE

A useful application of the model is to predict container offload rates of a given system configuration for a range of sea states. This can easily be done by incrementing the significant wave height and solving for the offload rate. It is also possible to repeat this exercise for other configurations.

Motion compensation options (MCO) of 0 and 1, which is a standard crane and a crane with a rider block tagline respectively, are used, along with significant wave heights (H13) of 1 to 8 feet. The initial condition of BCF = 4.0 rad/sec is interpreted by the TFB subroutine as no breakwater, since this cutoff frequency is sufficiently high to have no effect.

The output of this computer run is given in Table 4.1. Figure 4.2 is a plot of these results. Container offload rate is shown versus wave height for a standard crane and a crane with a rider block (RBTS). The five to six foot wave heights represent an upper sea state 3, the highest operating range of a container offload and transfer system using the LCM-8 lighters. The seaworthiness of these lighters becomes an operational, limiting factor, although the theoretical offload rates are shown above sea state 3 for comparison purposes. Container offload rate decreases rapidly with increasing wave height for wave heights above about one foot for both standard and RBTS cranes. In a sea state 3, the offload rate of a standard crane is reduced to about 25% of its value in calm water. As sea conditions worsen, the offload rate of the standard crane decreases more rapidly than the RBTS crane.

TABLE 4.1. EFFECT OF SEA STATE ON COST AND PRODUCTIVITY OF COTS WITH NO BREAKWATER

INCIDENT WAVE HEIGHT (FT)	TRANSMITTED WAVE HEIGHT (FT)	BREAKWATER COST ($1000)	CRANE COST ($1000)	TOTAL SYSTEM COST ($1000)	OFFLOAD RATE	
1.00	1.00	0.00	1467.61	11467.61	146.40	
2.00	2.00	0.00	1477.20	11477.20	132.52	
3.00	3.00	0.00	1482.14	11482.14	104.75	
4.00	4.00	0.00	1486.69	11486.69	74.12	STANDARD CRANE
5.00	5.00	0.00	1492.73	11492.73	51.94	
6.00	6.00	0.00	1499.84	11499.84	37.88	
7.00	7.00	0.00	1500.00	11500.00	29.03	
8.00	8.00	0.00	2500.00	12500.00	23.23	
1.00	1.00	0.00	1639.37	11639.37	151.09	
2.00	2.00	0.00	1649.92	11649.92	142.42	
3.00	3.00	0.00	1655.36	11655.36	122.67	
4.00	4.00	0.00	1660.36	11660.36	96.72	CRANE WITH RBTS
5.00	5.00	0.00	1667.00	11667.00	73.93	
6.00	6.00	0.00	1674.82	11674.82	57.12	
7.00	7.00	0.00	1675.00	11675.00	45.39	
8.00	8.00	0.00	1675.00	11675.00	37.16	

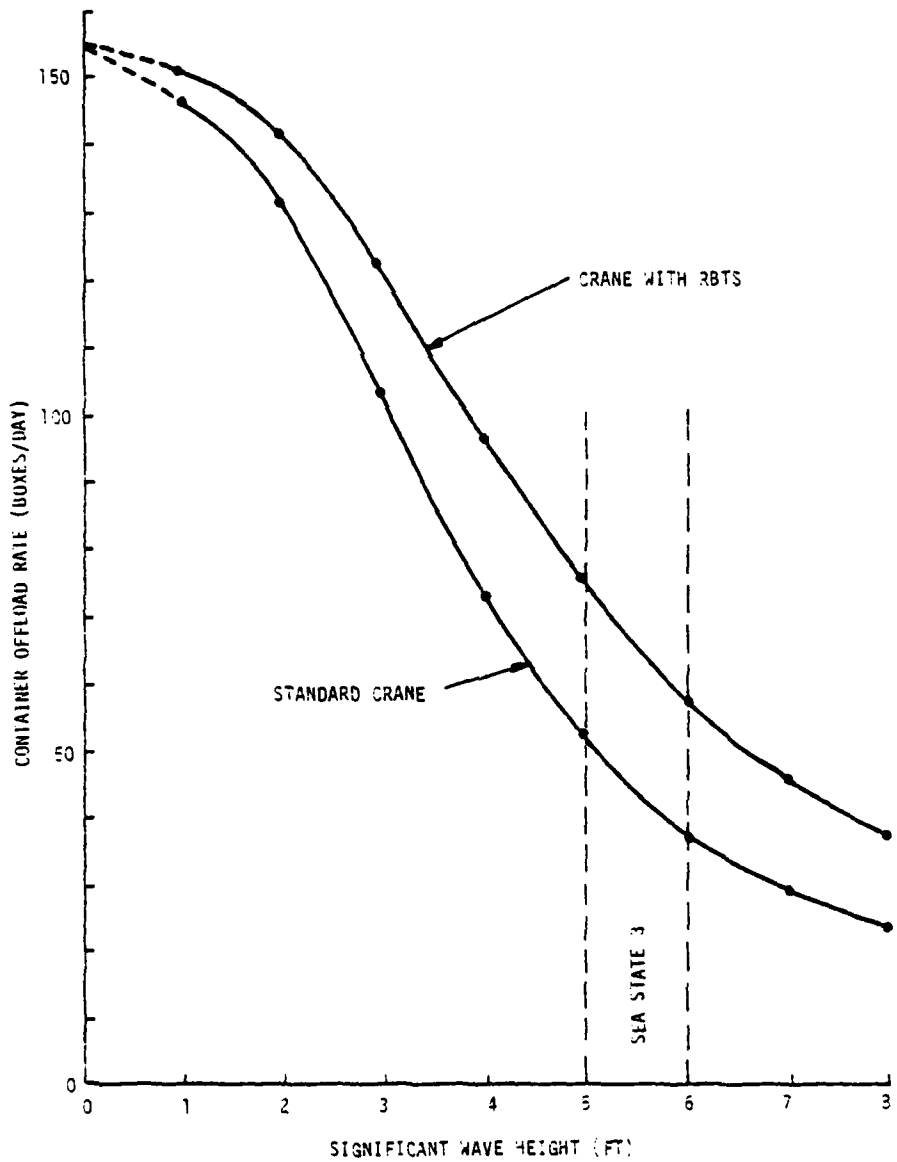

Figure 4.2. Effect of Wave Height on Productivity of Example COTS with Standard and RBTS Equipped Cranes

Figure 4.3 is a plot of the percentage increase in productivity and cost of the RBTS crane over the standard crane versus wave height. The benefits of the RBTS crane, in terms of increased productivity, increases with increasing wave height. In a sea state 3, the RBTS crane has an offload rate that is approximately 50% greater than a standard crane.

The added cost of the RBTS equipment is approximately 12% of the standard crane cost. This results in a 2-1/2 foot wave height as the economic break even point in the decision to make use of an RBTS crane. At wave heights less than this, the increased cost of the RBTS hardware over the standard crane is greater than the percentage increase in productivity derived from its use.

4.2.2 EFFECT OF BREAKWATERS

Another application of the COTS program is to examine the effect of variations in breakwater design on system productivity. This is easily done by varying the breakwater cutoff frequency (BCF) for a given sea condition. The changes to the computer program required to implement this are given in Appendix E.

Once again, the standard crane and the rider block option are compared. The breakwater cutoff frequency (BCF) is varied from 4.0 rad/sec to 0.5 rad/sec in increments of 0.5 rad/sec. The incident significant wave height (H13) in all cases is the initial input value of 6.0 feet. The output of this computer run is given in Table 4.2.

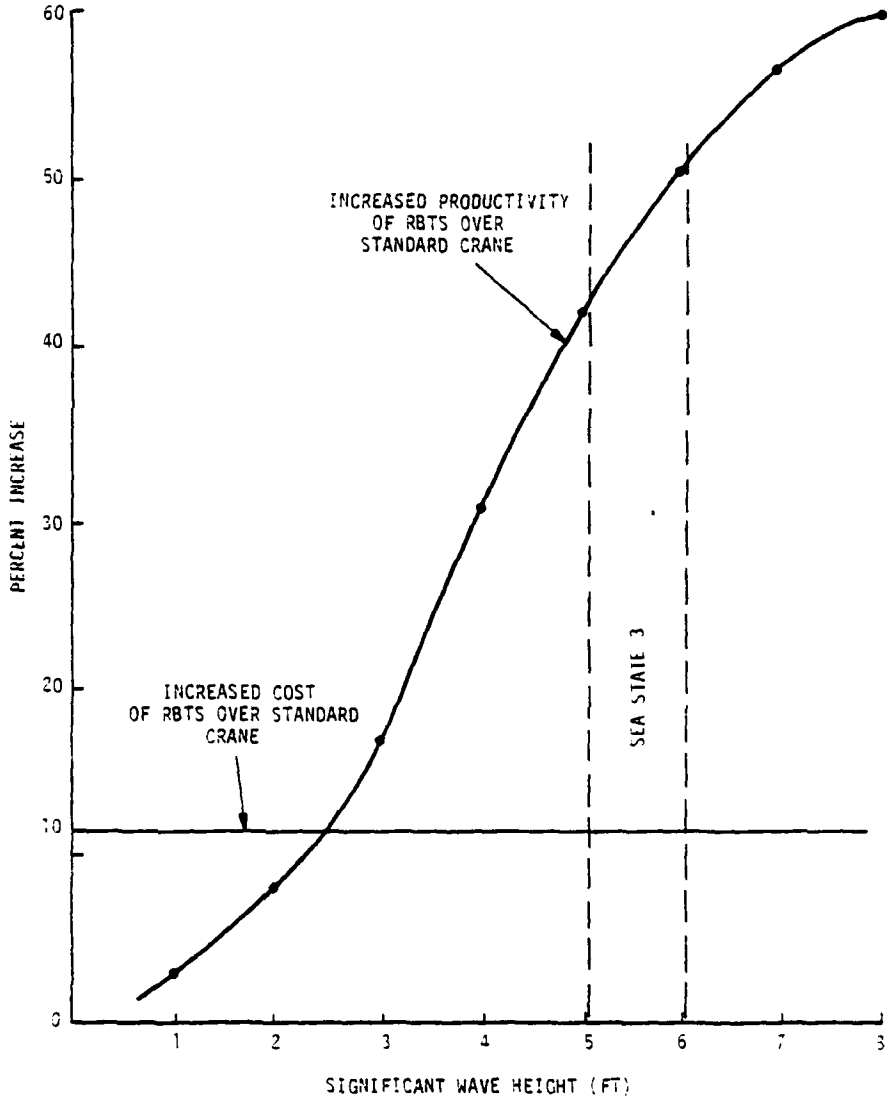

Figure 4.3. Percent Increase in System Cost and Productivity of RBTS Over Standard Cranes Versus Wave Height

TABLE 4.2. EFFECT OF BREAKWATER ON COST AND PRODUCTIVITY OF COTS IN SEA STATE 3

BREAKWATER CUTOFF FREQUENCY (RAD/SEC)	TRANSMITTED WAVE HEIGHT (FT)	BREAKWATER COST ($1000)	CRANE COST ($1000)	TOTAL SYSTEM COST ($1000)	OFFLOAD RATE	
4.00	6.00	0.00	1499.84	11499.84	37.88	
3.50	5.99	59.75	1487.97	11547.73	37.89	
3.00	5.96	107.34	1481.84	11589.18	37.89	
2.50	5.91	214.61	1475.93	11690.54	37.90	STANDARD CRANE
2.00	5.73	501.08	1469.61	11970.69	38.12	
1.50	5.01	1495.12	1461.91	12957.02	40.83	
1.00	2.43	6979.46	1441.00	18420.45	67.34	
.50	1.34	97215.53	1430.34	108645.86	108.50	
4.00	6.00	0.00	1674.82	11674.82	57.12	
3.50	5.99	59.75	1661.77	11721.52	57.13	
3.00	5.96	107.34	1655.02	11762.36	57.13	
2.50	5.91	214.61	1648.52	11863.13	57.14	CRANE WITH RBTS
2.00	5.73	501.08	1641.57	12142.65	57.45	
1.50	5.05	1495.12	1633.10	13128.21	61.25	
1.00	2.43	6979.46	1610.10	18589.55	92.54	
.50	1.34	97215.53	1598.37	108813.90	127.38	

Figure 4.4 is a plot of offload rate for the standard and RBTS cranes versus breakwater cutoff frequency from these results. Once again, as in the previous example, the RBTS crane is seen to provide a larger offload rate than the standard crane for the same conditions. As the breakwater cutoff frequency is reduced, thereby reducing the amount of wave activity, the offload rate of both crane designs increases. This increase is very slight between 4 rad/sec and 1.5 rad/sec but rises very sharply between 1.5 rad/sec and .5 rad/sec. This result is not too surprising upon review of the sea spectrum for six foot waves (Figure 3.1). The majority of its energy is found at frequencies below 1.5 rad/sec. At 1.5 rad/sec, the productivity of both cranes has increases less than 8% over the value for no breakwater (4.0 rad/sec). At 1.0 rad/sec, however, the standard crane shows a 77% increase and the RBTS crane, a 62% increase.

These productivity figures are accompanied by costs that also increase most rapidly where the greatest benefits are derived. (See Table 4.2). At first glance, these costs appear to make the breakwater far too expensive in comparison to its effect on the system. It should be noted that a single breakwater can shelter more than one crane. Two cranes could easily operate from the same crane platform, offloading the same containership. As the breakwater cost increases, the crane cost is reduced, because the reduction in the transmitted wave height reduces the dynamic loads experienced by the crane. This savings, times the number of cranes, can be deducted from the cost of the breakwater in making comparisons.

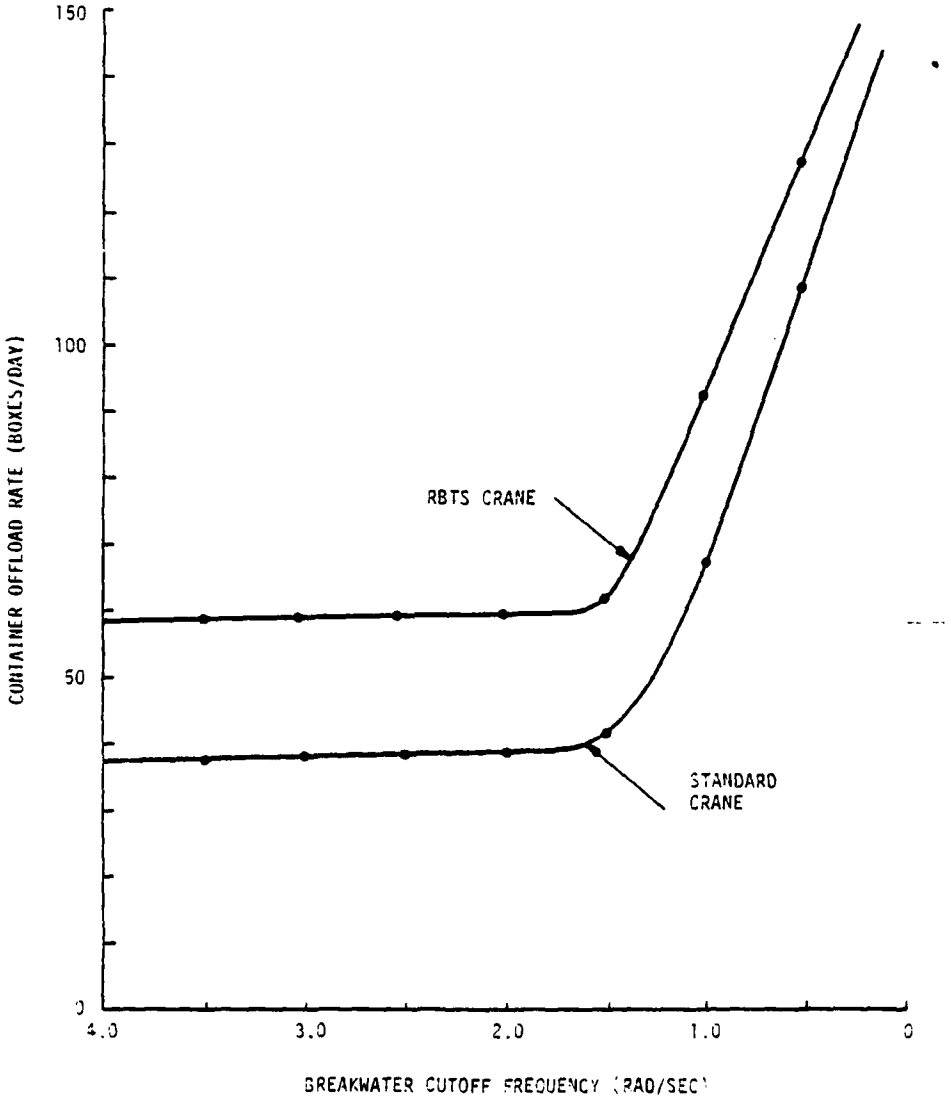

Figure 4.4. Effect of Breakwater Cutoff Frequency on Productivity of Example COTS with Standard and RBTS Cranes

The use of a 1.0 rad/sec breakwater in the example with two standard cranes results in an increase of 53% in the total system cost. This is more than offset by the increased productivity of 77%. On the other hand, the selection of a 2.0 rad/sec breakwater for this system would have resulted in a total system cost increase of over 3% with a corresponding increase in productivity of less than 1%.

Therefore, it appears, that if breakwaters are to be used in such a system, that one large enough to have a sufficiently low cutoff frequency would be more cost effective than the smaller, less costlier designs.

4.2.3 TRADEOFF ANALYSIS

Another use of the COTS computer model is in evaluating tradeoffs between two or more competing technologies. For the example COTS configuration under investigation, the tradeoff between motion compensating cranes and breakwaters will be examined.

For a two parameter system such as this, the brute force approach of evaluating the system over the ranges of both independent variables provides the designer with a quick look at the nature of the tradeoffs and the approximate values and locations of any optimal solutions.

The required lines of computer code to implement this two parameter evaluation technique are listed in Appendix E. The breakwater cutoff frequency is varied from 0.8 to 4.0 rad/sec. The motion compensation gain is varied from 0.0 to 10. The resulting offload rate, total system cost, and cost effectiveness (total system cost/offload rate) are shown in Figures 4.5, 4.6, and 4.7 respectively.

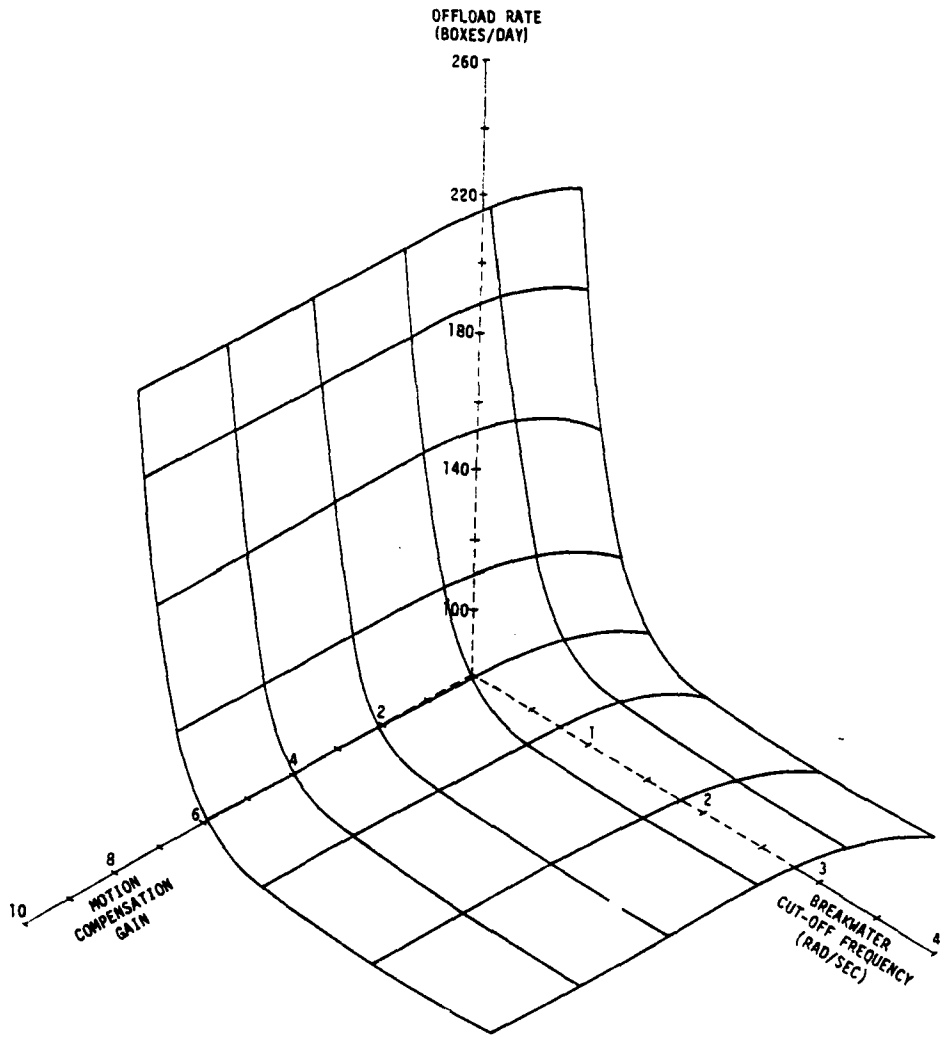

Figure 4.5. Combined Effect of Motion Compensation Gain and Breakwater Cutoff Frequency on Productivity of Example COTS

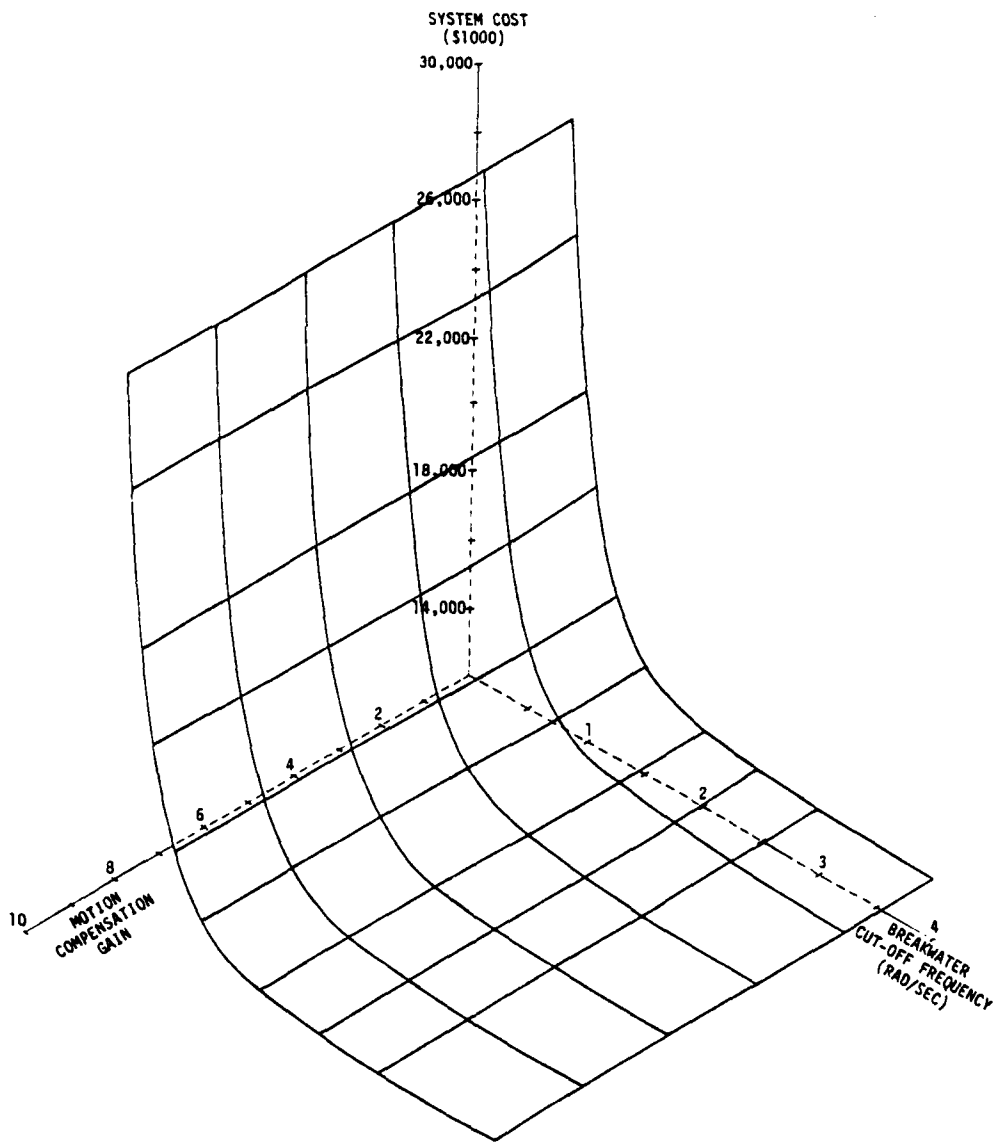

Figure 4.6. Combined Effect of Motion Compensation Gain and Breakwater Cutoff Frequency on Cost of Example COTS

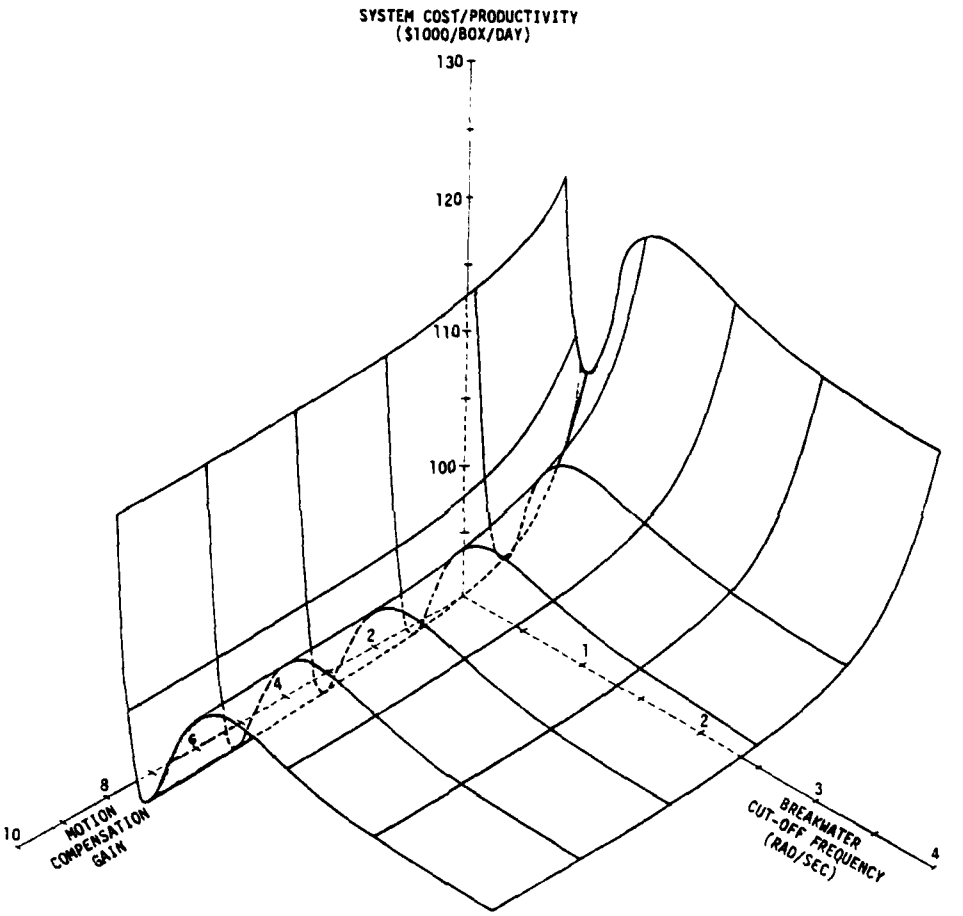

Figure 4.7. Combined Effect of Motion Compensation Gain and Breakwater Cutoff Frequency on Cost Effectiveness of Example COTS

The effect of breakwater cutoff frequency on container offload rate that was observed in the previous example (Section 4.3) is seen, in Figure 4.5, to be characteristic of the effect of breakwaters on offload rate regardless of the presence or magnitude of motion compensation gain. This characteristic is also observed with respect to system cost as shown in Figure 4.6.

The effect of motion compensation gain on offload rate is quite different from that of breakwaters. The addition of a small amount of gain results in a pronounced increase in offload rate. Further increases in gain result in successively smaller increases in offload rate. This is explained by the manner in which gain affects the motion compensating system's ability to track the motions of the crane platform. A measure of the control system's capability is its steady state error to a step input which equals 1/K+1, where K is gain. An increase in gain from 0 to 3 results in a reduction in this error from 100% to 25% or 75%. An additional increase in gain to 9, only results in an additional 15% reduction in steady state error.

Figure 4.6 shows that the effect of motion compensation gain on system cost is not significant. Once the initial cost of the motion compensating hardware is absorbed in the total system cost, the increased cost associated with the additional horsepower requirements, necessitated by increased gain, is not a major factor.

Figure 4.7 provides an interesting overview of the combined effects of breakwater cutoff frequency and motion compensation gain on the cost effectiveness of the system. The cost per box per day increases with

decreasing breakwater cutoff frequency between 4.0 rad/sec and 1.5 rad/sec. At this point the cost effectiveness, as measured in dollars per box per day, falls sharply with decreasing cutoff frequency to approximately 1.0 rad/sec. Decreasing cutoff frequencies below 1.0 rad/sec result in rapidly increasing costs per unit offload rate.

The effect of motion compensation gain on cost effectiveness is monotonic. At all points, an increase in gain results in a reduction in cost per unit offload rate, although the predominant reductions occur at the lower values of gain.

These results would lead a COTS designer to utilize the maximum motion compensation capability at his disposal and fill in with breakwater as required to obtain the necessary offloading capability. Two basic COTS configurations appear as potentially viable candidates from minimization of the system cost effectiveness:

a) Maximum motion compensation gain and no breakwater, and

b) Maximum motion compensation gain and a breakwater with a cutoff frequency in the neighborhood of 1.0 rad/sec.

System (a) provides an offload rate of 132 boxes/day at a cost of 13.8 million dollars for a six month duration. System (b) provides an offload rate of 208 boxes/day at a cost of 20.7 million dollars.

The two parameter system, as shown above, can be evaluated, the resulting surface plotted, and system tradeoffs readily identified. This approach breaks down, however, for systems with three or more variables. In these cases, optimal solutions could be found by gradient search techniques such as a steepest descent algorithm.[57,58] The

AD-A114 420 EG AND G WASHINGTON ANALYTICAL SERVICES CENTER INC R--ETC F/G 15/5
A METHODOLOGY FOR THE EVALUATION OF ALTERNATIVE OFFSHORE CONTAI--ETC(U)
APR 82 J D BIRD N00014-78-C-0787
UNCLASSIFIED WASC-TR-D200-0002 NL

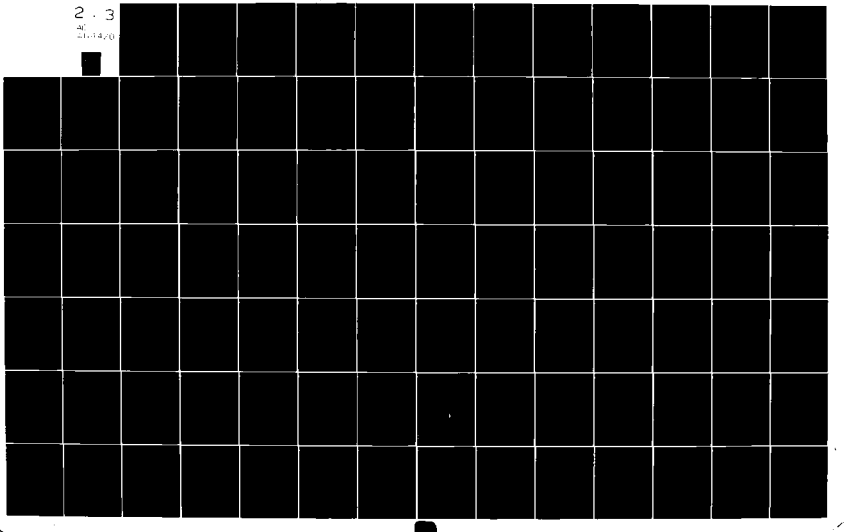

addition of penalty functions to the measure of effectiveness, permits the use of this technique for constrained optimization.

A simple minimization routine is performed on the cost effectiveness function. Partial derivatives of the cost effectiveness with respect to breakwater cutoff frequency and motion compensation gain are numerically evaluated by small variations about their present values. These numerical partial derivatives are used to calculate the unit vector in the direction of the gradient. A fixed size step is taken in the direction of the gradient. If a reduction in cost effectiveness is found, the process is repeated. If a reduction is not observed, the step size is repeatedly cut in half until a reduction is observed. If the step size is reduced to a sufficiently small value with no observed reduction in cost effectiveness, the process is stopped and the coordinates and related system parameters are printed. The required lines of computer code are listed in Appendix E. Depending upon the initial starting points, the routine either converges to the local minimum at a cutoff frequency of 4.0 rad/sec and a gain of 10.0 or the global minimum where cutoff frequency equals 1.05 rad/sec and gain equals 10.0.

An example of the use of the COTS model in a constrained minimization problem is to find the least cost configuration that will provide an offload rate of at least 170 boxes/day. This is done by adding to the cost function, a penalty function of the form:

$$500 \left(\frac{170}{OLR}\right)^{500},$$

where OLR is the offload rate. This penalty function becomes very large for offload rates less than 170 boxes/day, but almost vanishes for offload rates greater than 170 boxes/day.

The lines of computer code required to execute this procedure are also given in Appendix E. The solution obtained for this example is:

Motion Compensation Gain = 10.0

Breakwater Cutoff Frequency = 1.196 rad/sec

Offload Rate = 170.9 boxes/day

System Cost = $17.3 million

4.3 COMPARATIVE ANALYSIS WITH ACTUAL TEST DATA.

Program COTS was tested for validity by comparative analysis with actual data from two COTS test series: the RTBS harbor tests[59], and the TCDF ship tests (TECHEVAL and OPEVAL).[60, 61, 62]

4.3.1 HARBOR TESTS OF CRANE WITH RBTS.

With the Manitowoc 4100W COTS prototype crane installed on an Army B-DeLong Barge, container handling tests were conducted in Port Hueneme, CA, in November and December 1979. Tests were first conducted at dockside, where there was no appreciable platform motion. Data from the dockside evolutions provided an estimated PMT of 3.7 minutes for input to the COTS computer program.

Barge RAOs were computed with program "RAOS". Some estimates were required for section geometries needed by the program. The efficiency factor for transfer was assumed to be 1.0 since the test was fully controlled.

Following the dockside tests, the barge was moved to the inner harbor. Figure 4.8 shows the transfer scenario. Five transfer sequences were conducted:

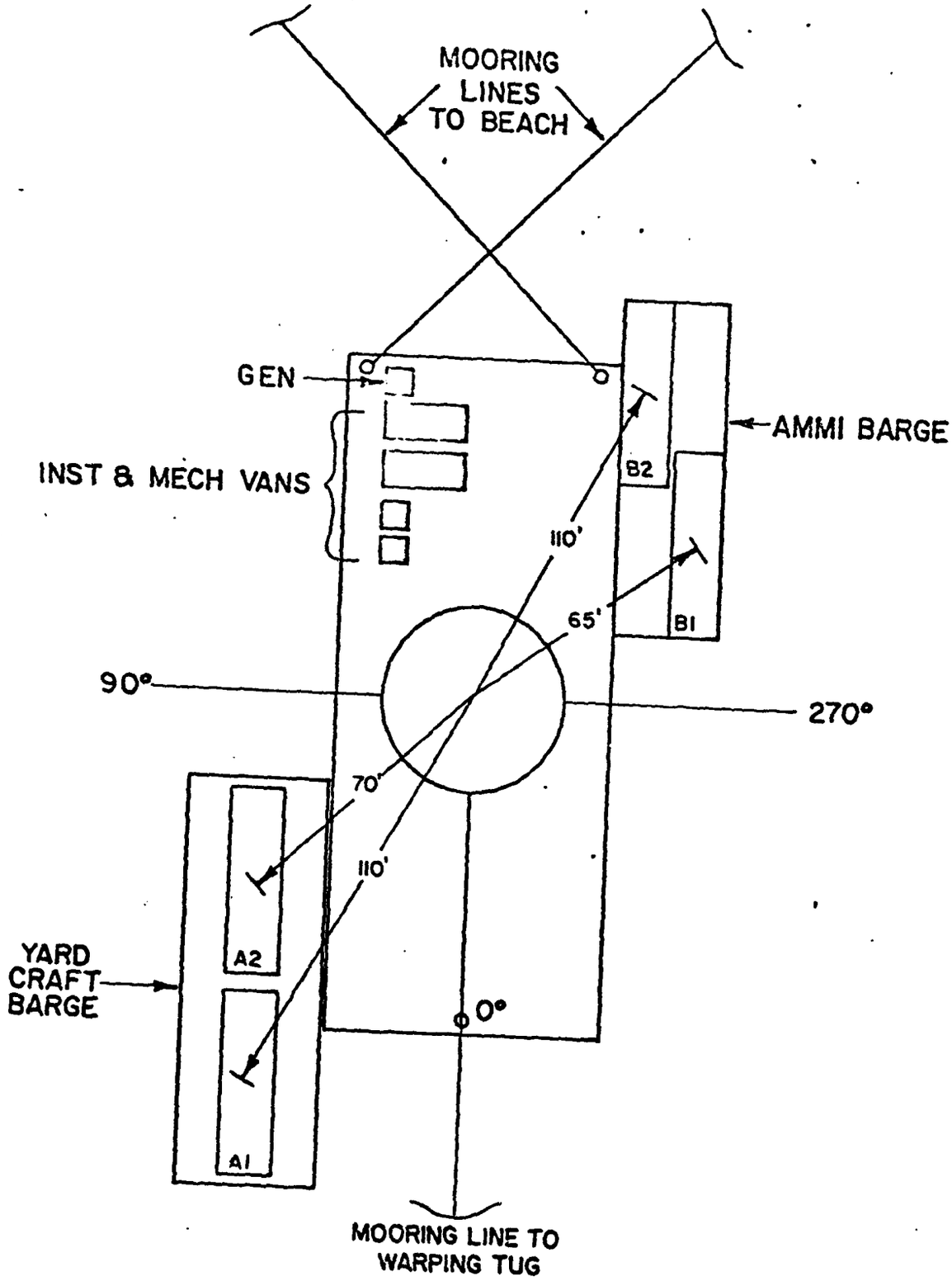

Figure 4.8 RBTS Test Arrangement

three with RBTS and two without. Table 4.3 contains important configuration parameters used in the computer programs.

A review of the test results revealed an anomaly which skewed the overall transfer rate average for the RBTS operation. Two of the RBTS sequences were performed by crane operator "A" and the other by "B", while each performed one of the without-RBTS sequences. Although B's non-RBTS sequence was significantly "better" than A's (13.73 containers/hour compared with 11.67 for A), his RBTS sequence was far less productive than A's (9.24 compared with 11.24 and 13.22 for A). With sufficient operator training, even at low seastates, productivity can be expected to increase when RBTS is used. Therefore, it can only be assumed that Operator B was not ready for a record-purposes sequence using the RBTS. Meanwhile, Operator A's RBTS performance of 11.24 and 13.22 (average 12.15) was better overall than his sequence without RBTS (11.67). This was to be expected, given the designed contribution of RBTS to the system, and providing that the operator is sufficiently trained and ready for the RBTS operation.

It is recognized that the sample-size is too small for any conclusions to be drawn on the validity of the computer program in this test. In view of the above, however, it was considered appropriate to reduce the sample even further by using only Operator A's performance for the analysis.

Table 4.4 shows a comparison between Operator A's test rates and the computer simulation rates. Since tests were conducted only in wave heights of $\leq$1 foot, a test rate slope cannot be obtained for comparison with the simulation rates slope.

Referring back to Table 4.3 and Figure 4.8, the "containership" and TCDF platform are barges. Together, they produce significantly greater movement, as wave heights increase, than do the ship platforms used for the OPEVAL (4.3.2.,

TABLE 4.3. RBTS TEST PARAMETERS

	CRANE SHIP	CONTAINER SHIP	LIGHTER
Length, ft	150	72	90
Beam, ft	60	25	30
Draft, ft	3.5	1.5	2
Displacement, long tons	900	77	154
Roll period	6.2	2.5	2.5

	CRANE
Boom length, ft	200
Vertical stiffness (VS), lb/in.	3500
Practical minimum transfer (PMT), sec	3.7

TABLE 4.4. RBTS TEST TRANSFER RATE
CONTAINERS PER HOUR

WITHOUT RBTS

WAVE HEIGHT H 1/3, Ft	TEST RATE	SIMULATION RATE
1	11.67	11.22
2	-	2.95
3	-	.94

WITH RBTS

WAVE HEIGHT H 1/3, Ft	TEST RATE	SIMULATION RATE
1	12.15	15.31
2	-	4.82
3	-	1.70

below). Therefore, the Table 4.4 simulation rates change dramatically as wave heights increase. Further, Wave Height 1 effects the ships relatively little, while barge movement is significantly greater than the ships at that wave height. This explains the greater improvement using RBTS in the barge scenario. Other features of Table 4.4 worthy of note: (1) Wave Height 1 rates are much higher than OPEVAL rates (Table 4.6), primarily due to the use of different efficiency factors; (2) the "Without RBTS" test rate compares favorably with the simulation rate, while the "With RBTS" test rate does not, being almost 3 containers/hour lower. Although (as stated earlier) the small sample size mitigates against conclusive findings, this could indicate high potential for improvement through RBTS operator training.

4.3.2 TCDF SHIP TESTS (TECHEVAL/OPEVAL).

These tests were performed in the Silver Strand Amphibious Beaching Area November-December, 1980. The crane was mounted on the ex-LSD16 (ex-CABILDO), the containership was the SS LINCOLN (a C-4 ship) and the lighter was modeled as an LCM-8. Table 4.5 contains the configuration parameters and Figure 4.9

TABLE 4.5. TCDF TEST PARAMETERS

	CRANE SHIP	CONTAINER SHIP	LIGHTER
Length, ft	458	563	51
Beam, ft	72	76	21
Draft, ft	17	15	2.5
Displacement, long tons	9000	14000	51
Roll Period	8	12.4	3

	CRANE
Boom Length, ft	200
Vertical stiffness, lb/in.	3500
Practical minimum transfer time, min.	5.2

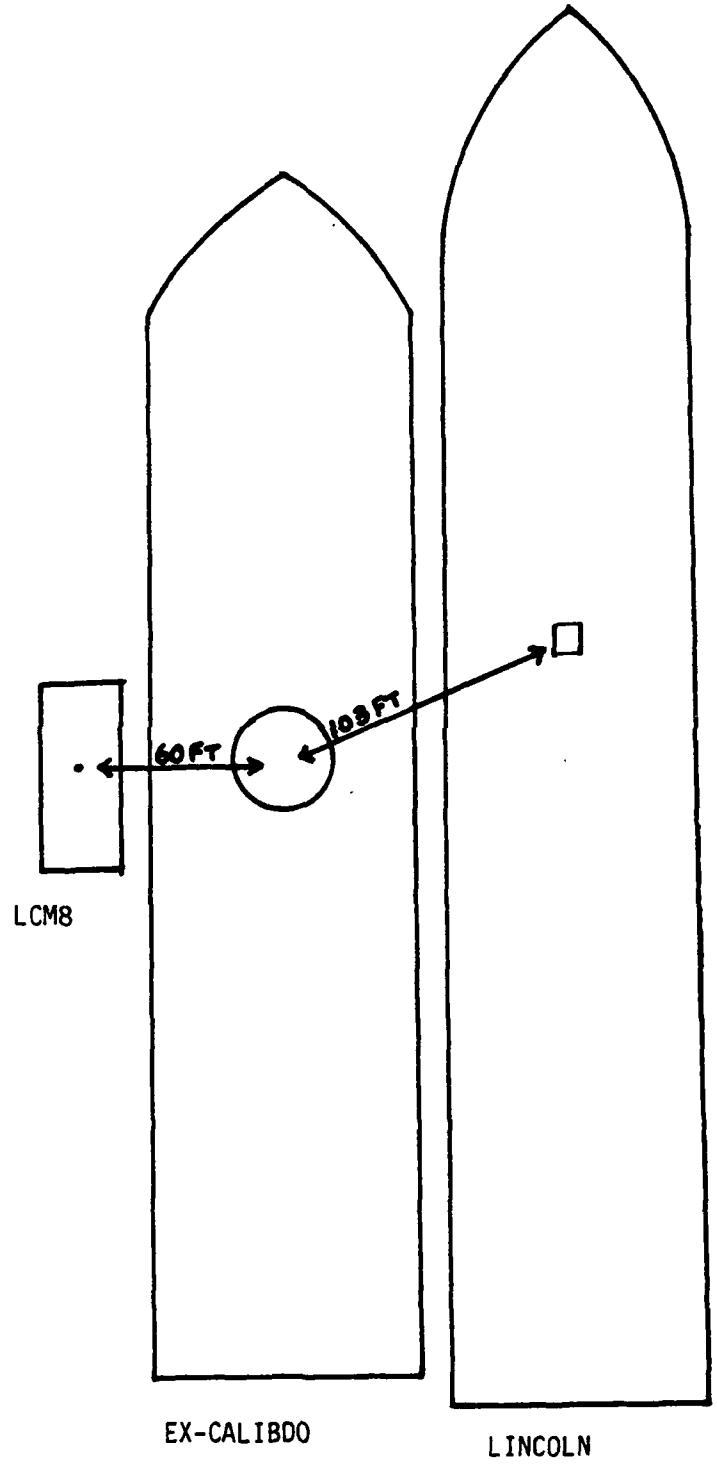

FIGURE 4.9 TCDF Test Arrangement

shows the scenario. The PMT was estimated by considering several factors: (1) time-motion analysis of the harbor test (4.3.1, above); (2) the physical lay-out of the TCDF scenario; and (3) the increased demands on operator performance imposed by the open-sea environment.

The tests were performed in sea states 1 and 2 (wave heights H 1/3 $\leq$3 ft). Efficiency was estimated to be 0.65 since this test represented actual operating conditions. Results were averaged from all available data, presented in Table 4.6, and graphed on Figure 4.10. Simulation data from the "COTS" computer program also is provided for comparison.

Figure 4.10 is a plot of "with RBTS" data only, since the tests were conducted using the RBTS throughout. The slope of the simulation curve compares favorably with overall TECH/OPEVAL results (the TECHEVAL/OPEVAL curve). Comparative slope is the singlemost important factor in validation of the computer program, since vertical displacement of the simulation curve is almost solely dependent upon selection of a realistic PMT and the appropriate efficiency factor.

It also should be noted that in low sea states (such as in these tests) the PMT is the dominant operational factor for transfer rate. As sea state increases, ship motions and crane parameters become more contributive.

It is recognized that sample size from these tests is too small for conclusive statistical analysis, but it is interesting to note that as sample size increases, the test data curve approaches the slope of the simulation curve. This is demonstrated in Figure 4.10 by plotting two test data curves: one for TECHEVAL only (128 samples), and one for TECHEVAL and OPEVAL (324 samples).

Comparative analysis between the test results and the simulation rates,

TABLE 4.6 TCDF TRANSFER RATES/CONTAINERS PER HOUR

WAVE HEIGHT H 1/3, Ft	SIMULATION (WITHOUT RBTS)	SIMULATION (WITH RBTS)	TEST RATES (ONLY WITH RBTS) OPEVAL ONLY	TEST RATES (ONLY WITH RBTS) OPEVAL AND TECHEVAL
1	7.46	7.48	6.34	6.10
1.5	7.26	7.37		
2	6.83	7.13		
2.5	6.22	6.77	6.34	5.59
3	5.53	6.31		

FIGURE 4.10 TRANSFER RATES FROM TABLE 4.6 (With RBTS)

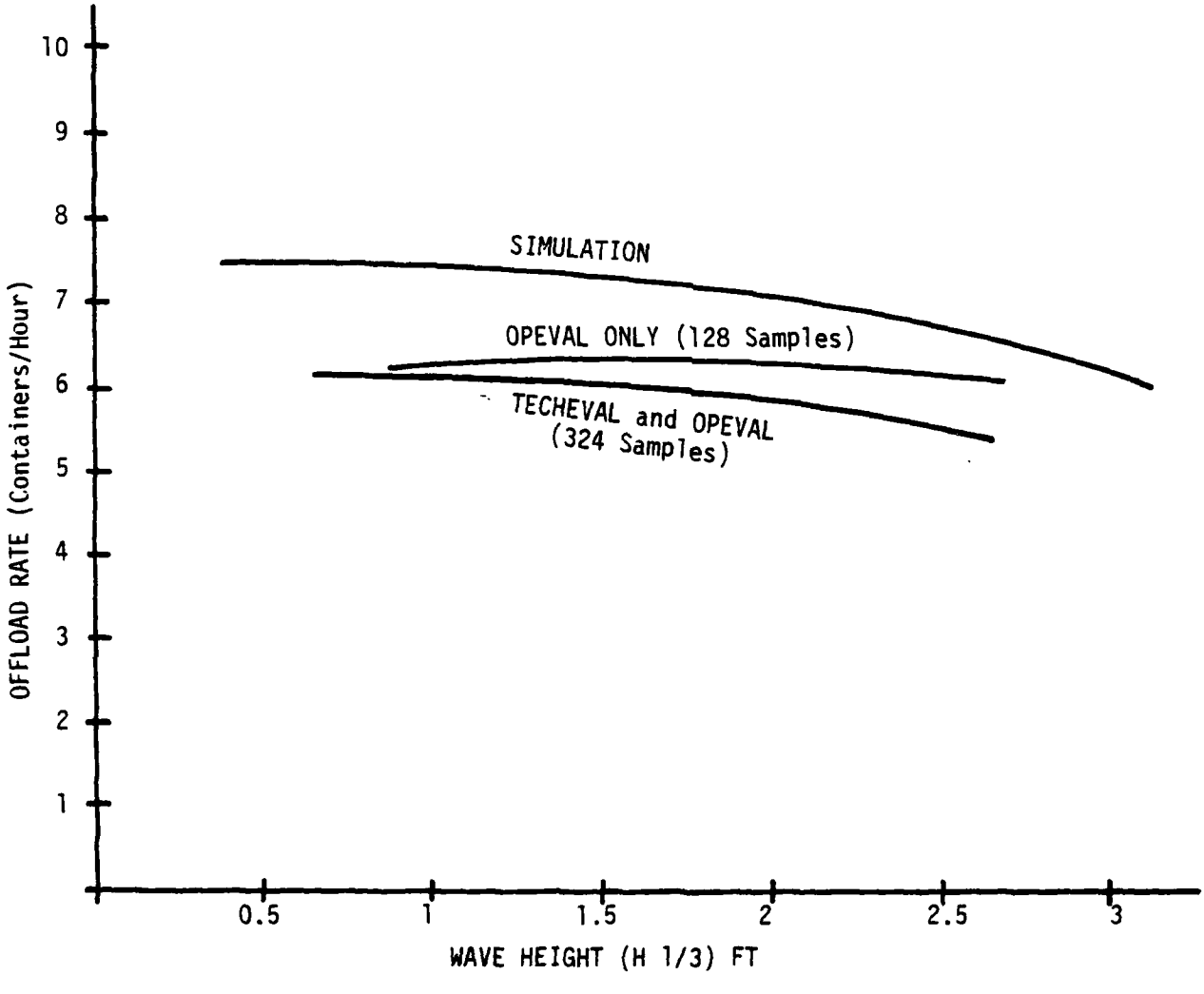

when all of the above factors are considered, tends to validate the "COTS" computer program. However, only through considerably more at-sea experience and the availability of more test data (making possible accurate estimates of PMT and efficiency factor) can accurate predictions of transfer rates be made.

SECTION V

CONCLUSIONS AND RECOMMENDATIONS

5.1 CONCLUSIONS

A methodology has been developed for the evaluation of the cost and effectiveness of a complex system of dynamic elements driven by a single random input. It has been shown that the interactions among the system elements, their environment, and the system measures of effectiveness can be grouped into two types of relationships - system dynamics and system evaluation. When the system dynamics are describable by linear differential equations and the input is a zero mean, Gaussian, random process, the system responses are completely described by their power density spectra. The significant and maximum expected values of those responses that are inputs to the system evaluation relationships can then be obtained. These evaluation relationships, that define the system measures of effectiveness, can be any function, linear or nonlinear, of the descriptive parameters of the system configuration and the significant and maximum expected values of the system's dynamic responses.

In particular, this methodology was developed for the evaluation of amphibious material handling systems and applied to the Navy's Container Offloading and Transfer system (COTS). An example system configuration has been examined in detail in order to demonstrate the application of the methodology and the type of data needed to develop the necessary system relationships. A variety of applications were

demonstrated, including determination of the effects of sea state and breakwaters and analysis of the tradeoff between breakwaters and motion compensating cranes. It was demonstrated that the methodology is easily adaptable to multidimensional optimization by the use of numerical techniques such as the steepest descent algorithm. Further, by comparative analysis with a limited sample of actual test data, it was demonstrated that Program "COTS" is a potentially useful tool for predicting crane performance at sea in the RBTS mode, given a sufficient sample size.

For the particular COTS configuration studied, it was determined that any requirement for additional offload capability should be obtained through the use of motion compensating cranes. Offload capability that could not be provided through the utilization of the maximum motion compensation capability could be obtained by the addition of breakwaters as required. Two basic COTS designs emerged as potentially viable candidates from the optimization of cost effectiveness: These were:

a) Maximum motion compensation gain and no breakwater, and

b) Maximum motion compensation gain and a breakwater with a cutoff frequency near the frequency of the peak energy density of the sea spectrum.

5.2 RECOMMENDATIONS FOR FURTHER RESEARCH

This methodology relies heavily upon Gaussian inputs, linearizable dynamic properties of the system elements, and a minimum of coupling between the dynamic elements. Future research should examine the possibility of handling non-Gaussian inputs, system dynamics that are not readily linearized, and systems where strong coupling exists between the dynamic elements.

In the particular case of the COTS problem, several areas warrant further investigation:

a) More complex forms of motion compensating crane strategies should be examined, such as those that track the relative displacement between the cargo and the adjacent craft or optimal strategies that anticipate relative motion and land the cargo on the peaks where relative velocity is minimized.

b) The interactions between the floating elements should be examined in greater detail. Particular attention should be given to the sheltering of one craft by another and the effects of secondary wave generation from the motions of the larger vessels.

c) Finally, additional data needs to be collected in order to more accurately establish the component cost models and to verify or develop improved expressions for the container offload cycle times.

Based upon the predicted performance of the simplified motion compensation system examined in this study, it is recommended that a prototype motion compensation system using this platform stabilization strategy be designed and tested on a floating crane. This will provide an interim motion compensation capability until the feasibility of the more complex systems is demonstrated.

BIBLIOGRAPHY

1. Gollobin, M. L., J. P. Scotch, Crane-On-Deck (COD) Selection Process, Presearch Incorporated, Arlington, Virginia, October 1976.

2. U.S. Department of the Navy, Navy Decision Coordinating Paper for the Container Offloading and Transfer System (COTS), NDCP-YP816SL, Chief of Naval Operations, Washington, D.C., July 1975.

3. U.S. Department of the Navy, Container Off-Loading and Transfer System (COTS), Naval Facilities Engineering Command, March 1977.

4. Clark, A. A., R. J. Lacavich, D. N. Brown, W. K. Dorbusch, R. W. Whalin, and F. B. Cox, Port Construction in the Theater of Operations, U.S. Army Engineering Waterways Experiment Station, Hydraulics Laboratory, Vicksburg, Mississippi, June 1973.

5. U.S. Department of the Navy, Program Management Plan for Container Off-Loading and Transfer System (COTS), Naval Facilities Engineering Command, March 1979.

6. Essoglou, Milon E., Army-Navy Test of Offshore Discharge of Containership OSDOC 1 5-9 December 1970, Naval Facilities Engineering Command, July 1971.

7. U.S. Department of Defense, Offshore Discharge of Containership II OSDOC II Test and Evaluation 3-14 October 1972, Evaluation Section, Joint Army-Navy Test Directorate, May 1973.

8. Rucker Shaffer, 200 Ton Crane Motion Compensator Product Description, Rucker Schaffer, Oakland, California, November 1976.

9. _____, "Kran med Bølgevegelses-Kompensator," Teknisk Ukeblad/ Teknikk, Oslo, Norway, January 5, 1978.

10. B. C. Research, Incorporated, Analysis of the Dynamics of a Motion Compensating Crane, Division of Engineering Physics, Vancouver, B. C., July 1976.

11. Casler, R., F. Browne, E. Foster, J. Eterno, W. Podgorski, The Design of Control Systems to Aid Cargo-Transfer Operations in Moderate Seas, Charles Stark Draper Laboratory, Cambridge, Massachusetts, December 1976.

12. U.S. Department of the Army, Shore Protection Manual, U.S. Army Coastal Engineering Research Center, 1973.

13. McWethy, P. J., S. B. Nelson, ed., Handbook for Offshore Port Planning, Marine Technology Society, Washington, D.C., 1974.

14. Kowalski, T. ed., 1974 Floating Breakwaters Conference Papers, National Oceanic and Atmospheric Administration, U.S. Department of Commerce, Washington, D.C., 1974.

15. Lliff, K. W., "Identification and Stochastic Control of an Aircraft Flying in Turbulence," Journal of Guidance and Control, Volume 1 Number 2, March-April 1978.

16. ORI Incorporated, Logistics Over the Shore (LOTS), ORI Incorporated, Silver Spring, Maryland, January 1979.

17. Bendat, J. S. and A. G. Piersol, Random Data: Analysis and Measurement Procedures, Wiley-Interscience, New York, 1971.

18. Kaplan, W., Operational Methods for Linear Systems, Addison-Wesley Publishing Company, Reading, Massachusetts, 1962.

19. St. Denis, Manley, "Seas, Ships, Statistics," Ocean Wave Spectra, Prentice-Hall, Englewood Cliffs, New Jersey, 1963.

20. Kinesman, Blair, Wind Waves: Their Generation and Propagation on the Ocean Surface, Prentice-Hall, Englewood Cliffs, New Jersey, 1965.

21. Meirovitch, Leonard, Elements of Vibration Analysis, McGraw-Hill, New York, 1975.

22. Longuet-Higgins, M. S., "On the Statistical Distribution of the Heights of Sea Waves," Journal of Marine Research, Volume XI, Number 3, 1958.

23. Seymour, R. J., Performance of Tethered Float Breakwaters in Deep Ocean Waves, California Department of Navigation and Ocean Development, November 1975.

24. Blagoveshchensky, S. N., Theory of Ship Motions, Dover Publications, New York, 1962.

25. Davis, D. A., H. S. Zwibel, The Relative Motion Between Ships in Random Head Seas, Technical Note N-1183, Civil Engineering Laboratory, Pt. Hueneme, California, September 1971.

26. Korvin-Kroukovsky, B. V., Theory of Seakeeping, The Society of Naval Architects and Marine Engineers, New York, 1961.

27. Kowalyshyn, R., R. A. Barr, and L. R. Sheldon, Model Tests of a Crane-Barge Combination, Hydronatutics, Incorporated, May 1979.

28. Davis, D. A., H. S. Zwibel, The Motion of Floating Advanced Base Components in Shoal Water--A Comparison Between Theory and Field Test Data, Technical Note N-1371, January 1975.

29. Finlay, Patrick, ed., Jane's Freight Containers, Franklin Watts Incorporated, New York, 1975.

30. Ford, Bacon, and Davis, Inc., Survey of Cranes Suitable for Use in a Temporary Container Discharge Facility, Civil Engineering Laboratory, Port Hueneme, California, November 1976.

31. Groh, G. A., D. L. Groh, NAVSEA COD System Crane Survey, Naval Ammunition Production Engineering Center, Crane, Indiana, July 1976.

32. Manitowoc Engineering, Product Literature, Manitowoc Engineering Company, Manitowoc, Wisconsin.

33. American Hoist and Derrick Company, Product Literature, American Hoist and Derrick Company, St. Paul, Minnesota.

34. Charrett, D. E. A. M. Hyden, "Dyanmic Factors for Offshore Cranes," Offshore Technology Conference, Dallas, Texas, 1976.

35. Johnson, Kenneth V., Theoretical Overload Factor-Effect of Sea State on Marine Cranes, Offshore Technology Conference, Dallas, Texas, 1976.

36. Kogan, Josef, Crane Design Theory and Calculations of Reliability, Halsted Press, Johnson Wiley & Sons, New York, 1976.

37. Traffalis, J. J., Powered Tagline Report, Civil Engineering Laboratory, Port Heuneme, California, June 1977.

38. Bonde, Leslie and David Dillon, A Concept for Improved Crane Performance in Offshore Operations, EG&G Washington Analytical Services Center, Rockville, Maryland, September 1976.

39. Goodyear Aerospace Corporation, Relative Motion Compensation Sensing System Study for Cargo Transfer in Rough Seas, Goodyear Aerospace Corporation, Akron, Ohio, December 1974.

40. Pope, W. S., J. M. Harris, A. M. Plummer, J. E. Drennan, and H. D. Harrison, Relative Motion Sensing Systems, Buttelle Columbus Laboratories, December 1976.

41. Goodyear Aerospace Corporation, Relative Motion Compensation Study for Cargo Transfer in Rough Seas, Goodyear Aerospace Corporation, Akron, Ohio, February 1973.

42. Goodyear Aerospace Corporation, Crane Power Requirements Study for Cargo Transfer in Rough Seas, Goodyear Aerospace Corporation, Akron, Ohio, May 1975.

43. Browne, F., R. Casler, and E. Foster, Preliminary Control System Design for a Conventional Crane Cargo Transfer System Operating in Moderate Seas, Charles Stark Draper Laboratory, Cambridge, Massachusetts, September 1976.

44. Michael, Waltern H., "Sea Spectra Simplified," Marine Technology, January 1968.

45. Bailey, R. F., A presentation on motion compensation systems, Naval Coastal Systems Center, Panama City, Florida, June 1979.

46. Pierson, William J. Jr., Lionel Moskowitz, "A Proposed Spectral Form for Fully Developed Wind Seas Based on the Similarity Theory of S. A. Kitaigorodskii," Journal of Geophysical Research, December 1964.

47. Raichlen, Frederick, Hydrodynamic Analysis of a Tethered Float Breakwater, California Institute of Technology, Pasadena, California, December 1976.

48. Seymour, R. J., M. H. Sessions, and K. M. Wallace, Preliminary Report: Model Evaluation of Tethered Float Breakwaters, Institute of Marine Resources, LaJolla, California, July 1974.

49. Moffatt and Nichol, Ogden Beeman, and International Maritime Associates, Feasibility Study to Evaluate the Commercial Market for a Tethered Float Breakwater System, United States Department of Commerce, Washington, D.C. December 1976.

50. Berkley, J. B. Jr., N. F. Johnson, Engineering Report: San Diego Bay Tethered Float Breakwater, Ocean Technology Department, Naval Undersea Center, San Diego, California, 1976.

51. Timoshenko, S. and D. H. Young, Vibration Problems in Engineering, D. Van Nostrand Company, Princeton, New Jersey, 1956.

52. _____, "Crane Structures Method of Test-SAE J987," 1967 Society of Automotive Engineers Handbook, Society of Automotive Engineers, 1967.

53. Bird, Dexter, J. III, Preliminary Report Joint Army-Navy Rider Block Tagline System Test, EG&G Washington Analytical Services Center, Rockville, Maryland, December 1977.

54. Davis, D. A. and J. J. Traffalis, OSDOC II Crane Platform Productivity as a Function of Sea State, TM 55-77-6, Civil Engineering Laboratory, Port Heuneme, California, July 1977.

55. J. J. Henry Company, Analysis of Containership Offloading at Advanced Operations Area, J. J. Henry Company, Hyattsville, Maryland August 1975.

56. U.S. Department of the Navy, Merchant Ship Expeditionary Logistic Facility, Naval Ship Research and Development Center, Annapolis, Maryland, October 1973.

57. Kirk, Donald E., Optimal Control Theory, Prentice-Hall, Englewood Cliffs, New Jersey, 1970.

58. Johnson, Lee W. and Dean R. Riess, Numerical Analysis, Addison-Wesley Publishing Company, Reading, Massachusetts, 1977.

59. U.S. Department of the Navy, Rider Block Tagline System COTS-TCDF Crane System Sea Tests S1-S3, S4B-S4D, Naval Coastal Systems Center Test Note 4, May 30, 1980.

60. U.S. Department of the Navy, Container Offloading and Transfer System (COTS) Technical Evaluation of Temporary Container Discharge Facility (TCDF), Naval Civil Engineering Laboratory, Port Hueneme, CA, Technical Memorandum 55-81-07, September 1981.

61. U.S. Department of the Navy, CNO Project 299-2-OT-IID-1 Letter Report of Operational Evaluation, Commander, Operational Test and Evaluation Force, April 2, 1981.

62. U.S. Department of the Navy, Request for Provisional Approval For Service Use (PASU) For the Temporary Container Discharge Facility (TCDF), Commander, Naval Facilities Engineering Command, Alexandria, VA, August 14, 1981. (Enclosure (3))

APPENDIX A

CRANES

A.1 Standard Crane Cost

A.2 Motion Compensating Cranes

APPENDIX A.1

STANDARD CRANE COST

The large number of crawler cranes in the larger capacities currently in service in the commercial construction industry make them viable candidates for use in the COTS application. As discussed in Sections 2.2.4 and 3.2.4, the parameters that most strongly influence the cost of a candidate crane are type, lift capacity, and reach requirements. For a crawler crane, the weight of the lifted load, W, herein after referred to as the lift, and the reach, R, can be used to approximate the cost. The load moment will be defined as the lift times the reach, WR. Commercially available crawler cranes have load moments up to about 7×10^6 lb-ft. If crawler cranes were made with lift-reach capabilities above this, they would most likely be more expensive than specially modified cranes like the Manitowoc 4100W Ringer. This is a standard crawler crane, outfitted with an extra long mast and heavy duty boom, mounted in the center of a 36 foot diameter steel ring. Extra counterweights are supported by rollers on this ring behind the crane and the boom base is supported in a similar fashion in front of the crane. The cost of this type of crane, installed, on a ship, is approximately 1.5 million dollars and it has lift-reach capabilities in excess of 16×10^6 lb-ft.

For lift-reach requirements below 7×10^6 lb-ft, where standard crawler cranes provide the more economical alternative, a reasonable cost model is required.

The lift capability of crawler cranes drops off sharply with increasing reach. Because overturning of the crane is one of the primary rating criteria for these types of cranes, the plot of load moment, WR, versus reach, R, should be close to a constant. A plot of load moment versus reach for three different commercially available cranes is shown in Figure A.1. They slope downward because at longer reaches, the weight of the boom and rigging reduce the useful capacity of the crane. They are not straight lines because the tipping moments are not counteracted at the center of rotation but at some point between this and the tips of the crawlers. Straight line approximations are useful, however, for reach requirements of container handling operations (from 50 to 130 feet). It can be observed that the larger capacity cranes have more negative slopes of their load moment curves. If these slopes are plotted against an arbitrary measure of capacity, such as load moment at 70 feet reach, M_{70}, Figure A.2, there appears to be a reasonable linear relationship.

$$S = -.00463\ M_{70},$$

where S is the slope of the load moment curve.

The cost of cranes varies with the options available on a particular model, the economic conditions at the time of purchase and the commission structure of the particular dealer. The prices of several crawler cranes obtained from telephone interviews with dealers is plotted with a ten percent confidence interval against their respective load moments at seventy feet, M_{70} (Figure A.3). A reasonably linear

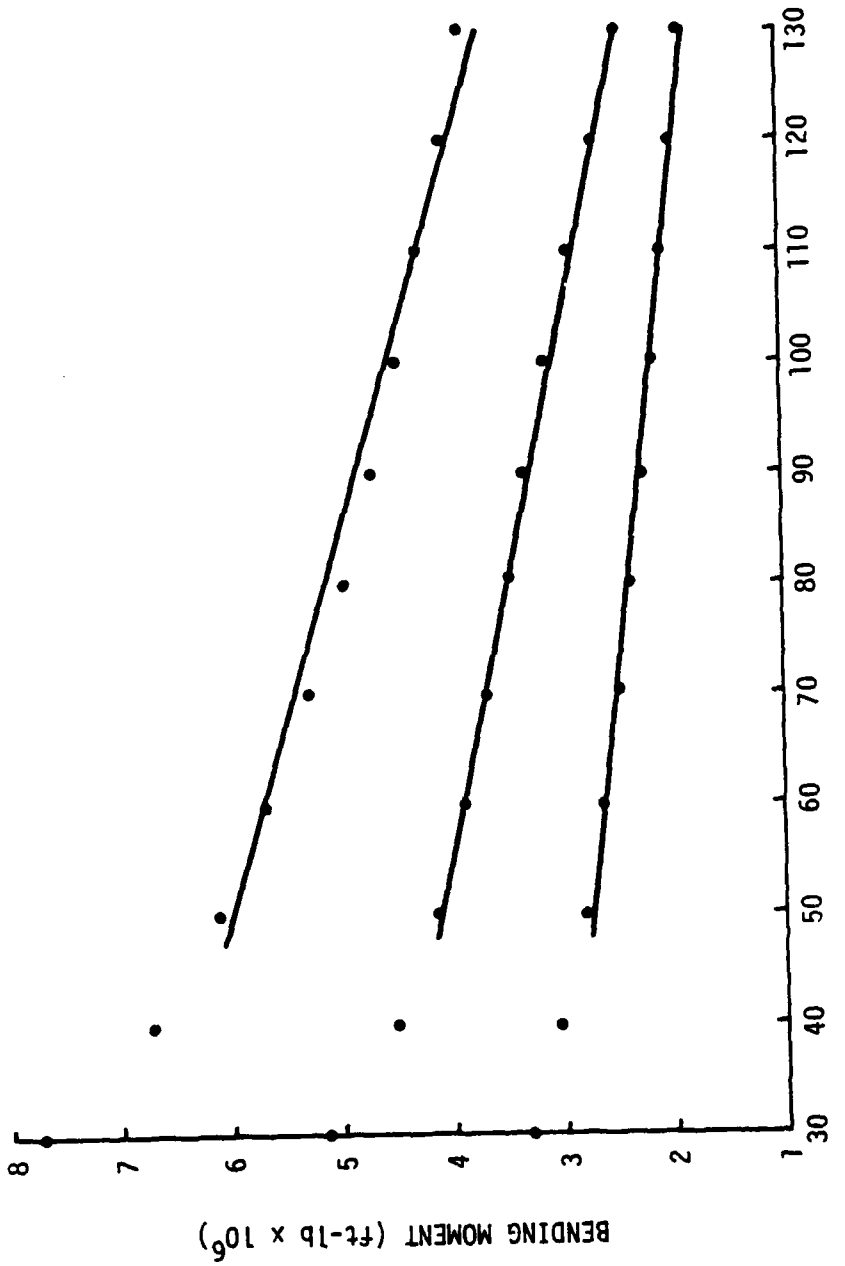

Figure A.1. Plot of Load Moment Versus Reach for Several Commercial Crawler Cranes Showing Linearized Portions

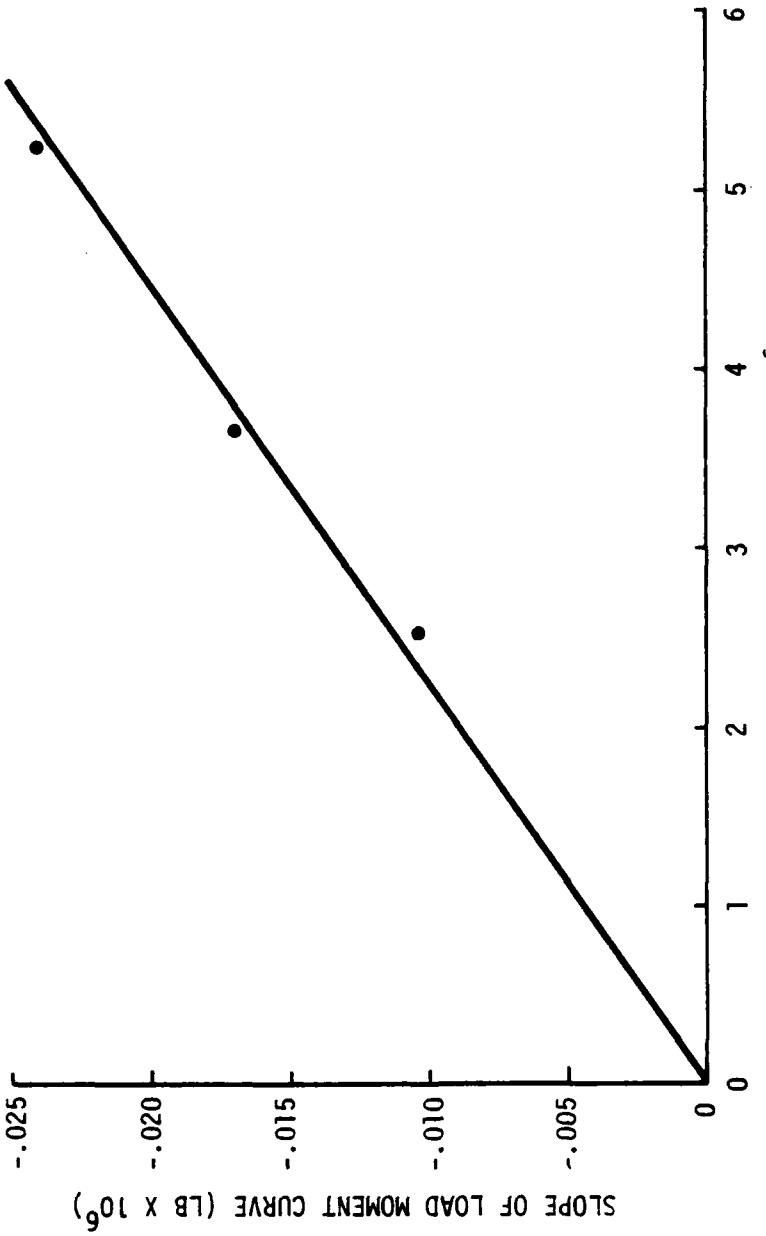

Figure A.2. Linear Trend of Relationship Between Slope Of Load Moment Curve and Load Moment at 70 Feet

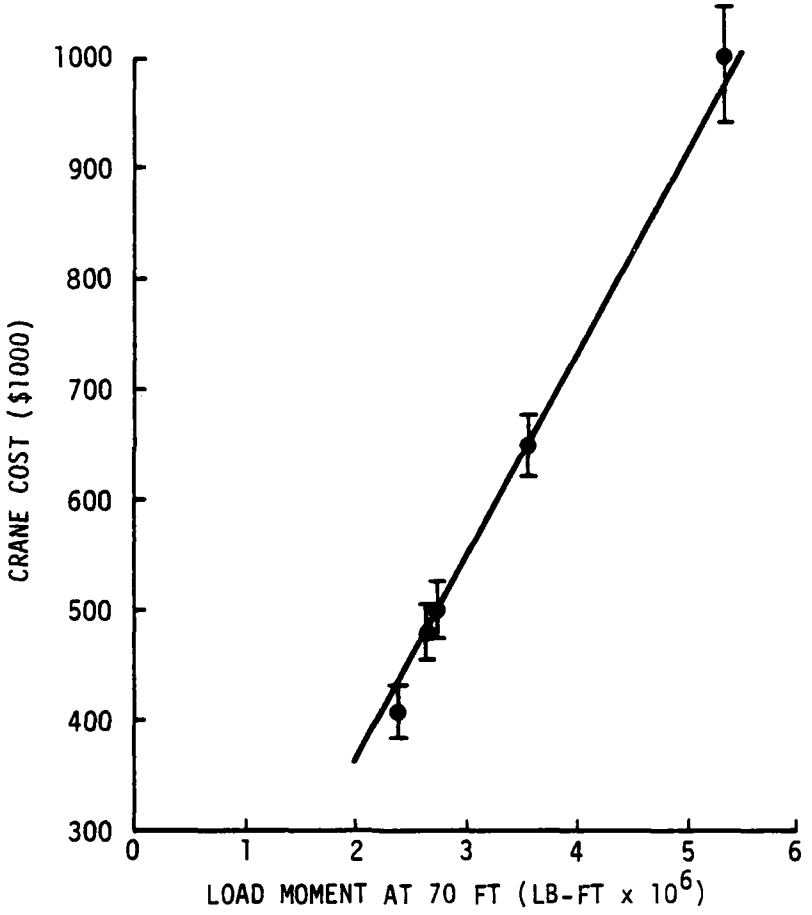

Figure A.3. Plot of Crane Cost Versus Load Moment at 70 Feet.

relationship is found.

$$COST = .18\ M_{70}.$$

The linearized load moment equations can be written,

$$WR = SR + B,$$

where the "y intercept", B, is a function of crane capacity.

It follows that,

$$M_{70} = (-.00463\ M_{70})\ 70 + B.$$

$$B = 1.3741\ M_{70}.$$

Therefore, $$WR = (-.00463\ M_{70})\ R + 1.3241\ M_{70}.$$

This can be solved for M_{70} as a function of lift and reach.

$$M_{70} = \frac{WR}{1.3241 - .00463\ R}.$$

Since, $$Cost = .18\ M_{70},$$

$$Cost = \frac{.18\ WR}{1.3241 - .00463\ R} = \frac{\$1000\ WR}{7356 - 25.76\ R}.$$

Crawler crane cost is now defined as a function of lift and reach. If lift and reach define a cost greater than $1.5 million, it will be assumed that the ringer crane described earlier would be chosen, otherwise a standard crawler crane will be assumed.

APPENDIX A.2

MOTION COMPENSATING CRANES

A number of researchers have addressed the problems associated with the development of cranes that will automatically compensate for relative motion between two vessels when transferring loads at sea.[8, 9,10,11,38,39,40,41,42] The COTS design goal of operational capability in a sea state 3 results in significant maximum relative velocities in the neighborhood of 10 ft/sec (3 m/sec).[39] For container weights up to 35 tons, peak synchronization horsepowers above 1200 HP will be required.

One of the major hurdles to be overcome is the design of a motion compensating crane is the stabilization of the feedback control system. The control loop includes the dynamics of the control strategy, the dynamics of the winch or other motion compensating machinery (i.e., hydraulic cylinders, counterweights, etc), and the lightly damped strucural resonance of the crane itself.

One study [11] has shown that this problem alone is a formidable one because of the proximity between the natural structural resonance of the crane and the frequency range of the lighter motions.

The design requirements of a motion compensating crane include rapid response to control inputs, machinery dynamics that are well above the bandwidth of the expected disturbances and relatively insensitive to load, and a capability of transmitting large amounts of horsepower. These requirements are best met by hydrostatic transmissions.

A hydrostatic transmission consists of a variable displacement pump driven by a prime mover, directly connected by a closed hydraulic loop to a fixed displacement hydraulic motor. The stroke of the pistons in the pump are controlled by the angle of a swashplate, which can be electrically actuated. This lends itself readily to series compensation stabilization techniques. A typical transfer function for such a system is:

$$\frac{\dot{x}(s)}{u(s)} = \frac{K}{(1 + \tau s)\left(1 + \frac{2\zeta s}{\omega_{n_h}} + \frac{s^2}{\omega_{n_h}^2}\right)}$$

where $\dot{x}$ = output speed

u = control input

K = system gain

τ = swashplate motion time constant

ω_{n_h} = hydrualic system resonance

ζ = damping ratio .

The term,

$$(1 + \tau s),$$

represents the lag response of the swashplate position and the term,

$$\left(1 + \frac{2\zeta s}{\omega_{n_h}} + \frac{s^2}{\omega_{n_h}^2}\right),$$

represents the second order effects due to the masses of the moving machinery elements, the damping characteristics of the hydraulic oil and

the compressibility of the oil trapped between the pump and the motor. Typical values for these constants are:

$$\tau \approx .3 \text{ sec}$$

$$\omega_{n_n} \approx 10 \text{ rad/sec}$$

$$\zeta \approx .5$$

The stability problem can be more readily appreciated when a system block diagram is examined.

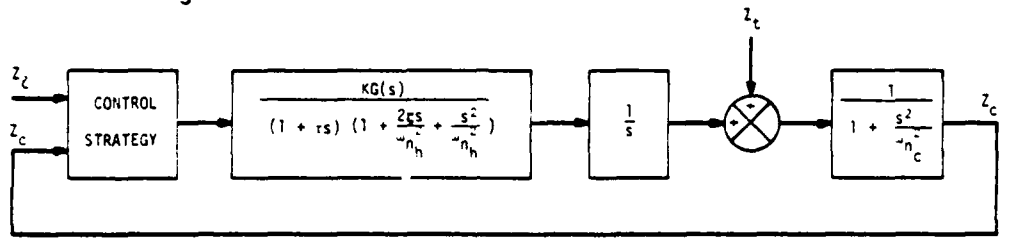

Z_ℓ = vertical displacement of the lighter

Z_c = vertical displacement of the cargo

Z_t = vertical motion of crane boom tip if crane were a rigid body

ω_{n_c} = natural resonance of crane structure

Standard feedback control strategies such as proportional or proportional plus rate for the above system can only be stabilized at very low loop gains or by a complex network of compensation lags and leads resulting in conditional stability. Since the structural resonance varies with both the load and boom position, a computer will probably be required to continually fine tune the system in order to assure global stability.

A great deal more research must be conducted before the total, relative motion compensation/adaptive touchdown strategies, currently under investigation are developed to a point that they can be effectively included and analyzed in this present tradeoff study.

Crane platform roll is the greatest contributer to the total displacement, but, because of its relatively low frequency, is a minor contributer to the total relative velocity. This indicates that a motion compensating crane that works to stabilize the platform may be an approach requiring significantly less horsepower. A simplified motion compensating crane design is proposed here as a technologically feasible alternative. The key elements of the proposed scheme are:

a. Compensate for crane platform motions only,

b. Use velocity feedback instead of position control,

c. Do not close the loop around the structural resonance of the crane,

d. Take maximum advantage of the adaptivity and anticipatory characteristics of the human operator.

A block diagram of this platform stabilized motion compensating crane is shown below.

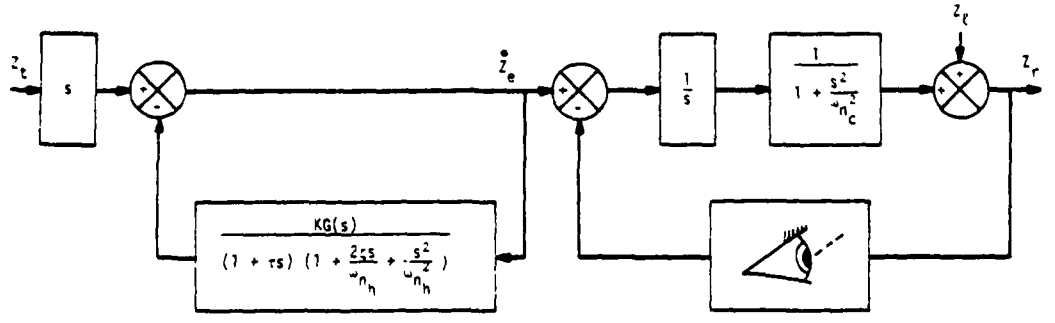

Z_e = motion compensated, effective boom tip motion

Z_r = vertical relative motion between cargo and lighter.

The first control loop reduces the effects of the absolute vertical motions of the boom tip. If the feedback in this loop had sufficient bandwidth and gain, it could hold the cargo still in inertial space as the boom tip rose and fell, leaving the crane operator free to focus his attention on the motion of the lighter only.

The transfer function,

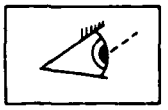

represents all of the characteristics of the human operator from prediction to automatic gain control. The human operator closes the control loop around the structural resonance of the crane. This is normally done in conventional crane operation. If a lighter had a heave RAO of 1, it would have a significant amplitude somewhat less than 3 feet and a predominant period around 6 seconds, in sea state 3. It is not unrealistic to expect the human operator to be able to anticipate peaks in this motion and land the cargo accordingly.

One problem in implementing this strategy is obtaining the Z_t signal free from contamination by the structural resonance of the crane. This can be best accomplished by measuring the motion of the platform, assuming the crane is a rigid body and calculating the theoretical motion of the boom tip. A second problem is stability. Even this relatively simple system, in the absence of compensation, G(s) is unstable

for significant values of loop gain, K. High loop gain is important in this system because the low frequency motion attenuation is approximately equal to $\frac{1}{K+1}$.

A simple analysis using Bode plots, indicates that acceptable stability can be achieved with gains as high as 10 if a lag-lead, lead-lag series compensation, G(s), is chosen.

$$G(s) = \frac{(1 + .3s)\ (1 + .1s)}{(1 + s)\ (1 + .01s)} .$$

The resulting closed loop transfer function between rigid body boom tip motion and the effective boom tip motion is,

$$\frac{Z_e}{Z_t} = \frac{(1 + s)\ (1 + .1s + .01s^2)\ (1 + .01s)}{(1 + s)\ (1 + .1s + .01s^2)\ (1 + .01s) + K\ (1 + .1s)} .$$

The hoisting velocity, is the difference between the boom tip velocity and the effective boom tip velocity.

$$V = \dot{Z}_t - \dot{Z}_e .$$

The transfer function between the boom tip motion and the hoisting velocity, V, is,

$$\frac{V}{Z_t} = \frac{s\ K\ (1 + .1s)}{(1 + s)\ (1 + .1s + .01s^2)\ (1 + .01s) + K\ (1 + .1s)} .$$

The significant hoisting velocity and the weight of the cargo can be used to determine the approximate value of the horsepower required to implement this motion compensating strategy. The transfer functions

given in this Appendix will be used in the COTS model to calculate the motion attenuation characteristics and horsepower requirements for this design of motion compensating cranes.

A plot of commercially available diesel engine costs versus horsepower is given in Figure A.4.. In general, the size and cost of the major power transmission components of the motion compensating system tend to increase with horsepower requirements. The cost of the electronic controls, sensing elements and installation, however, will tend to remain a constant for a range of horsepowers as these items do not change significantly.

Based on the procurement costs of the hydraulic power pack and winch system for the prototype RBTS, a cost of approximately $400.00 per horsepower was chosen for the variable cost of the motion compensating hardware.

Based on current projected motion compensating crane cost estimates,[2] a fixed cost of approximately $250,000.00 appears to be reasonable at this time.

This leads to a motion compensation cost model of the form,

$$\text{COST} = \$250{,}000 + \$400\ \text{HPs},$$

where HPs is the significant horsepower as defined in Section 3.2.4.

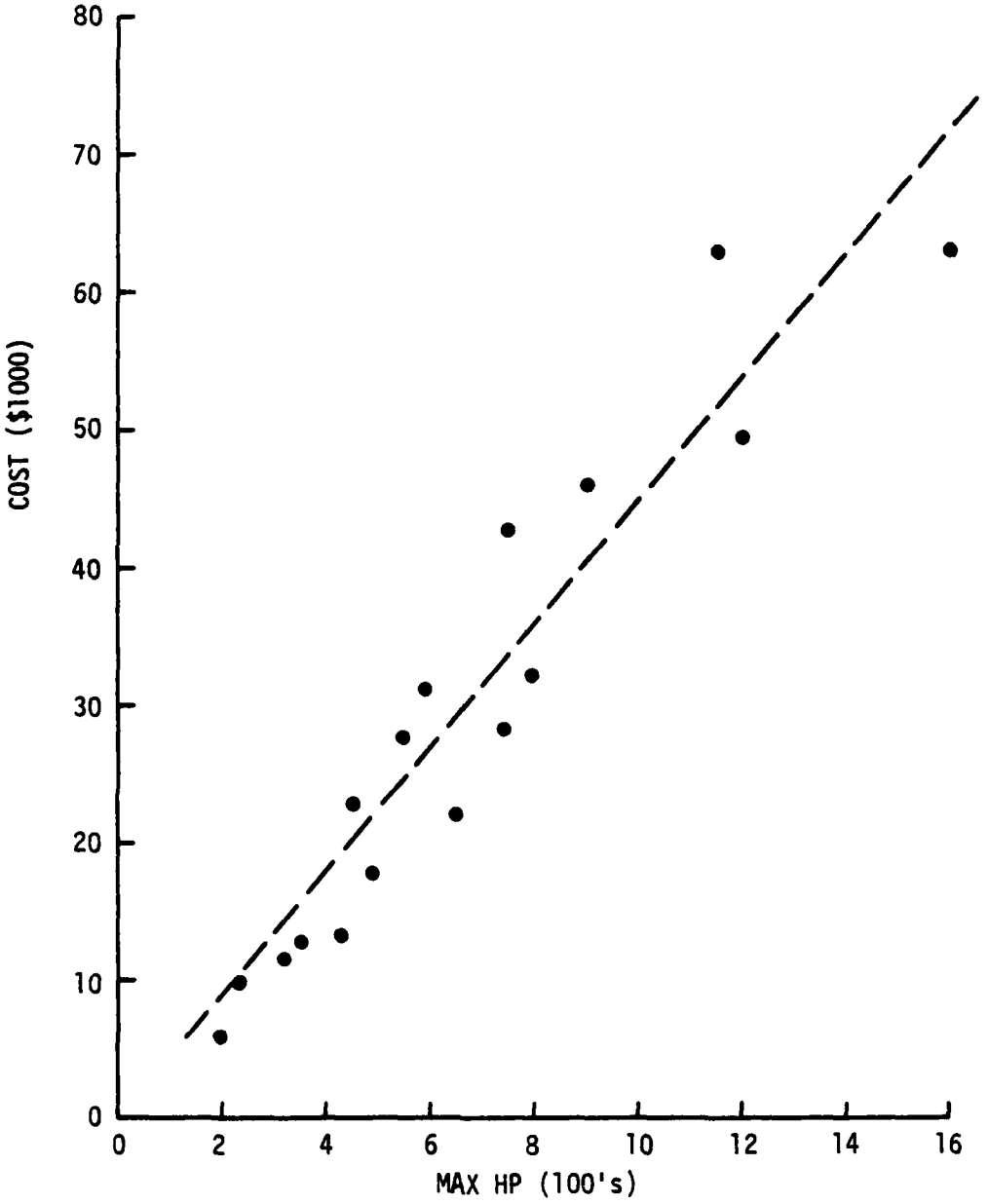

Figure A.4. Diesel Engine Cost Versus Horsepower

APPENDIX B

PRODUCTIVITY

B.1. Minimum Time to Position a Pendulum

B.2. Cycle Time

APPENDIX B.1

MINIMUM TIME TO POSITION A PENDULUM

In the development of the lost time expressions in the productivity model (Section 3.3.2), an analogy is made between the crane operator's task of positioning the cargo and the idealized problem of positioning a simple pendulum. It is assumed that an operator might perform positioning tasks in a suboptimal manner in times that are longer than, but approximately proportional to the minimum time obtained by the optimal solution. This minimization problem forms the basis for the use of $\sqrt{\ell}$ in the lost time expressions of the productivity model.

Given an ideal pendulum at rest, that can be moved in a horizontal line at its fulcrum; find the minimum time and optimal trajectory that will move the pendulus mass to an adjacent point at a state of rest in the minimum time if the maximum velocity of the fulcrum is limited.

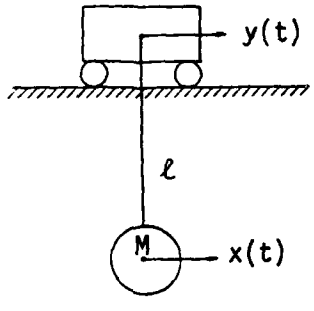

$$x(0) = \dot{x}(0) = \ddot{x}(0) = 0$$

$$y(0) = 0$$

$$x(t_f) = y(t_f) = x_f$$

$$\dot{x}(t_f) = \ddot{x}(t_f) = 0$$

$$|\dot{y}(t)| \leq V$$

x = displacement of pendulus mass

y = displacement of fulcrum

ℓ = pendulum length

M = pendulus mass

g = acceleration of gravity

Equation of Motion

$$M\ddot{x} = \frac{Mg}{\ell}(y-x)$$

$$\ddot{x} + \frac{g}{\ell}x = \frac{g}{\ell}y$$

Let $$\omega^2 = \frac{g}{\ell}$$

$$\ddot{x} + \omega^2 x = \omega^2 y$$

Because the constraint is on $\dot{y}$ rather than y, a more useful form of the equation is:

$$\dddot{x} + \omega^2\dot{x} = \omega^2\dot{y}$$

Find $\dot{y}^*(t)$ that minimizes

$$J = \int_o^{tf} dt$$

State Equations

Let $x = x_1$, $\dot{x} = x_2$, $\ddot{x} = x_3$, $\dot{y} = u$

Therefore $$\dot{x}_1 = x_2$$

$$\dot{x}_2 = x_3$$

$$\dot{x}_3 = -\omega^2 x_2 + \omega^2 u$$

Hamiltonian

$$H = 1 + P_1 x_2 + P_2 x_3 - P_3 \omega^2 x_2 + P_3 \omega^2 u$$

Co-State Equations

$$\dot{P}_1 = 0$$

$$\dot{P}_2 = -P_1 + \omega^2 P_3$$

$$\dot{P}_3 = P_2$$

Solution of the Co-State Equations

$$P_1 = \text{constant} = K_1$$

$$\ddot{P}_3 = -\dot{P}_2 = P_1 - \omega^2 P_3$$

$$\ddot{P}_3 + \omega^2 P_3 = K_1$$

$$\therefore \quad P_3 = K_2 \sin(\omega t + \phi) + \frac{K_1}{\omega^2}$$

where K_1, K_2, and ϕ are constants of integration.

Optimal Control

$u^*(t)$ is the value of $u(t)$ that minimizes the Hamiltonian. Therefore,

$$u^*(t) = -\text{sgn}(P_3)\ V.$$

If $x_f \leq \frac{2\pi V}{\omega}$, the optimal control is of the form

$$\{+V, -V, +V\}\ .$$

Solution of Differential Equation

$$\dddot{x} + \omega^2 \dot{x} = \pm\ \omega^2 V$$

$$x(t) = A \sin(\omega t) + B \cos(\omega t) + C \pm Vt$$

Let t_1, t_2, and t_3 be the length of time that the +V, -V, and +V control is applied respectively. Substituting these times into the above solution to the differential equation, using the initial and final conditions of the original problem, and using final conditions of each phase for the initial conditions of the next, the following set of algebraic equations result.

$$\sin(\omega t_1 + \omega t_2 + \omega t_3) - 2 \sin(\omega t_2 + \omega t_3) + 2 \sin(\omega t_3) = 0$$

$$\cos(\omega t_1 + \omega t_2 + \omega t_3) - 2 \cos(\omega t_2 + \omega t_3) + 2 \cos(\omega t_3) = 1$$

$$t_1 - t_2 + t_3 = \frac{x_f}{V}$$

The following substitution of variables,

$$z_1 = \omega t_1 + \omega t_2 + \omega t_3$$

$$z_2 = \omega t_2 + \omega t_3$$

$$z_3 = \omega t_3$$

results in a set of equations which lend themselves nicely to Newton-Raphson techniques of solution.

$$\sin(z_1) - 2\sin(z_2) + 2\sin(z_3) = 0 .$$

$$\cos(z_1) - 2\cos(z_2) + 2\cos(z_3) = 1 .$$

$$z_1 - 2z_2 + 2z_3 = \frac{\omega x_f}{V}$$

Note that

$$t_f^* = \frac{z_1}{\omega} .$$

Application

The above technique was used to solve for the minimum time to reposition a pendulum a distance of two feet at a maximum speed of two feet/second for a range of pendulum lengths. The basic computer program used to implement this analysis is given in Figure B.1. The results are plotted in Figure B.2.

Values of pendulum length between 14 feet and 130 feet are plotted. It can be seen that,

$$T = 1 + .36\sqrt{\ell} ,$$

provides a reasonable fit to these data. Since the minimum time to reposition a rigid body two feet at a maximum speed of two feet/second is one second, the lost time attributed to the pendulum is

$$T_{lost} = .36\sqrt{\ell} .$$

In general, therefore, for pendulum movements that are small with respect to the pendulum length, it can be shown that the extra time

```
100 DIM P(3,3),X(3,1),F(3,1),T(3,1),W(3,3),F(3,1)
110 PRINT  "  OPTIMAL MINIMUM TIME TO POSITION A PENDULUM OF LENGTH L,"
120 PRINT  "  A DISPLACEMENT OF 2 FT WITH A MAXIMUM ERROR OF 1 FT/SEC"
130 PRINT
140 PRINT
150 X(1,1)=0
160 X(2,1)=4
170 X(3,1)=2
180 PRINT "W","L","T1","T2","T3","TF"
190 PRINT
200 Z=6.3
210 FOR I=1 TO 61
220 Z=Z-.1
230 P(1,1)=SIN(X(1,1))-2*SIN(X(2,1))+2*SIN(X(3,1))
240 P(2,1)=COS(X(1,1))-2*COS(X(2,1))+2*COS(X(3,1))-1
250 P(3,1)=X(1,1)-2*X(2,1)+2*X(3,1)-2
260 P(1,1)=COS(X(1,1))
270 P(1,2)=-2*COS(X(2,1))
280 P(1,3)=2*COS(X(3,1))
290 P(2,1)=-SIN(X(1,1))
300 P(2,2)=2*SIN(X(2,1))
310 P(2,3)=-2*SIN(X(3,1))
320 P(3,1)=1
330 P(3,2)=-2
340 P(3,3)=2
350 MAT Q=INV(P)
360 MAT T=Q*F
370 MAT Y=X-T
380 D=ABS(T(1,1))+ABS(T(2,1))+ABS(T(3,1))
390 MAT X=Y
400 IF D >.0005 THEN 230
410 L1=32.2/Z/7
420 T1=(X(1,1)-X(2,1))/Z
430 T2=X(2,1)-X(3,1))/Z
440 T3=X(3,1)/Z
450 T4=X(1,1)/Z
460 PRINT Z,L1,T1,T2,T3,T4
470 NEXT I
480 END
```

Figure B.1. Basic Program Used to Find the Minimum Time to Reposition a Pendulum a Distance of Two Feet at a Speed of 2 Feet/Second for a Range of Pendulum Lengths

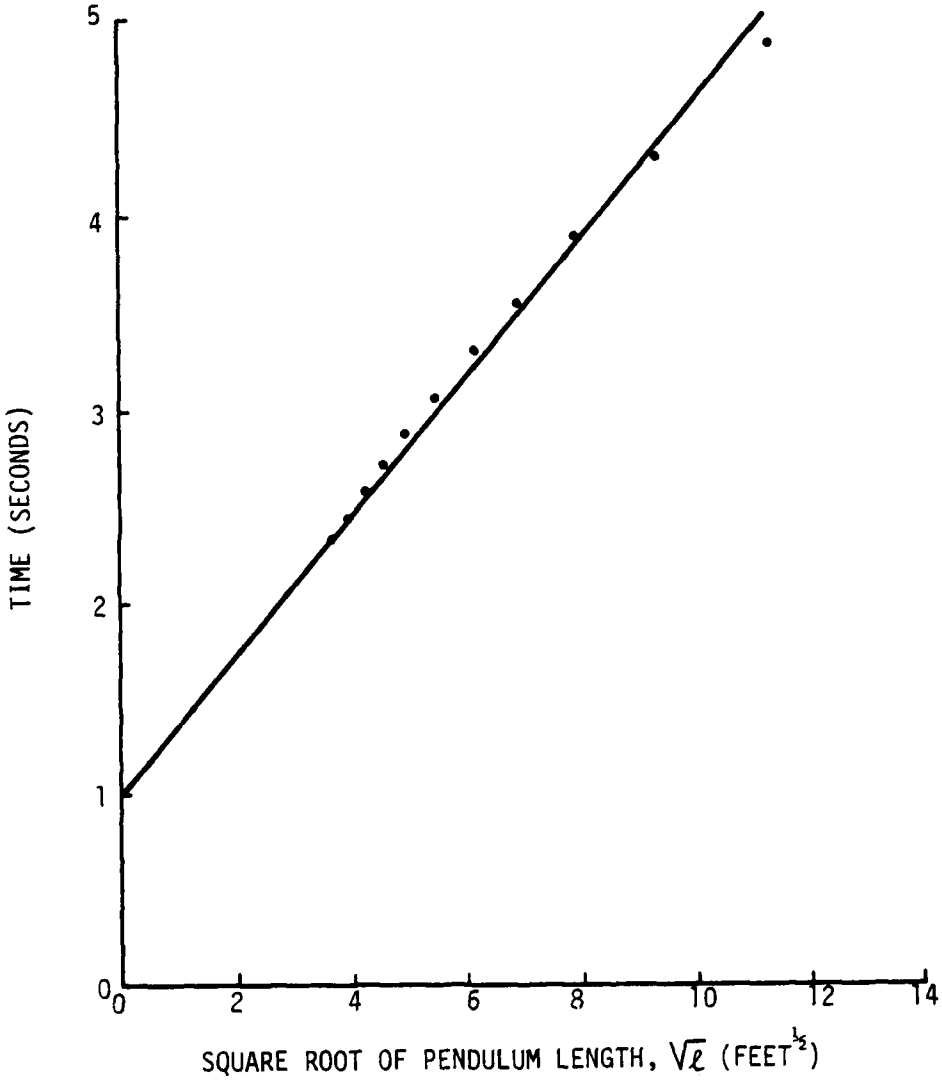

Figure B.2. Results of - Minimum Time to Reposition a Pendulum a Distance of Two Feet at a Speed of 2 Feet/Second for a Range of Pendulum Lengths

(lost time) required to complete a positioning task is approximately proportional to the square root of pendulum length.

APPENDIX B.2

CYCLE TIME

An estimate of the container offload cycle time is required as part of the productivity model developed in Section 3.3.2. A cycle time model of the form,

$$CT = T_m + T_s + T_\ell ,$$

was chosen, where

CT = cycle time,

T_m = minimum time to move a container under ideal conditions,

T_s = average time lost over the ship,

T_ℓ = average time lost over the lighter.

It was hypothesized that the lost times could be approximated by a power function of the two parameters that most directly influenced it - relative vertical displacement between the cargo and the adjacent vessel and pendulum length beneath the crane.

$$T = A\sigma^{\alpha}\ell^{\beta},$$

where

T = lost time

A = constant

σ = standard deviation of vertical displacement

ℓ = pendulum length

α and β = exponents

After the OSDOC II exercises, several observers, knowledgeable in the field of marine operations and Naval material handling, extrapolated the data to generate estimates of offload cycle times for sea states 1 through 4.[55] The minimum time, T_m,[56] was subtracted from these estimates to obtain the total lost time. A review of the data indicated that the time lost over the ship, T_s, was approximately 70% greater than the time lost over the lighter, T_ℓ.[7] This data is presented in Table B.1. along with estimates of the standard deviation of relative vertical displacements over the ship and lighter for the respective sea states. The vertical displacements were obtained from analysis of a typical container offloading configuration by the RELMO computer program.

These cycle times were for standard cranes, and therefore, the pendulum lengths were assumed to be 120 feet over the ship and 150 feet over the lighter. In Appendix B.1, it was shown that the exponent, β, could be taken as $\frac{1}{2}$.

There are now only two unknowns in each equation - A and α. A log-log plot of the data in Table B.1 (Figures B.3 and B.4) allows these remaining two unknowns to be approximated.

The resulting lost time expressions over the ship and the lighter respectively are:

$$T_s = .82\sigma_s \ell_s^{\frac{1}{2}}$$

and

$$T_\ell = .3\sigma_\ell^2 \ell_\ell^{\frac{1}{2}} .$$

TABLE B.1. DATA FOR EVALUATION OF SHIP AND LIGHTER LOST TIME EXPRESSIONS

SEA STATE	WAVE HEIGHT (ft)	CYCLE[1] TIME (min)	LOST[2] TIME (min)	σ_ℓ(4) (ft)	T_ℓ(3) (min)	σ_s(4) (ft)	T_s(3) (min)
1	1.2	5.0	1.0	.28	.37	.06	.63
2	3.0	6.0	2.0	.50	.74	.14	1.26
3	5.0	12.0	8.0	.82	2.96	.58	5.04
4	7.5	29.5	25.5	1.73	9.44	1.74	16.06

(1) Analysis of Containership Offloading at Advanced Operations Area, Prepared by: J.J. Henry Co., Inc., Hyattsville, Md., 15 August 1975, Page G-4.

(2) Based on 4.0 min practical minimum time, Tm, Merchant Ship Expeditionary Logistic Facility, N.S.R.D.C., Bethesda, Md. Report 4154, October 1973, page B-70.

(3) OSDOC II, Test and Evaluation, Vol. 1 Surface Operations, May 1973, page C-21.

(4) Results of application of RELMO Computer program to typical configurations.

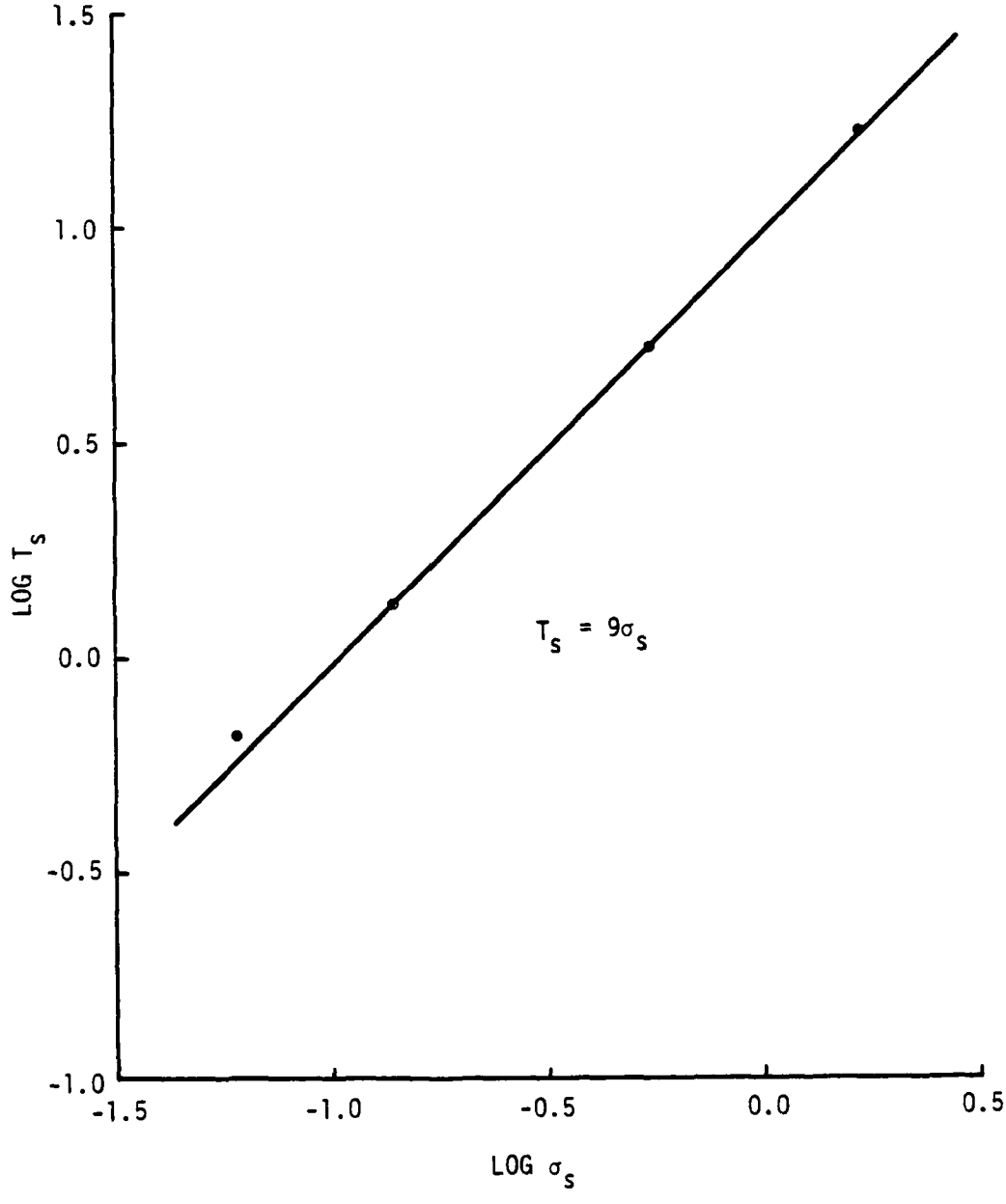

Figure B.3. Log-Log Plot of Time Lost Over Container Ship Versus Relative Vertical Displacement Over Container Ship

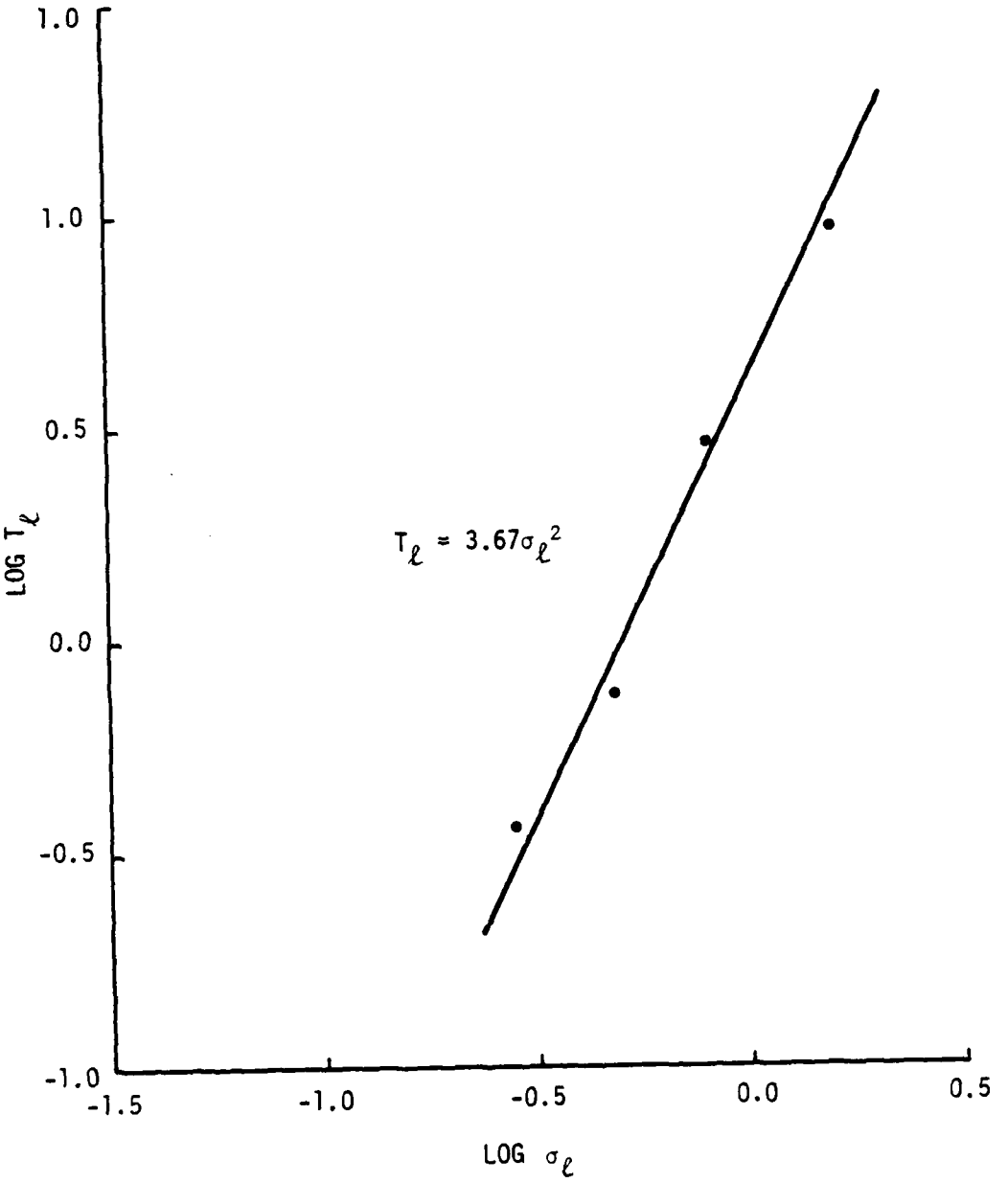

Figure B.4. Log Plot of Time Lost Over Lighter Versus Relative Vertical Displacement Over Lighter

APPENDIX C

TETHERED FLOAT BREAKWATER

APPENDIX C

TETHERED FLOAT BREAKWATER

This Appendix contains correspondence between the author and faculty at Scripps Institution of Oceanography regarding cost and performance of the tethered float breakwater. The data contained herein were used to develop the functional relationships given in Section 3.2.2 and used in the TFB subroutine of the COTS computer model discussed in Section 3.4.

THE
TETHERED FLOAT
BREAKWATER
OCEAN
EXPERIMENT
Mail Code A022
UCSD
La Jolla
Ca. 92093
714·452·2561

A
FEDERAL·STATE
COOPERATIVE
DEMONSTRATION
PROGRAM
UNITED STATES NAVY
Facilities Engineering Command
STATE OF CALIFORNIA
Department of Navigation
& Ocean Development
UNITED STATES ARMY
Corps of Engineers
MARITIME ADMINISTRATION

February 25, 1977

Mr. Dexter Bird
Washington Analytical Services
Center, Inc.
EG&G
2150 Fields Road
Rockville, Maryland 20850

Dear Dexter:

It was a pleasure to meet with you and Les this week and to discuss the Crane/TFB Optimization Study. I have given it some considerable thought since you left and I feel that the approach you are taking is quite sound and should result in a good feel for the optimum system.

When you have decided on your example sea states (or representative Pierson-Moskowitz spectra), send them along and I will respond with families of transfer functions as we discussed and with costing formulas.

Best of luck on your work.

Sincerely,

R. J. Seymour

cc: Mr. Leslie Bonde
Mr. M. E. Essoglou

EG&G

WASHINGTON ANALYTICAL SERVICES CENTER, INC.
HYDROSPACE-CHALLENGER GROUP
2150 Fields Road
Rockville, Maryland 20850
(301) 948-4350

J-5772-15
29 March 1977
JWB:nbt

Dr. R. J. Seymour
The Tethered Float Breakwater Ocean Experiment
Mail Code A033
UCSD
La Jolla, California 92093

Re: Breakwater Characteristics and Costs

Dear Sir:

In accordance with your recommendations, I am beginning the Breakwater/Motion Compensation trade-off analysis based upon sea state 3 only.

It is most convenient for me to use the following formulation of the Pierson-Moskowitz sea spectrum:

$$S(\omega) = \frac{8.4}{\omega^5} \exp\left\{\frac{-33.6}{H_S^2 \omega^4}\right\}$$

where H_S = significant wave height in ft.

ω = angular frequency in rad/sec

and $\int_0^\infty S(\omega)\, d\omega = \sigma^2$

where σ^2 = variance of sea level distribution about the mean in ft^2.

I would like to define sea state 3 as having a significant wave height of 5 ft. This yields a sea spectrum with a variance of approximately 1.5625 ft^2.

As we discussed earlier, I need some information on the Energy Transmission Ratio (ETR) and the related breakwater costs. For example, if the ETR can be described by a function of the form:

$$ETR = ETR\ (\omega_c,\ \alpha),$$

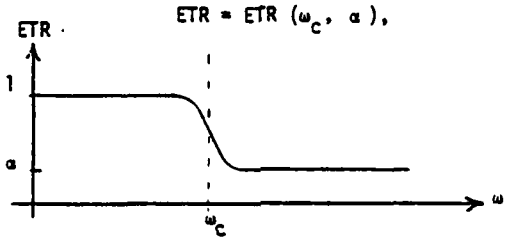

it would be preferable to have a cost function of the form:

$$Cost = C_B\ (\omega_c,\ \alpha).$$

If this formulation introduces unrealistic constraints, please let me know and we will try another approach.

Thank you again for your continuing assistance in this effort.

Cordially,

EG&G WASHINGTON ANALYTICAL
SERVICES CENTER, INC.

J. Dexter Bird, III

J. Dexter Bird, III

Copy to:
Mr. M. E. Essoglou, NAVFAC 031A

THE
TETHERED FLOAT
BREAKWATER
OCEAN
EXPERIMENT
Mail Code A022
UCSD
La Jolla
Ca. 92093
714·452·2561

A
FEDERAL·STATE
COOPERATIVE
DEMONSTRATION
PROGRAM
UNITED STATES NAVY
Facilities Engineering Command
STATE OF CALIFORNIA
Department of Navigation
& Ocean Development
UNITED STATES ARMY
Corps of Engineers
MARITIME ADMINISTRATION

May 20, 1977

Mr. Dexter Bird
Washington Analytical Services
Center, Inc.
EG&G
2150 Fields Road
Rockville, Maryland 20850

Dear Mr. Bird:

The performance and cost of a tethered float breakwater for a given sea state are related to several design parameters. For example, float characteristics, tether length, and the number of rows are all significant. However, all functional relationships which exist between these variables are highly nonlinear, which makes even a simple analysis somewhat complicated.

I have investigated the performance and costs for several different breakwater designs subject to sea state three, with a significant wave height of 5.2 feet, in water of depth equal to 50 feet. For each design I have enclosed a plot of energy transmission ratio (ETR) vs. Frequency (ω), and an estimate of the cost per foot of breakwater provided by Dick Seymour. ETR(ω) is defined as the ratio of transmitted energy at frequency ω to incident energy at frequency ω.

There are several bits of information contained on each plot. They have the following meanings: Teth is the effective tether length in cm, σ is the specific gravity of the float, N is the number of rows of breakwater, and ETR overall is the ratio of total energy transmitted to total energy incident. Please ignore the line labled "measured." Keep in mind that a value of ETR at a certain frequency has meaning if there is a reasonable amount of incident energy at that frequency. For the sea state considered, the range of incident energy is approximately from 0.08 to 0.5 hertz.

For some sea states and breakwater designs, the TFB functions very much like a low pass filter. For such a system, performance can be approximated by a function of the form:

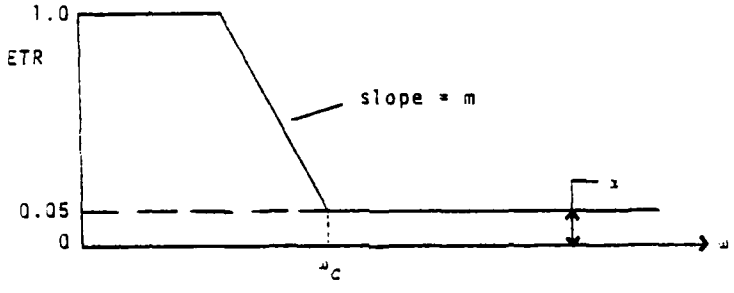

where:

(1) $ETR = 1 + m(\omega-\omega_c-.95/m)H(\omega-\omega_c-.95/m) - m(\omega-\omega_c)H(\omega-\omega_c)$.

$$H(arg) = \begin{cases} 0 \text{ for } arg<0 \\ 1 \text{ for } arg\geq 0 \end{cases}$$

ω_c and m are defined in diagram.

It appears that this approximation is valid for the following designs:

Design #	ω_c(hz)	m(hz^{-1})	Cost ($/Foot)
1	.306	-13	300
3	.275	-13	750
6	.244	-13	1050
10	.213	-14	2250
14	.205	-13	2400
17	.197	-13	3000
21	.190	-13	3000
25	.182	-13	3000
29	.160	-16	5250

I have attempted to express cost as a function of ω_c. I found

$$\text{cost} = 5.4\ \omega_c^{-3.8}$$

$/foot ω in (hz)

for $.306 \geq \omega_c \geq .160$ hz

and for $\alpha = 0.05$

The other designs (with $\alpha > 0.05$) produce curves which do not lend themselves to simple approximations. So I have included copies of all of the designs with their associated costs. You may be able to construct functions for these that will meet your needs.

Let me know if there is any additional information I can provide, (714) 452-2561.

Very truly yours,

Daniel Hanes

Enclosures
cc: Mr. Don B. Jones

UNIVERSITY OF CALIFORNIA, SAN DIEGO

BERKELEY · DAVIS · IRVINE · LOS ANGELES · RIVERSIDE · SAN DIEGO · SAN FRANCISCO SANTA BARBARA · SANTA CRUZ

SCRIPTS INSTITUTION OF OCEANOGRAPHY LA JOLLA, CALIFORNIA 92093

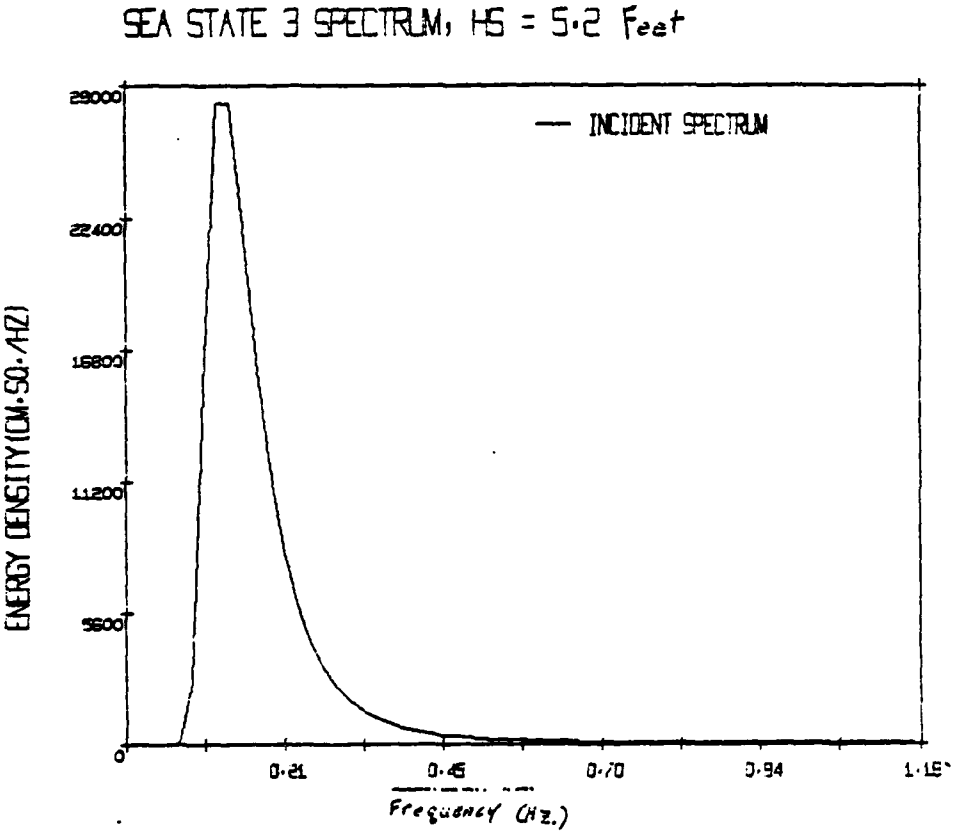

UNIVERSITY OF CALIFORNIA, SAN DIEGO

BERKELEY • DAVIS • IRVINE • LOS ANGELES • RIVERSIDE • SAN DIEGO • SAN FRANCISCO SANTA BARBARA • SANTA CRUZ

SCRIPPS INSTITUTION OF OCEANOGRAPHY LA JOLLA, CALIFORNIA 92093

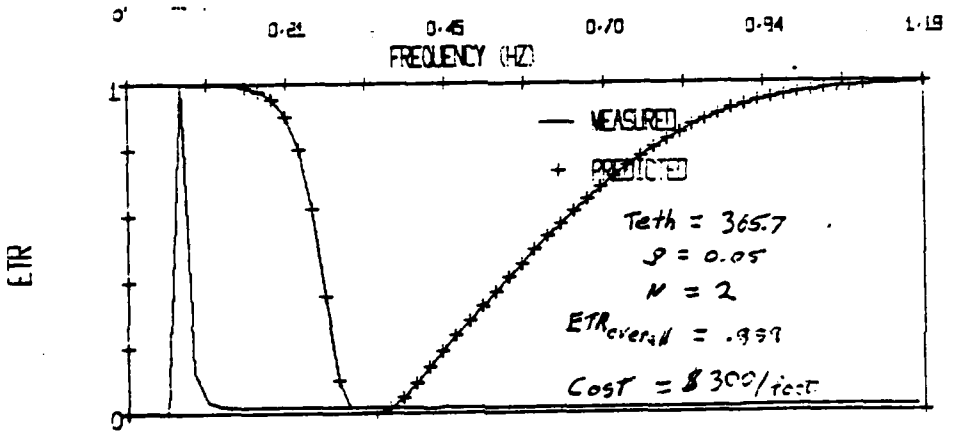

Design 1

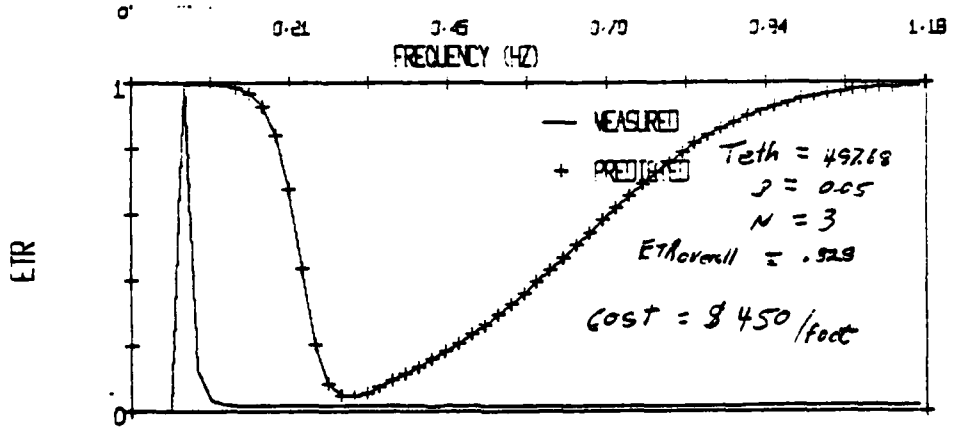

Design 2

UNIVERSITY OF CALIFORNIA, SAN DIEGO

BERKELEY · DAVIS · IRVINE · LOS ANGELES · RIVERSIDE · SAN DIEGO · SAN FRANCISCO SANTA BARBARA · SANTA CRUZ

SCRIPPS INSTITUTION OF OCEANOGRAPHY LA JOLLA, CALIFORNIA 92093

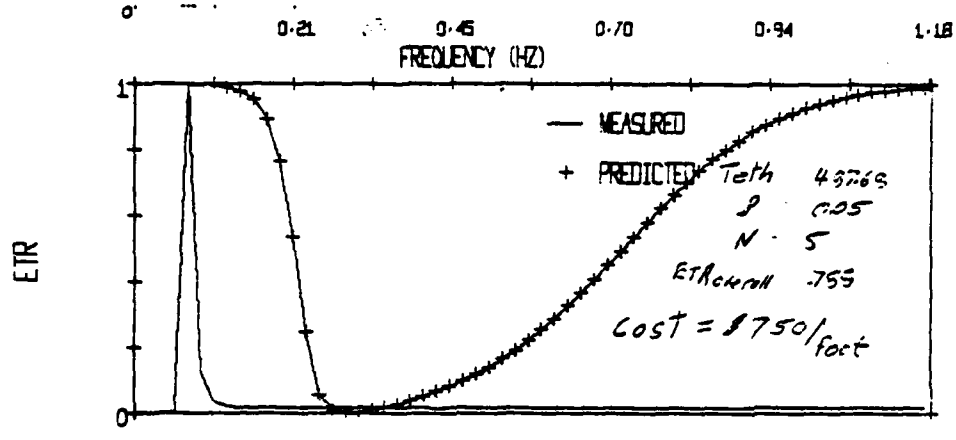

Design 3

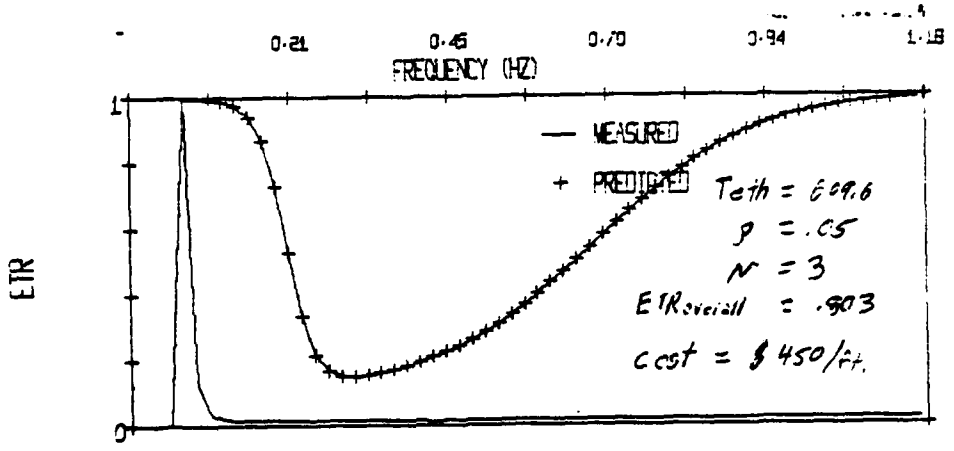

Design 4

UNIVERSITY OF CALIFORNIA, SAN DIEGO

BERKELEY · DAVIS · IRVINE · LOS ANGELES · RIVERSIDE · SAN DIEGO · SAN FRANCISCO SANTA BARBARA · SANTA CRUZ

SCRIPPS INSTITUTION OF OCEANOGRAPHY LA JOLLA, CALIFORNIA 92093

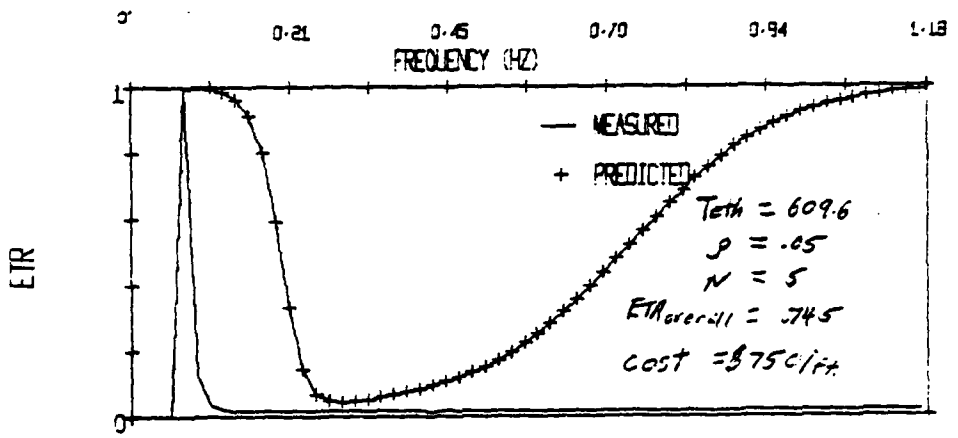

Design 5

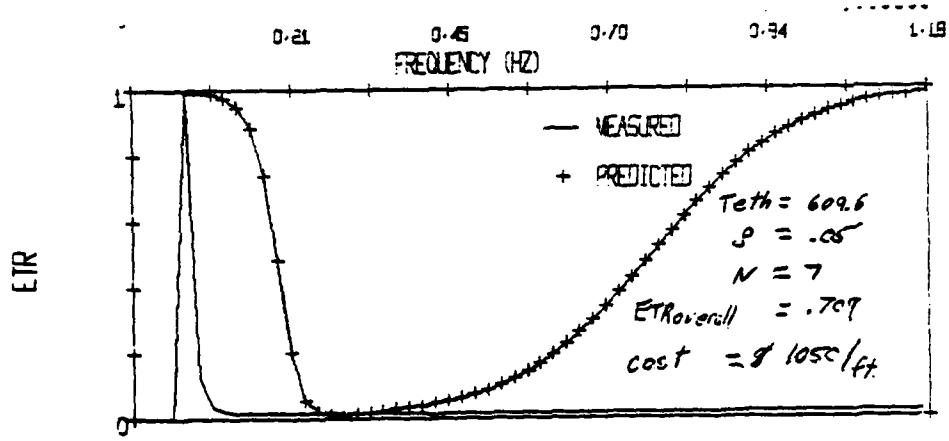

Design 6

UNIVERSITY OF CALIFORNIA, SAN DIEGO

BERKELEY • DAVIS • IRVINE • LOS ANGELES • RIVERSIDE • SAN DIEGO • SAN FRANCISCO SANTA BARBARA • SANTA CRUZ

SCRIPPS INSTITUTION OF OCEANOGRAPHY LA JOLLA, CALIFORNIA 92093

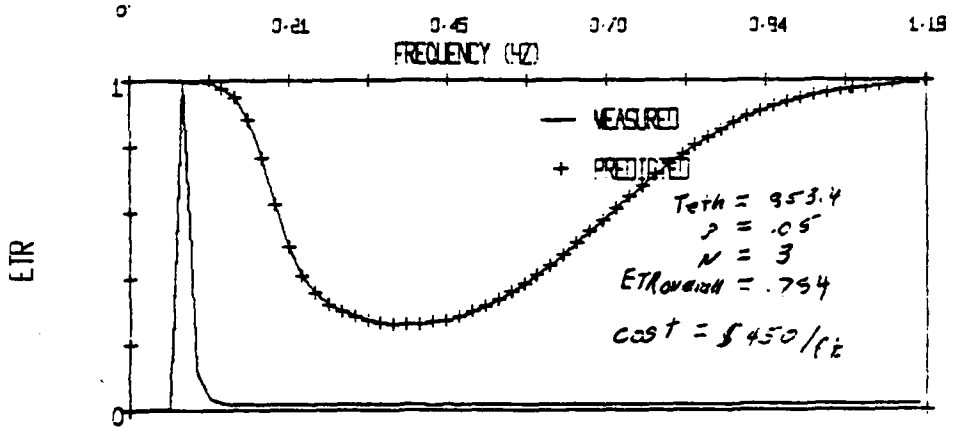

Design 7

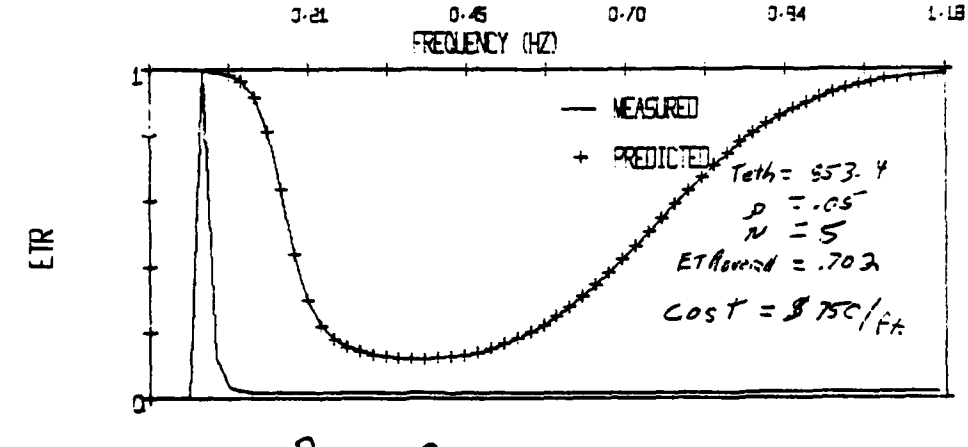

Design 8

UNIVERSITY OF CALIFORNIA, SAN DIEGO

BERKELEY · DAVIS · IRVINE · LOS ANGELES · RIVERSIDE · SAN DIEGO · SAN FRANCISCO SANTA BARBARA · SANTA CRUZ

SCRIPPS INSTITUTION OF OCEANOGRAPHY LA JOLLA, CALIFORNIA 92093

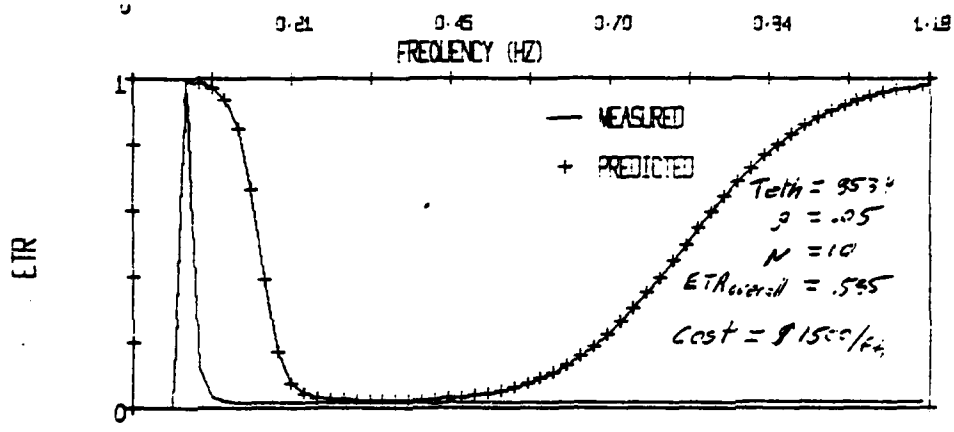

Design 9

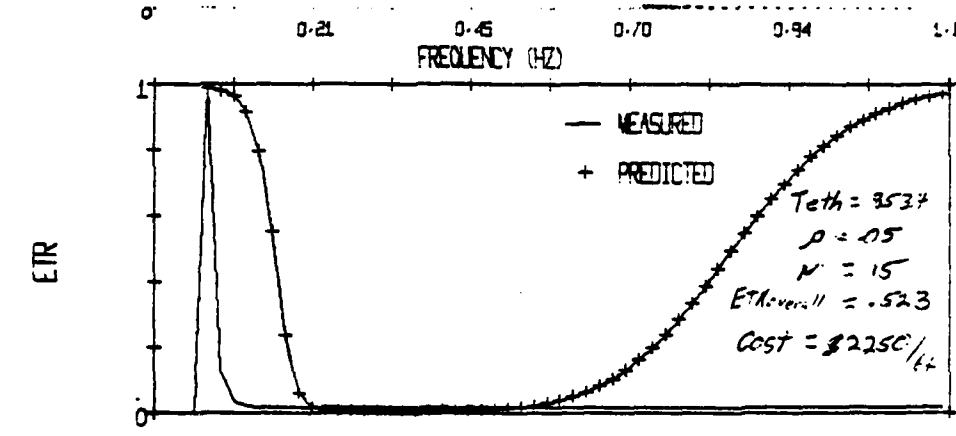

Design 10

UNIVERSITY OF CALIFORNIA, SAN DIEGO

BERKELEY · DAVIS · IRVINE · LOS ANGELES · RIVERSIDE · SAN DIEGO · SAN FRANCISCO

SANTA BARBARA · SANTA CRUZ

SCRIPPS INSTITUTION OF OCEANOGRAPHY

LA JOLLA, CALIFORNIA 92093

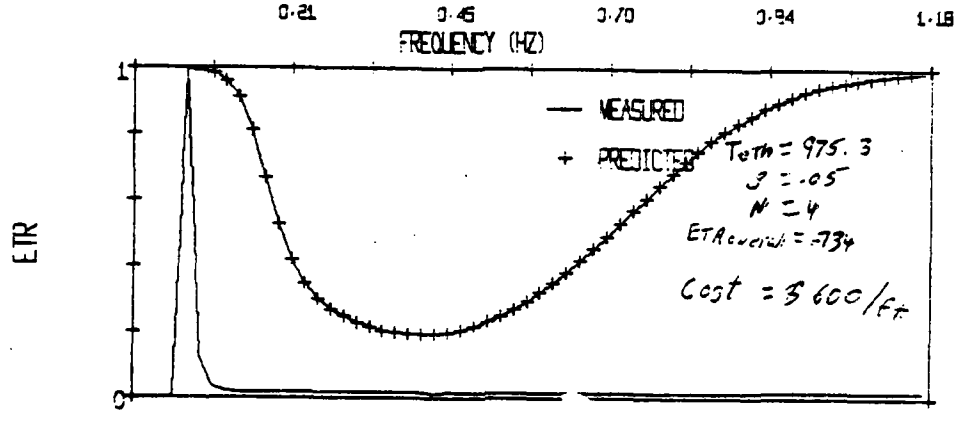

Design 11

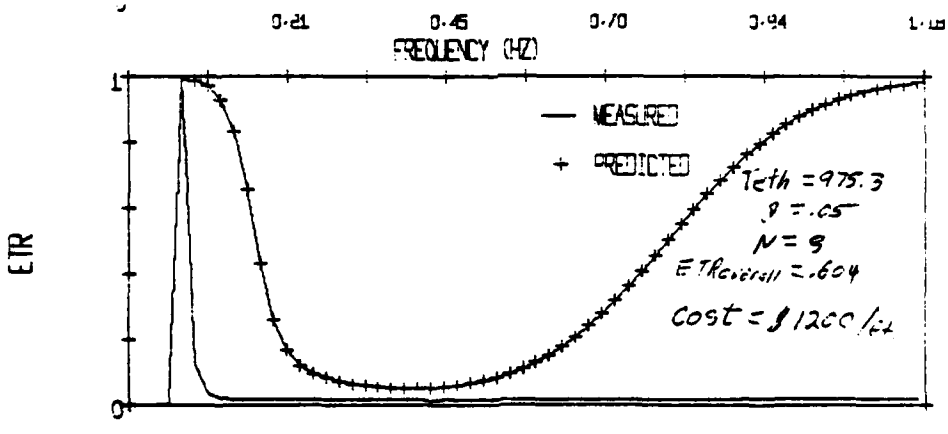

Design 12

UNIVERSITY OF CALIFORNIA, SAN DIEGO

BERKELEY · DAVIS · IRVINE · LOS ANGELES · RIVERSIDE · SAN DIEGO · SAN FRANCISCO SANTA BARBARA · SANTA CRUZ

SCRIPPS INSTITUTION OF OCEANOGRAPHY LA JOLLA, CALIFORNIA 92093

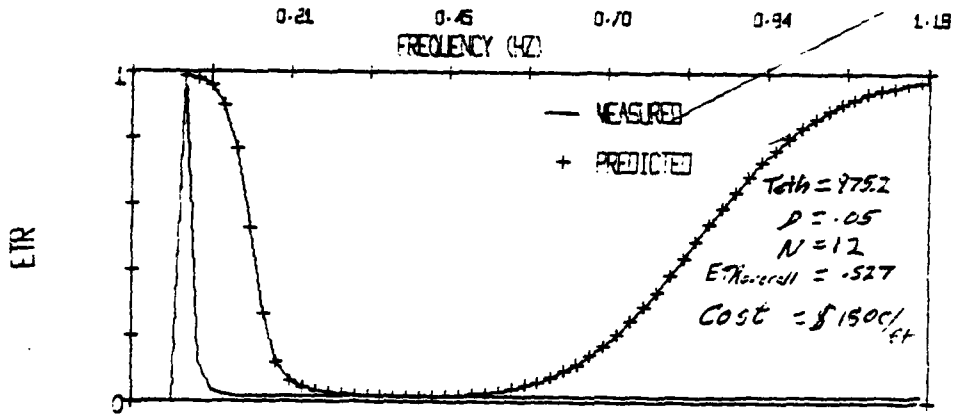

Design 13

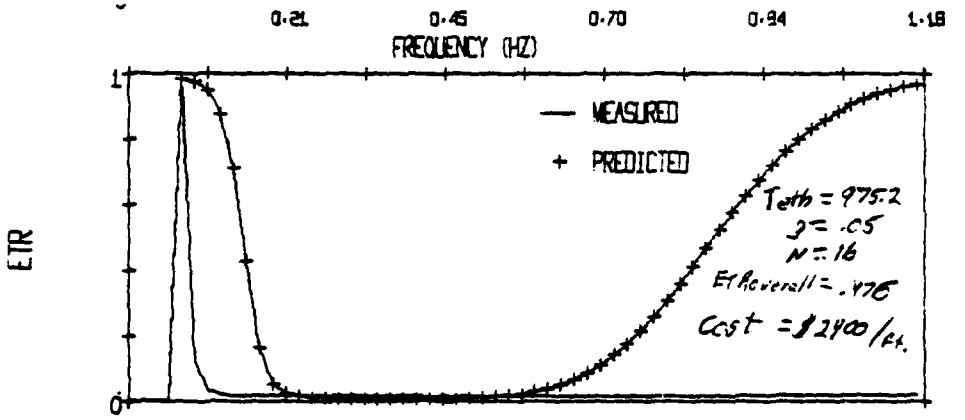

Design 14

UNIVERSITY OF CALIFORNIA, SAN DIEGO

BERKELEY · DAVIS · IRVINE · LOS ANGELES · RIVERSIDE · SAN DIEGO · SAN FRANCISCO

SANTA BARBARA · SANTA CRUZ

SCRIPPS INSTITUTION OF OCEANOGRAPHY

LA JOLLA, CALIFORNIA 92093

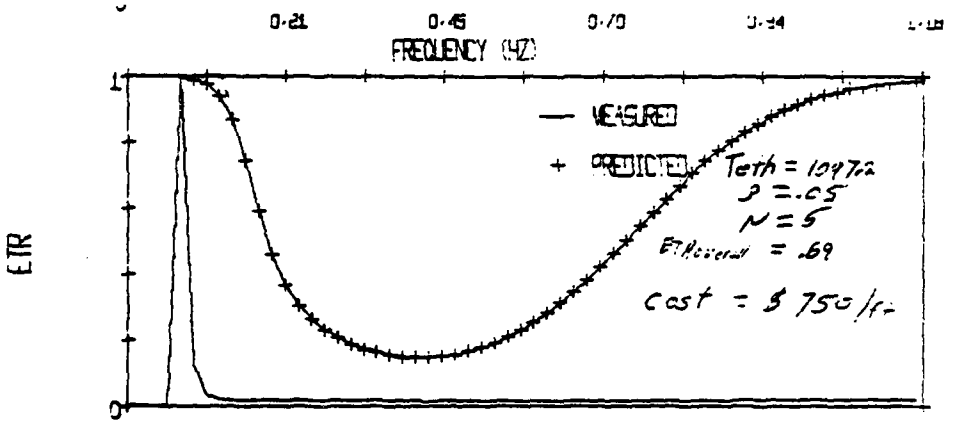

Design 15

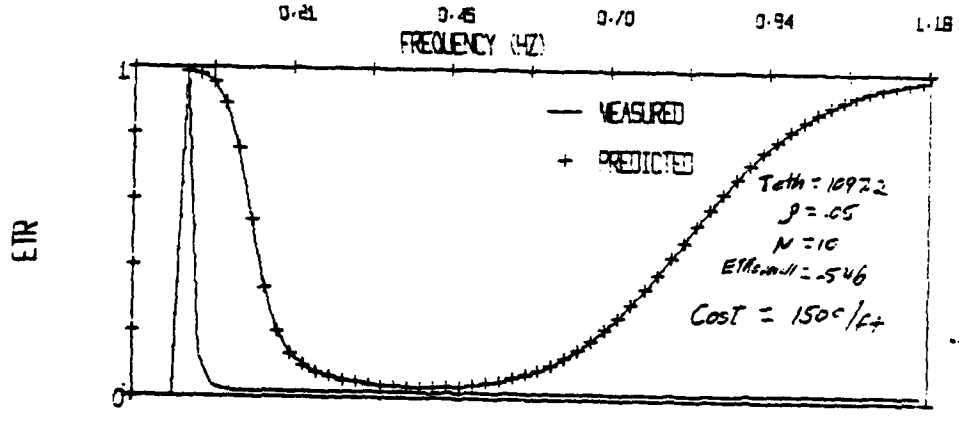

Design 16

UNIVERSITY OF CALIFORNIA, SAN DIEGO

BERKELEY • DAVIS • IRVINE • LOS ANGELES • RIVERSIDE • SAN DIEGO • SAN FRANCISCO SANTA BARBARA • SANTA CRUZ

SCRIPPS INSTITUTION OF OCEANOGRAPHY LA JOLLA, CALIFORNIA 92093

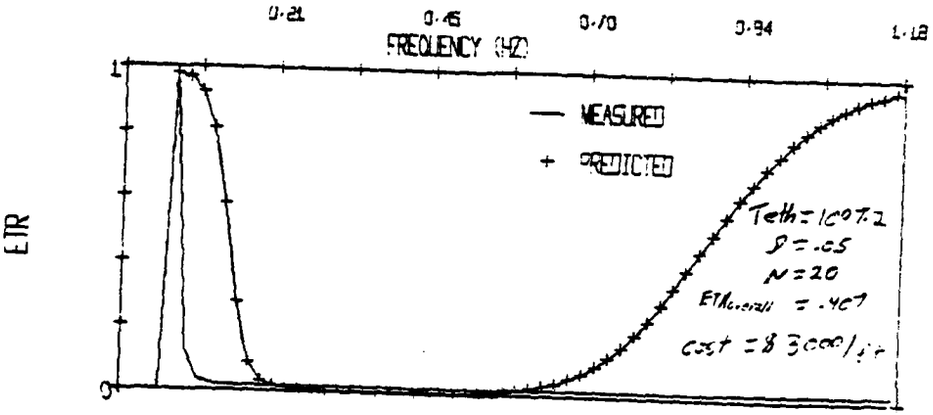

Design 17

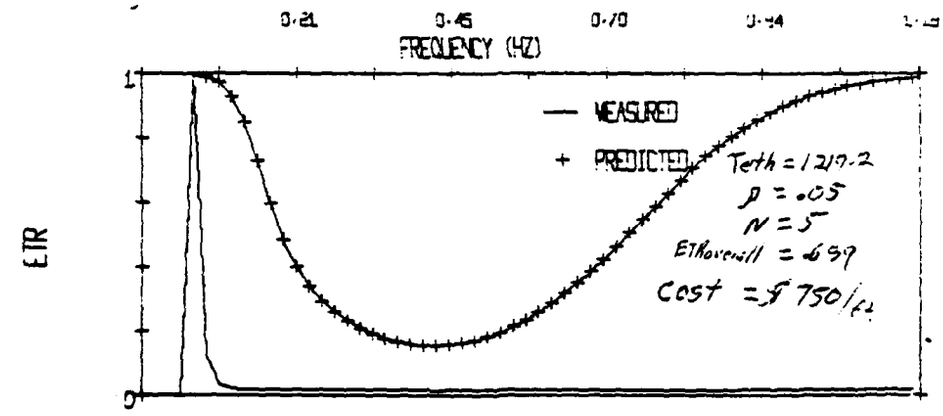

Design 19

UNIVERSITY OF CALIFORNIA, SAN DIEGO

BERKELEY • DAVIS • IRVINE • LOS ANGELES • RIVERSIDE • SAN DIEGO • SAN FRANCISCO SANTA BARBARA • SANTA CRUZ

SCRIPPS INSTITUTION OF OCEANOGRAPHY LA JOLLA, CALIFORNIA 92093

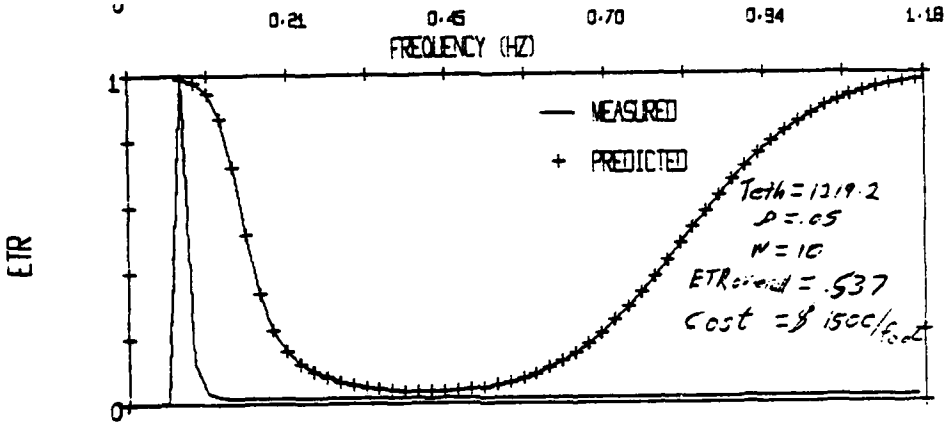

Design 19

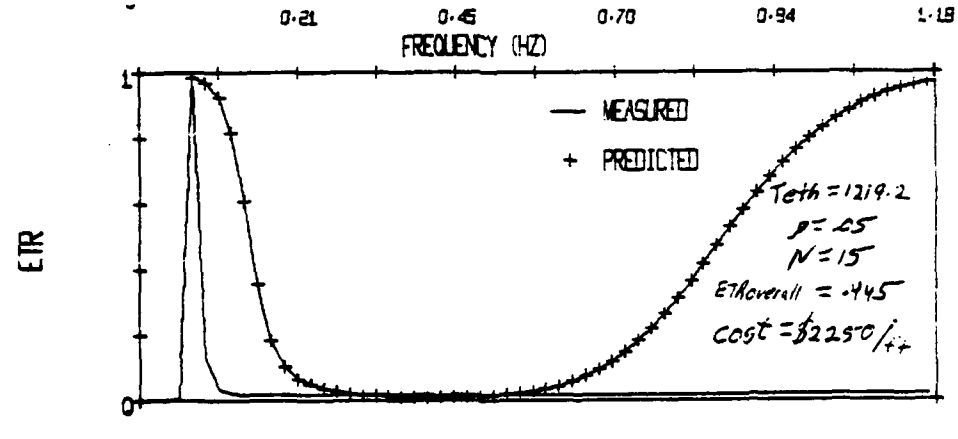

Design 20

UNIVERSITY OF CALIFORNIA, SAN DIEGO

BERKELEY • DAVIS • IRVINE • LOS ANGELES • RIVERSIDE • SAN DIEGO • SAN FRANCISCO SANTA BARBARA • SANTA CRUZ

SCRIPPS INSTITUTION OF OCEANOGRAPHY LA JOLLA, CALIFORNIA 92093

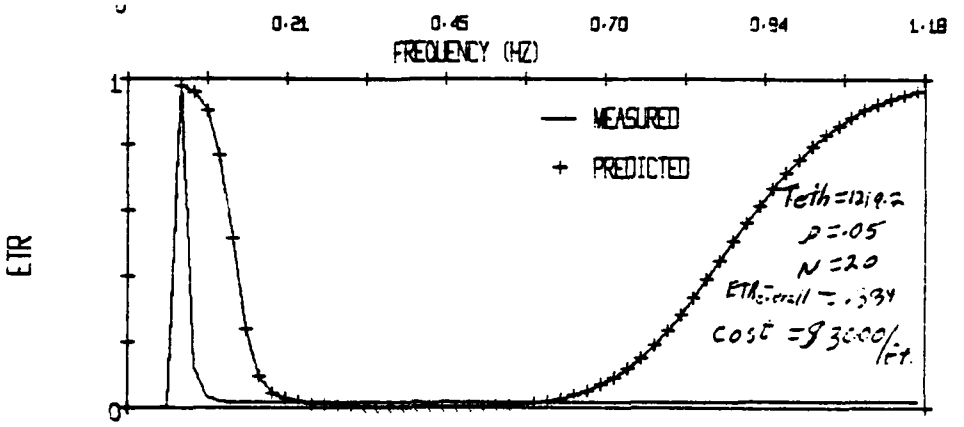

Design 21

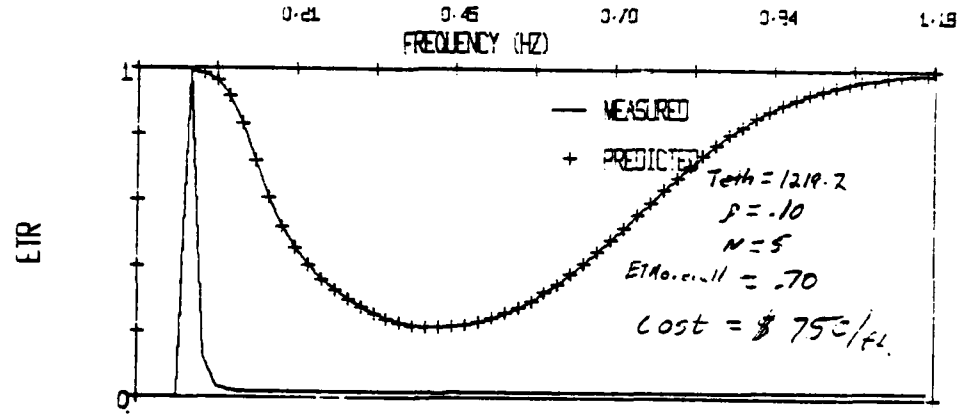

Design 22

UNIVERSITY OF CALIFORNIA, SAN DIEGO

BERKELEY · DAVIS · IRVINE · LOS ANGELES · RIVERSIDE · SAN DIEGO · SAN FRANCISCO SANTA BARBARA · SANTA CRUZ

SCRIPPS INSTITUTION OF OCEANOGRAPHY LA JOLLA, CALIFORNIA 92093

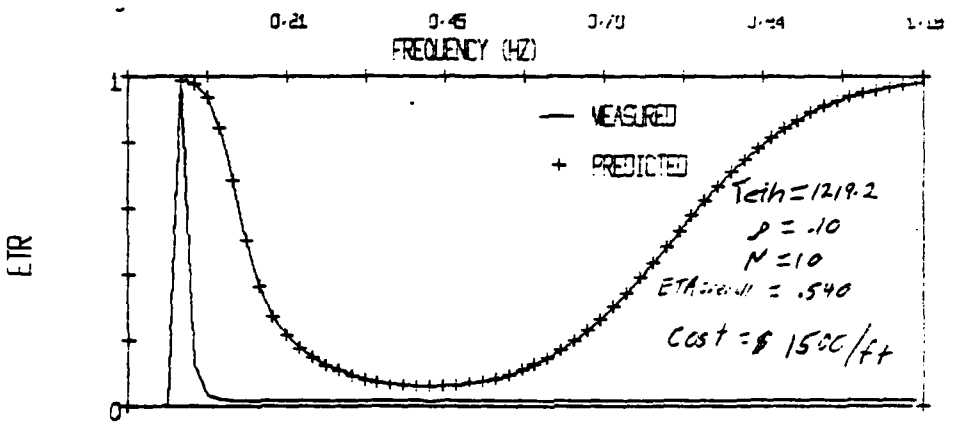

Design 23

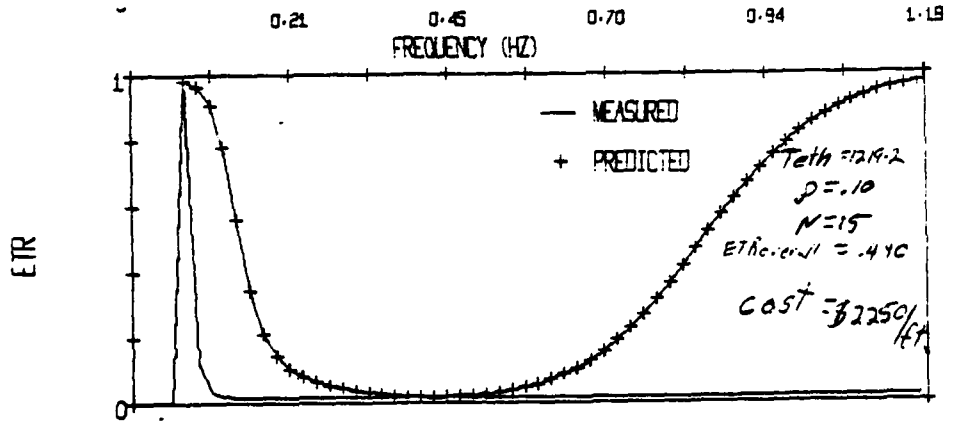

Design 24

UNIVERSITY OF CALIFORNIA, SAN DIEGO

BERKELEY • DAVIS • IRVINE • LOS ANGELES • RIVERSIDE • SAN DIEGO • SAN FRANCISCO — SANTA BARBARA • SANTA CRUZ

SCRIPPS INSTITUTION OF OCEANOGRAPHY — LA JOLLA, CALIFORNIA 92093

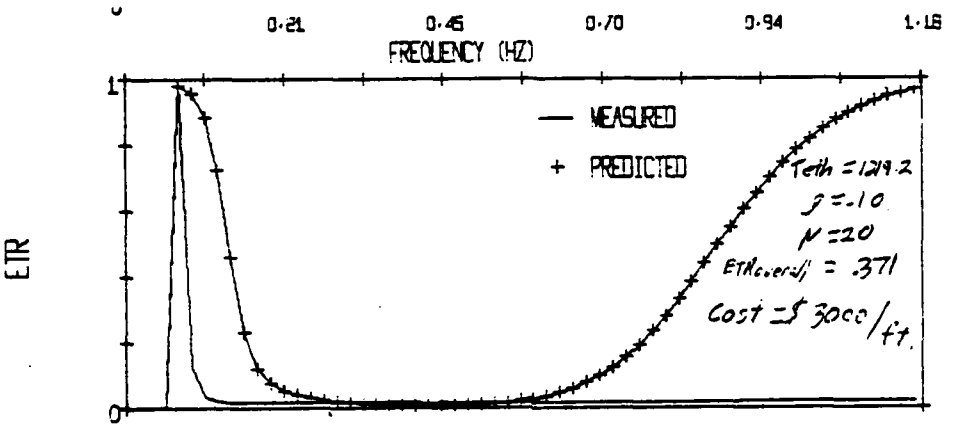

Design 25

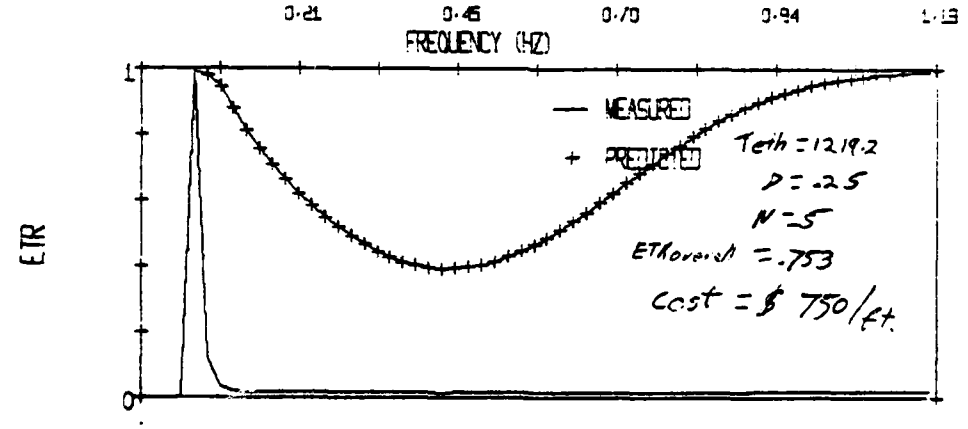

Design 26

UNIVERSITY OF CALIFORNIA, SAN DIEGO

BERKELEY • DAVIS • IRVINE • LOS ANGELES • RIVERSIDE • SAN DIEGO • SAN FRANCISCO SANTA BARBARA • SANTA CRUZ

SCRIPPS INSTITUTION OF OCEANOGRAPHY LA JOLLA, CALIFORNIA 92093

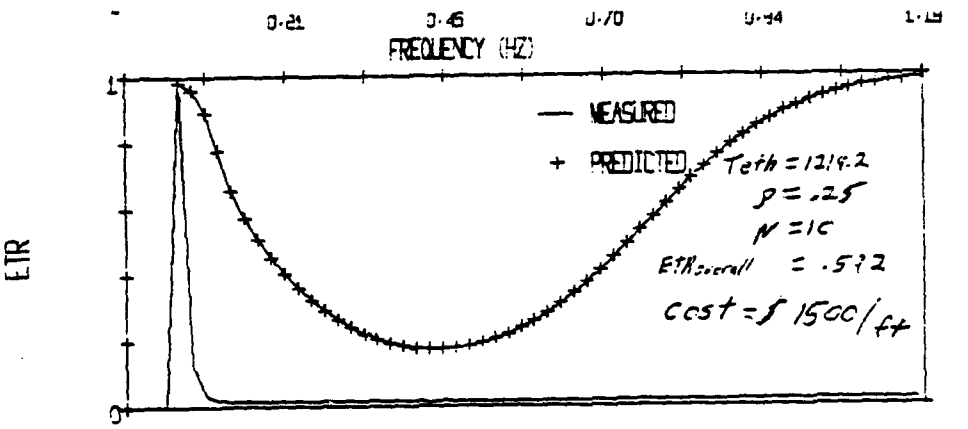

Design 27

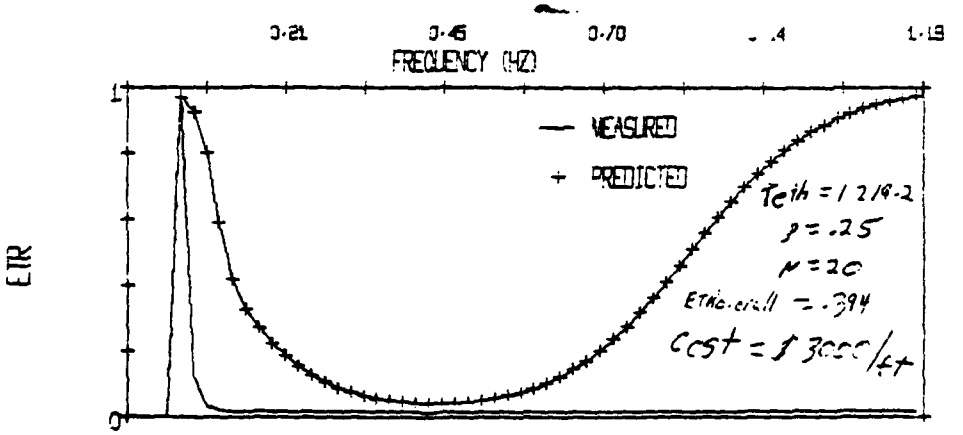

Design 28

UNIVERSITY OF CALIFORNIA, SAN DIEGO

BERKELEY • DAVIS • IRVINE • LOS ANGELES • RIVERSIDE • SAN DIEGO • SAN FRANCISCO SANTA BARBARA • SANTA CRUZ

SCRIPPS INSTITUTION OF OCEANOGRAPHY LA JOLLA, CALIFORNIA 92093

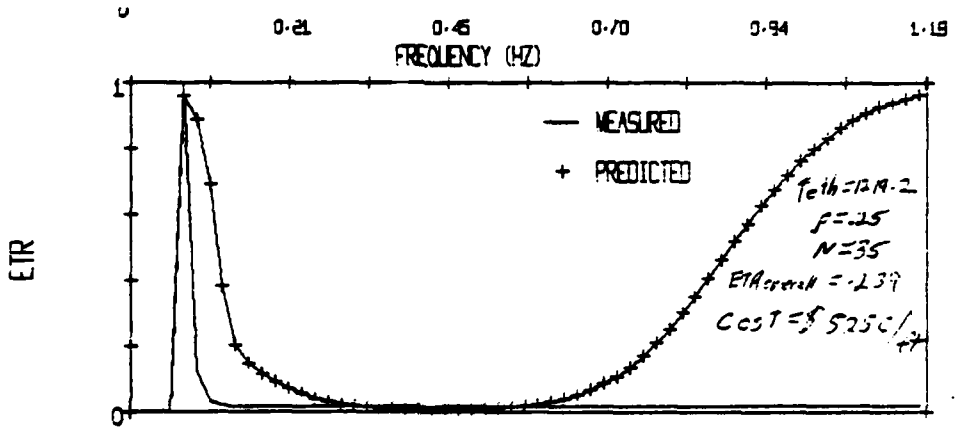

Design 29

APPENDIX D

EVALUATION OF RAOS

APPENDIX D

EVALUATION OF RAOS

Program Description

This appendix describes the input data required by the RAOS program given in Appendix E in order to generate the response amplitude operators of the floating vessels. The RAOS program is a modified version of RELMO, a computer program developed by the Navy to solve for relative motion between ships in random seas. A complete description of the original RELMO program can be found in Technical Note N-1371, The Motion of Floating Advanced Base Components in Shoal Water -- A Comparison Between Theory and Field Test Data by D.A. Davis and H.S. Zwibel of the Civil Engineering Laboratory, Port Hueneme, California.

The modified program, RAOS, makes use of that portion of RELMO necessary to evaluate the vessels response amplitude operators and writes them on disc files to be recalled later by the COTS program (also listed in Appendix E). The RAOS program consists of a MAIN program that formats the data output and four subroutines as follows:

RAO: Reads input data and calls other subroutines.

FREQ: Generates angular frequencies and wave numbers to be used in computing frequency-dependent terms in equations of motion. Computes associated depth-dependent wave lengths.

ADMAB: Computes added-mass and damping coefficients by Grim's method.

COEF: Computes force coefficients appearing in equation of motion. Dynamic force coefficients are functions of added-mass and damping coefficients computed in subroutine ADMAB. Solves for the frequency-dependent ship coordinates (heave, pitch, surge, yaw, roll, and sway). These are the response amplitude operators for each ship as all exciting waves are assumed to have unit amplitudes. The process involves inversion of the force and moment coefficient matrix and multiplication of inverted matrix with the wave force and moment matrix.

Program Inputs

Data are entered on two types of input cards: INPUT and SHIP.

INPUT: Data needed to define the period, length, and direction of the unit amplitude, incident regular waves is placed on this card. Card variables are defined as follows:

DEPTH: The mean water depth, in feet, at a station beneath the center of gravity of the ship.

NFREQ: The number of angular frequencies to be used in computing the ship response amplitude operators. This variable and the one designating the number of ship transverse sections (NSEC) have a predominant effect on the amount of computational time required. Computional time will increase roughly as the product of NFREQ and NSEC. NFREQ, however, should be

at least 50 to insure sufficient accuracy in most ship motion problems.

FREMIN: The minimum angular wave frequency (rad/sec) desired.

FREMAX: The maximum angular wave frequency (rad/sec) desired. Intermediate wave frequencies, totalling NFREQ-2 in number, will be spaced equally between the extremes defined by FREMIN and FREMAX.

BETA: The angle of approach (degrees) of the incident unit amplitude waves. BETA equal to zero designates waves approaching sternon (see figure below).

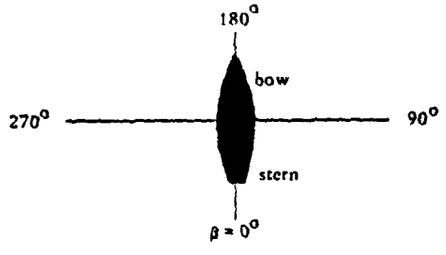

ISTOP: This is a control variable. For any ISTOP value (integer) other than zero, the computer reads a new set of data cards (beginning with INPUT) and repeats an entire set of computations.

SHIP: Data concerning ship characteristics are inputed on this card. All weights are in pounds, and distances are in feet.

ISHIP: Used by RELMO to designate ship 1 or 2. In the modified version, RAOS, it is always assigned a value of 1.

NSEC: The number of transverse ship sections. There can be as few as one, but the usual number is 10 or 20.

W: The weight (displacement) of the ship (lbs).

BG: The vertical separation between the ship's center of gravity (CG) and center of buoyancy (CB). BG is positive if CG lies above CB.

RG: The radius of gyration of the ship in pitch. If unknown, it should be set equal to 1/4 of the ship length.

XCGFS: The logitudinal distance of the ship CG from the aft perpendicular.

B: The ship beam at the waterline for each transverse section.

SECOE: The ship section coefficient at each transverse section. Note: Bulbous sections will have coefficients greater than unity. Grim's method for computing the section added-mass and damping will provide rather poor estimates if SECOE greatly exceeds one.

DRAFT: The vertical distance from the waterline to the keel at each transverse section.

SECL: The thickness of each transverse section. Usually the thinkness is the same for all sections.

KX: The effective surge mooring spring constant in units of lb/ft, assumed to be 0.0 if not entered on SHIP card.

ZCBM: The vertical center of buoyancy at each transverse section.

TPHI: The vessel natural roll period in seconds. If unknown, the roll period can be estimated from the following expression:

$$TPHI = \frac{CB}{\sqrt{GMT}}$$

where B is the beam of the vessel, GMT is the transverse metacentric height, and C is an empirical constant which varies from 0.44 for full-formed merchant ships to 0.39 for more round hull ships.

OG: The vertical distance between the ship's CG and the water plane. OG is positive if the CG lies above the water plane.

RGZ: The radius of gyration of the vessel in yaw. If unknown, it should be set equal to the radius of gyration in pitch.

ZETA: The roll damping coefficient. Use ZETA = 0.04 for round hull vessels and ZETA = 0.08 for vessels with flat bottom hulls.

The input data used to generate the RAO's for the example system configuration described in Section 4.1 are given below:

- Heavily loaded C7 container ship:

```
$INPUT DEPTH=50.,NFREQ=80,FREMIN=.05,FREMAX=4.,BETAD=135.,ISTOP=0 $
$SHIP ISHIP=1,NSEC=20,W=6.502E+7,BG=16.1,RG=176.,XCGFS=326.,NOMORE=1,
B(1)=20.5,40.5,55.3,65.8,72.9,78.1,82.1,84.4,85.0,85.0,85.0,84.0,81.1,76.4,
69.7,60.2,47.1,31.6,16.6,4.8,SECOE(1)=.394,.359,.508,.639,.753,.838,.895,
.937,.965,.977,.976,.968,.958,.941,.906,.856,.813,.792,.843,1.000,
DRAFT(1)=18.0,31.2,30.9,30.6,30.4,30.1,29.8,29.5,29.3,29.1,28.8,28.5,28.2,
27.9,27.7,27.4,27.2,27.0,26.8,13.4,SECL(1)=20*33.5,ZCBM(1)=9.0,15.6,15.5,
15.3,15.2,15.1,14.9,14.8,14.7,14.6,14.4,14.3,14.1,14.0,13.9,13.7,13.6,13.5,
13.4,13.2,TPHI=30.2,GMT=1.53,OG=2.9,RGZ=176.,ZETA=.06 $
```

- Medium loaded C4 container ship:

```
$INPUT DEPTH=50.,NFREQ=80,FREMIN=.05,FREMAX=4.,BETAD=135.,ISTOP=0 $
$SHIP ISHIP=1,NSEC=20,W=3.624E+7,BG=12.4,RG=143.5,XCGFS=287.0,NOMORE=0,
B(1)=5.6,18.8,33.8,46.5,61.7,71.7,78.2,81.3,3*82.0,81.4,77.7,70.0,59.4,47.0,
34.1,21.7,11.2,3.4,SECOE(1)=.400,.453,.505,.553,.612,.689,.775,.855,.917,.946,
.933,.893,.846,.808,.779,.758,.753,.798,1.0,1.0,DRAFT(1)=12.3,19*24.6,
SECL(1)=20*27.225,ZCBM(1)=6.2,19*12.3,TPHI=12.4,GMT=8.0,OG=7.4,RGZ=143.5,
ZETA=.06 $
```

- LCM8, landing craft:

```
$INPUT DEPTH=50.,NFREQ=80,FREMIN=.05,FREMAX=4.,BETAD=135.,ISTOP=0 $
$SHIP ISHIP=1,NSEC=17,W=1.15E+5,BG=4.13,RG=17.89,XCGFS=34.3,NOMORE=0,
B(1)=21.,21.1,12*21.2,21.1,20.9,20.6,SECOE(1)=1.,1.,.982,.953,.920,.889,
.866,4*.850,.847,.840,.826,.805,.767,.681,DRAFT(1)=.26,.76,1.24,1.66,1.98,
2.20,2.34,4*2.50,2.35,2.22,2.05,1.83,1.51,1.01,SECL(1)=17*3.0,ZCBM(1)=.13,
.38,.62,.83,.99,1.10,1.17,4*1.25,1.18,1.11,1.03,.92,.76,.51,TPHI=3.0,
GMT=18.3,OG=3.2,RGZ=17.89,ZETA=.08,KX=0. $
```

APPENDIX E

PROGRAM LISTING

PROGRAM COTS

Implements Methodology Developed

For COTS Evaluation

PROGRAM COTS

```
      PROGRAM COTS(INPUT,OUTPUT,TAPE5=INPUT,TAPE6=OUTPUT,TAPE3,
     + TAPE2,TAPE1)
      DIMENSION XCG(3),YCG(3),XR(3),YR(3),ZR(3),SS(80),ETR(80),TSS(80),
     +KWN(80),OMEGA(80),WNXX(80),WNYY(80),VDSD(3),ALS(80),SLS(80),
     +VDS(80),PAS(80),BC(3),EC(3),IC(3)
      COMPLEX VM(80),VMA(80),AL(80),SL(80),VD(80),PA(80),X(3,80),
     +Y(3,80),Z(3,80),THETA(3,80),PHI(3,80),PSI(3,80),STR(80),PNDL(80),
     +CMC(80),CLS(80),PHL
      COMMON/BLK1/NFREQ,FREMIN,FREMAX,OMEGA(80),KWN(80),BETA,
     +WNXX(80),WNYY(80)
      COMMON/XXX/ XCG(3),YCG(3),XR(3),YR(3),ZR(3),CFCOST,BWL,MCO,NC,PMT,
     + EFF,WC,VS,FK,BCF,H13,S2,AMS,AML,PAE
1F,VDSD(3),SL13M,ICM,BCC,
     + EMC,DEL,X(3,80),Y(3,80),Z 3,80),THETA(3,80),PHI(3,80),PSI(3,80)
      NAMELIST/CONFIG/XCG,YCG,XR,YR,ZR,CFCOST,BWL,MCO,NC,PMT,EFF
      NAMELIST/VARIAB/WC,VS,FK,BCF,H13
      XCG(1)=0.
      YCG(1)=0.
      DRP=.01
      DRV=.01
      ZR(1)=0.
      ZR(2)=0.
      ZR(3)=0.
      NS=3
      HGT=100.
      REWIND 5,(CONFIG)
```

```
      READ(5,VARIAB)
      CALL RADG(NS,X,Y,Z,THETA,PHI,PSI)
      DEL=(FREMAX-FREMIN)/FLOAT(NFREQ-1)
      DO 90 I=1,2
      NCO=I-1
      DO 80 J=1,8
      H13=FLOAT(J)
      CALL EVAL(TCCOST,BWCOST,TSCOST,OLR)
      WRITE(6,50)H13,S2,BWCOST,TCCOST,TSCOST,OLR
   50 FORMAT(1H ,6F12.2/)
   80 CONTINUE
   90 CONTINUE
      STOP
      END
      SUBROUTINE RADG(NS,X,Y,Z,THETA,PHI,PSI)
      COMPLEX X(3,80),Y(3,80),Z(3,80),THETA(3,80),PHI(3,80),PSI(3,80)
      COMMON /BLK1/ NFREQ,FREMIN,FREMAX,OMEGA(80),K(80),BETA,
     1 WNXX(80),WNYY(80)
      DIMENSION OMEGA(80),K(80),WNXX(80),WNYY(80)
      REAL K
      DO 70 I=1,NS
      IF(I.GT.1) GO TO 30
      READ(1) N,NFREQ,FREMIN,FREMAX,BETA
      DO 10 J=1,NFREQ
   10 READ(1) K(J),OMEGA(J),WNXX(J),WNYY(J)
      DO 20 J=1,NFREQ
      READ(1) X(1,J),Y(1,J),Z(1,J)
   20 READ(1) THETA(1,J),PHI(1,J),PSI(1,J)
      GO TO 60
   30 CONTINUE
      READ(1) N,NF,F1,F2,B
      DO 40 J=1,NFREQ
   40 READ(1) W1,W2,W3,W4
```

These lines determine the application of the program. Shown here is the required code for evaluating the effect of sea state. Other applications are implemented by Inserts I through IV that follow this listing.

```
      DO 50 J=1,NFREQ
      READ(I) X(I,J),Y(I,J),Z(I,J)
   50 READ(I) THETA(I,J),PHI(I,J),PSI(I,J)
   60 CONTINUE
   70 CONTINUE
      RETURN
      END
      SUBROUTINE FIERMOS(H13,SS)
      DIMENSION SS(80)
      COMMON/BLK1/NFREQ,FREMIN,FREMAX,OMEGA(80),K(80),BETA
      DO 10 I=1,NFREQ
      A = H13*H13*OMEGA(I)**4
      B = 8.4/OMEGA(I)**5
      SS(I)=0.
      IF(A.LT..05) GO TO 10
      SS(I) = B*EXP(-33.6/A)
   10 CONTINUE
      RETURN
      END
      SUBROUTINE TFB(WC,ETR,COST)
      DIMENSION ETR(80)
      COMMON/BLK1/NFREQ,FREMIN,FREMAX,OMEGA(80),K(80),BETA
      WC1 = WC-.459
      DO 100 I=1,NFREQ
      ETR(I)=1.
      IF(WC.GE.4.) GO TO 80
      IF (OMEGA(I) .LT. WC1) GO TO 80
      ETR(I) = 1.-2.07*(OMEGA(I)-WC1)
      IF (OMEGA(I) .LT. WC) GO TO 80
      ETR(I)=.05
   80 CONTINUE
   90 CONTINUE
  100 CONTINUE
```

```
      COST = 5.4/(WC/6.28)**(3.8)
      COST=COST/1000.
      IF(WC.GE.4.) COST=0.
      RETURN
      END
      SUBROUTINE CRANE(VS,WC,MCO,DRV,DRP,STR,PNDL)
      COMPLEX STR(80),PNDL(80)
      DIMENSION OMEGA(80)
      COMMON/BLK1/N,F1,F2,OMEGA(80)
      CM=WC/32.2+300.
      VSF=VS*12.
      WN2=VSF/CM
      WN=SQRT(WN2)
      DF=2.*DRV*WN
      DO 10 I=1,N
      W=OMEGA(I)
      A=DF*W
      B=WN2-W*W
   10 STR(I)=CMPLX(WN2,A)/CMPLX(B,A)
      PL=100.
      IF(MCO.GT.0) PL=24.
      WN2=32.2/PL
      WN=SQRT(WN2)
      DF=2.*DRP*WN
      DO 20 I=1,N
      W=OMEGA(I)
      A=DF*W
      B=-W*W/PL
      C=WN2-W*W
   20 PNDL(I)=CMPLX(B,0.)/CMPLX(C,A)
      RETURN
      END
      SUBROUTINE ARCOMP(MCO,FE,CAC,PLS)
```

```
      COMPLEX CMC(80),CLS(80),A,B,C,D,E,F
      COMMON/BLK1/N,F1,F2,OMEGA(80)
      DIMENSION OMEGA(80)
      IF(MCO.EQ.2) GO TO 20
      DO 10 I=1,N
      CMC(I)=CMPLX(1.0,0.0)
   10 CLS(I)=CMPLX(0.0,0.0)
      GO TO 40
   20 F=CMPLX(FK,0.0)
      DO 30 I=1,N
      W=OMEGA(I)
      A=CMPLX(1.,W)
      T=.1*W
      B=CMPLX(1.,T)
      T=.01*W
      C=CMPLX(1.,T)
      T=.14*W
      T1=1.-.01*W*W
      D=CMPLX(T1,T)
      E=A*C*D
      CMC(I)=E/(E+F*B)
   30 CLS(I)=F*B/(E+F*B)*CMPLX(0.,W)
   40 CONTINUE
      RETURN
      END
      SUBROUTINE INTEG(F,S,N,D)
      DIMENSION F(N)
      S=0.
      DO 10 I=1,N
   10 S = S+D*F(I)
      RETURN
      END
      SUBROUTTOE CKCOST(MCO,ALH,UC,REA,PAM,SL13,BC,EC,IC,F)
```

```
FF=SIN(PAN)/.02
IF(MCO.GT.0) FF=SIN(PAN)/.07
FV=1.+ALM/32.2
F=FF
IF(FV.GT.FF) F=FV
W=F*WC
IC=1
BC=W*REA/(7356.-25.72*REA)
IF(BC.GT.1500.) IC=2
IF(IC.EQ.2) BC=1500.
RW=REA*W
IF(RW.GT.18000000.) IC=3
IF(IC.EQ.3) BC=2500.
EC=0.
IF(MCO.GT.0) EC=25.+.1*BC
EM=0.
IF(MCO.EQ.2) EM=250.+WC*SL13*.000455
EC=EC+EM
RETURN
END
SUBROUTINE PROD(VD13,PMT,EFF,MCO,OLR)
DIMENSION VD13(3)
PL=100.
IF(MCO.GT.0)PL=24.
PL3=PL+25.
T2=.82*(VD13(2))*SQRT(PL)
T3=.3*(VD13(3)**2.)*SQRT(PL3)
T=PMT+T2+T3+1.0
OLR=1200./T
OLR=EFF*OLR
RETURN
END
SUBROUTINE EVAL(TCCOST,BWCOST,TSCOST,OLR)
```

```
      DIMENSION XCG(3),YCG(3),XR(3),YR(3),ZR(3),SS(80),ETR(80),TSS(80),
     +RWN(80),OMEGA(80),WNXX(80),WNYY(80),VDSD(3),ALS(80),SLS(80),
     +VDS(80),PAS(80),BC(3),EC(3),IC(3)
      COMPLEX VM(80),VMA(80),AL(80),SL(80),VD(80),PA(80),X(3,80),
     +Y(3,80),Z(3,80),THETA(3,80),PHI(3,80),PSI(3,80),STR(80),PNDL(80),
     +CMC(80),CLS(80),PHL
      COMMON/BLK1/NFREQ,FREMIN,FREMAX,OMEGA(80),RWN(80),BETA,
     +WNXX(80),WNYY(80)
      COMMON/XXX/ XCG(3),YCG(3),XR(3),YR(3),ZR(3),CFCOST,BWL,MCO,NC,PMT,
     + EFF,WC,VS,FK,BCF,H13,S2,AMS,AML,PAMM,DLF,VDSD(3),SL13M,ICM,BCC,
     + EMC,DEL,X(3,80),Y(3,80),Z(3,80),THETA(3,80),PHI(3,80),PSI(3,80)
      XCG(1)=0.
      YCG(1)=0.
      DRP=.01
      DRV=.01
      ZR(1)=0.
      ZR(2)=0.
      ZR(3)=0.
      NS=3
      HBT=100.
      CALL FIERMOS(H13,SS)
      IF(BWL.LT.1.) BCF=4.0
      CALL TFB(BCF,ETR,BWC)
      BWCOST=BWC*BWL
      CALL INTEG(SS,S,NFREQ,DEL)
      A=H13*H13/16./S
      DO 10 J=1,NFREQ
10    SS(J)=A*SS(J)
      CALL CRANE(VS,WC,MCO,DRV,DRP,STR,PNDL)
      CALL MOCOMP(MCO,FK,CMC,CLS)
      DO 50 I=2,3
      REA=SQRT((XCG(I)+XR(1)-XR(1))**2+(YCG(I)+YR(I)-YR(1))**2)
      DO 20 J=1,NFREQ
```

```
      VM(J)=Z(1,J)+PHI(1,J)*(YCG(I)+YR(I))-THETA(I)*(XCG(I)+XR(I))
      VMA(J)=Z(I,J)-THETA(I,J)*XR(I)+PHI(I,J)*YR(I)
      AL(J)=-VM(J)*STR(J)*OMEGA(J)*OMEGA(J)
      SL(J)=VM(J)*CLS(J)
      PHL=CEXP(CMPLX(0.,-WNXX(J)*XCG(I)-WNYY(J)*YCG(I)))
      VD(J)=VM(J)*CMC(J)*STR(J)-PHL*VMA(J)
      PA(J)=(Y(1,J)-PHI(1,J)*HBT)*PNDL(J)
20    CONTINUE
      DO 30 J=1,NFREQ
      TSS(J)=SS(J)*ETR(J)
      ALS(J)=TSS(J)*CABS(AL(J))**2
      SLS(J)=TSS(J)*CABS(SL(J))**2
      VDS(J)=TSS(J)*CABS(VD(J))**2
      PAS(J)=TSS(J)*CABS(PA(J))**2
30    CONTINUE
      CALL INTEG(SS,S1,NFREQ,DEL)
      S1=4.*SQRT(S1)
      CALL INTEG(TSS,S2,NFREQ,DEL)
      S2=4.*SQRT(S2)
      CALL INTEG(ALS,S,NFREQ,DEL)
      ALM=3.7*SQRT(S)
      IF(I.EQ.2) AMS=ALM
      IF(I.EQ.3) AML=ALM
      CALL INTEG(SLS,S,NFREQ,DEL)
      SL13=2.*SQRT(S)
      CALL INTEG(VDS,S,NFREQ,DEL)
      VDSD(I)=SQRT(S)
      CALL INTEG(PAS,S,NFREQ,DEL)
      PAM=3.7*SQRT(S)
      IF(I.EQ.2) PAMM=PAM
      IF(PAMM.LT.PAM) PAMM=PAM
      CALL CRCOST(MCO,ALM,WC,REA,PAM,SL13,BC(I),EC(I),IC(I),F)
      IF(I.EQ.2) DLF=F
```

```
      IF(F.GT.OLF) OLF=F
50    CONTINUE
      KBC=2
      IF(BC(3).GT.BC(2)) KBC=3
      KEC=2
      IF(EC(3).GT.EC(2)) KEC=3
      BCC=BC(KBC)
      EMC=EC(KEC)
      TCCOST=(BC(KBC)+EC(KEC))*FLOAT(NC)
      TSCOST=BWCOST+TCCOST+CFCOST
      CALL PROD(VDSD,PMT,EFF,MCO,OLR)
      OLR=OLR*FLOAT(NC)
90    CONTINUE
      RETURN
      END
```

INSERT I

Changes To The COTS Program Required To

Evaluate Effect of Breakwaters (Section 4.3)

```
      DO 90 I = 1,2
      MCO = I-1
      DO 80 J = 1,8
      J1 = 9-J
      BCF = FLOAT (J1)/2.
      CALL EVAL (TCCOST, BWCOST, TSCOST, OLR)
      WRITE (6,50) BCF, S2, BWCOST, TCCOST, TSCOST, OLR
   50 FORMAT (1H, 6F12.2/)
   80 CONTINUE
   90 CONTINUE
```

INSERT II

Changes To The COTS Program Required To

Implement The Two Parameter Evaluation Technique (Section 4.4)

```
      MCO=2
      NC=2
      DO 90 I=1,6
      I1=I-1
      FK=2.*FLOAT(I1)
      DO 80 J=1,10
      J1=11-J
      BCF=.75+.05*FLOAT(J1)
      B1=.25*FLOAT(J1)-.25
      IF(J1.GT.5) BCF=B1
      CALL EVAL(TCCOST,BWCOST,TSCOST,OLR)
      X1=FK
      X2=BCF
      X3=S2
      X4=BWCOST
      X5=TCCOST
      X6=TSCOST
      X7=OLR
      X8=TSCOST/OLR
      FK=1.1*FK+.1
      CALL EVAL(TCCOST,BWCOST,TSCOST,OLR)
      X9=(TSCOST-X6)/(OLR-X7)
      FK=X1
      BCF=.9*BCF
      CALL EVAL(TCCOST,BWCOST,TSCOST,OLR)
      X10=(TSCOST-X6)/(OLR-X7)
      WRITE(6,49) X1,X2,X3,X4,X5,X6,X7,X8,X9,X10
49    FORMAT(1H ,3F6.2,3F8.0,4F8.2,/)
```

INSERT III

Changes To The COTS Program Required To

Minimize Cost Effectiveness (Section 4.4)

```
      NIT=0
      MCO=2
      NC=2
      X0=1.5
      Y0=0.0
      TAU=.2
      EPS=.02
10    BCF=X0
      FK=Y0
      CALL EVAL(TCCOST,BWCOST,TSCOST,OLR)
      Z1=BCF
      Z2=FK
      Z3=TSCOST/OLR
      FK=1.1*FK+.05
      CALL EVAL(TCCOST,BWCOST,TSCOST,OLR)
      Z4=(TSCOST/OLR-Z3)/(FK-Z2)
      FK=Z2
      BCF=.98*BCF
      CALL EVAL(TCCOST,BWCOST,TSCOST,OLR)
      Z5=(TSCOST/OLR-Z3)/(BCF-Z1)
      Z6=SQRT(Z4*Z4+Z5*Z5)
      STS=TAU
20    NIT=NIT+1
      IF(NIT.GT.1000) GO TO 40
      X1=X0-STS*Z5/Z6
      Y1=Y0-STS*Z4/Z6
      IF(X1.GT.4.0) X1=4.0
      IF(X1.LT.0.0) X1=0.0
      IF(Y1.GT.10.0) Y1=10.0
      IF(Y1.LT.0.0) Y1=0.0
      ASTS=SQRT((X1-X0)**2+(Y1-Y0)**2)
      IF(ASTS.LT.EPS) GO TO 40
      BCF=X1
      FK=Y1
      CALL EVAL(TCCOST,BWCOST,TSCOST,OLR)
      Z7=TSCOST/OLR
      IF(Z7.GE.Z3) GO TO 30
      X0=X1
      Y0=Y1
      GO TO 10
30    STS=STS/2.
      GO TO 20
40    WRITE(6,50) X0,Y0,Z3,NIT
50    FORMAT(1H ,3(5X,F12.4),3X,I5)
```

AD-A114 420 EG AND G WASHINGTON ANALYTICAL SERVICES CENTER INC R--ETC F/G 15/5
A METHODOLOGY FOR THE EVALUATION OF ALTERNATIVE OFFSHORE CONTAI--ETC(U)
APR 82 J D BIRD N00014-78-C-0787
UNCLASSIFIED WASC-TR-0200-0002 NL

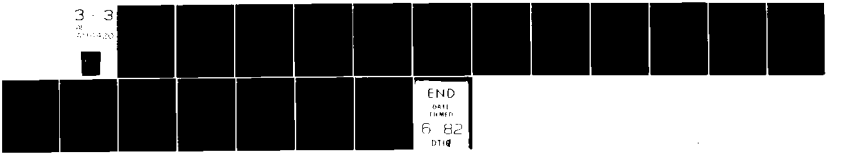

INSERT IV

Changes To The COTS Program Required

To Implement Constrained Optimization (Section 4.4)

```
      NIT=0
      OLRM=1.70
      MCO=2
      NC=2
      XO=1.5
      YO=10.0
      TAU=.2
      EPS=.0002
   10 BCF=XO
      FK=YO
      CALL EVAL(TCCOST,BWCOST,TSCOST,OLR)
      Z1=BCF
      Z2=FK
      Z3=TSCOST+500.*(OLRM/OLR)**500
      FK=1.1*FK+.05
      CALL EVAL(TCCOST,BWCOST,TSCOST,OLR)
      Z4=TSCOST+500.*(OLRM/OLR)**500
      Z4=(Z4-Z3)/(FK-Z2)
      FK=Z2
      BCF=.995*BCF
      CALL EVAL(TCCOST,BWCOST,TSCOST,OLR)
      Z5=(TSCOST/OLR-Z3)/(BCF-Z1)
      Z5=TSCOST+500.*(OLRM/OLR)**500
      Z5=(Z5-Z3)/(BCF-Z1)
      Z6=SQRT(Z4*Z4+Z5*Z5)
      STS=TAU
   20 NIT=NIT+1
```

```
      IF(NIT.GT.1000) GO TO 40
      X1=X0-STS*Z5/Z6
      Y1=Y0-10.*STS*Z4/Z6
      IF(X1.GT.4.0) X1=4.0
      IF(X1.LT.0.0) X1=0.0
      IF(Y1.GT.10.0) Y1=10.0
      IF(Y1.LT.0.0) Y1=0.0
      ASTS=SQRT((X1-X0)**2+(Y1-Y0)**2)
      IF(ASTS.LT.EPS) GO TO 40
      BCF=X1
      FK=Y1
      CALL EVAL(TCCOST,BWCOST,TSCOST,OLR)
      Z7=TSCOST+500.*(OLRM/OLR)**500
      IF(NIT.LT.50) GO TO 25
      IF(Z7.GE.Z3) GO TO 30
25    CONTINUE
      X0=X1
      Y0=Y1
      GO TO 10
30    STS=STS/2.
      GO TO 20
40    WRITE(6,50) X0,Y0,Z3,NIT
      WRITE(6,50) TSCOST,OLR,Z3,NIT
      BCF=X0
      FK=Y0
      CALL EVAL(TCCOST,BWCOST,TSCOST,OLR)
      WRITE (6,50) TSCOST,OLR,Z7,NIT
50    FORMAT(1H ,3(5X,F12.4),8X,I5)
```

PROGRAM RAOS

Generates Response Amplitude Operators

For The Floating Vessels

PROGRAM RAOS

```
      PROGRAM MAIN(INPUT,OUTPUT,TAPE5=INPUT,TAPE6=OUTPUT,TAPE3)
      COMPLEX X(3,80), Y(3,80), Z(3,80), THETA(3,80),
     1 PHI(3,80), PSI(3,80)
      COMMON /BLK1/ NFREQ, FREMIN, FREMAX, OMEGA(80),
     1 K(80), BETA, WNXX(80), WNYY(80)
      COMMON /BLK3/ X,Z,THETA,Y,PSI,PHI
      REAL K
      NS=1
      CALL RAO(NS)
      WRITE(3) NS,NFREQ,FREMIN,FREMAX,BETA
      DO 20 I=1,NFREQ
20    WRITE(3) K(I), OMEGA(I), WNXX(I), WNYY(I)
      DO 60 N=1,NS
      DO 40 I=1,NFREQ
      WRITE(3) X(N,I), Y(N,I), Z(N,I)
40    WRITE(3) THETA(N,I), PHI(N,I), PSI(N,I)
60    CONTINUE
      STOP
      END
      SUBROUTINE RAO(NS)
      COMMON G,NSEC,B(21),QUANT(21),ABAR(21),SECOE(21),DRAFT(21),RHOG,
     1 SECL(21),W,KX,CZ,CTHETA,BG,RG,DEPTH,ISHIP,XCG(3),OG,CY,CPSI,ZETA,
     2ZCBM(21),GMT,TPHI,KY,KPSI,RMZ
      COMMON/BLK1/NFREQ,FREMIN,FREMAX,OMEGA(80),K(80),BETA
     1,WNXX(80),WNYY(80)
      COMMON/BLK3/X,Z,THETA,Y,PSI,PHI
      COMMON/BLK4/WC
```

```
      REAL K,KX,KY,KPSI
      COMPLEX X(3,80),Z(3,80),THETA(3,80),Y(3,80),PSI(3,80),PHI(3,80)
      NAMELIST /INPUT/ DEPTH, NFREQ, FREMIN, FREMAX, BETAD, ISTOP
      NAMELIST/SHIP/ NSEC,B,SECOE,DRAFT,SECL,W,KX,BG,RG,ISHIP,XCGFS,
     1 NOMORE,KXOVER,ISHOUT,ZETA,ZCBM,GMT,TPHI,OG,RGZ
      DO 1000 N=1,80
      DO 1000 J=1,NS
      Y(J,N) = (0.0,0.0)
      PSI(J,N) = (0.0,0.0)
      PHI(J,N) = (0.0,0.0)
      X(J,N) = (0.0,0.0)
      Z(J,N) = (0.0,0.0)
1000  THETA(J,N) = (0.0,0.0)
      ZETA = .05
      KY = 0.0
      KPSI = 0.0
      CY = 1.0
      CPSI = 1.0
      KX = 0.0
      CZ = 1.0
      RHOG = 64.0
      CTHETA = 1.0
      DEPTH = 60.0
      PI = 3.14159
      BETAD = 180.0
      KXOVER = 1
      G=32.2
      READ(5,INPUT)
      BETA = BETAD * PI / 180.0
      CALL FREQ(DEPTH,BETAD)
      XCG(1) = 0.0
      XCG(2) = 0.0
      XCG(3) = 0.0
```

```
      DO 150 NSH=1,NS
      READ(5,SHIP)
      ISHIP=NSH
      XCG(ISHIP) = XCGFS
      WC = 0.0
      SL = 0.0
      DO 25 J=1,NSEC
      SL = SL + SECL(J)
25    WC = WC + SECOE(J)*B(J)*DRAFT(J)*SECL(J)
      WC = WC*RHOG
      DO 100 N=1,NFREQ
      OMEG = OMEGA(N)
      CALL ADMAB(OMEG)
      CALL COEF(N)
100   CONTINUE
150   CONTINUE
      RETURN
      END
      SUBROUTINE ADMAB(OMEG)
      COMMON G,NS,BSTAR(21),QUANT(21),ABAR(21),SECOE(21),DRAFT(21),RHOG
      DIMENSION SSB(10),SFB(10),SDB(10),SSA(10),SFA(10),SDA(10),
     1SLW(10),EFA(5,6),EQA(5,6),EFC(5),EFB(5),EFX(5),EQX(5),EFY(5),
     2EQY(5),SY(10),SZ(10)
      PI = 3.14159
      DO 7499 I=1,NS
      SFRFA=((OMEG**2)/(2.*G))*BSTAR(I)
      IF(SFRFA) 7001,7001,7002
7001  QUANT(I) = 0.0
      ABAR(I) = 0.0
      GO TO 7499
7002  SBBB = SECOE(I)
      SBB = BSTAR(I)
      SBH=BSTAR(I)/(2.*DRAFT(I))
```

```
      SFRPB = SFRPA
 7003 SAN=PI+(SBEB*4.0-PI)*SBH/(SBH+1.0)**2
      SWA = 5.55165-1.57078*SAN
      SAZN=(2.35619 + SQRT(SWA))/SAN
      SA = (SBH-1.0)*SAZN/(SBH+1.0)
      SB = SAZN-1.0
      SW = SFRPA/(1.0+SA+SB)
 8003 SY0 = SFRPA
      SSB0=PI*SIN(SY0)
      SSA0=SIN(SY0)*ALOG(1.781*SY0)-1.57078*COS(SY0)-SY0
      SSA0 = SSA0+0.30556*SY0**3-0.01903*SY0**5
      SFF1=0.0
      SFQ1 = 0.0
      SQ = -0.05236
      SWF = 0.0
      SLWM = 0.0
      DO 8004 LS=1,10
      SLS = LS
      SLSP=SLS*0.15708
      SNSL = SIN(SLSP)
      SN3SL=SIN(3.0*SLSP)
      SY(LS)=SW*((1.0+SA)*COS(SLSP)+SB*COS(3.0*SLSP))
      SZ(LS)=SW*((1.0-SA)*SNSL-SB*SN3SL)
      SEZ = PI*EXP(-SZ(LS))
      SSB(LS) = SEZ*SIN(SY(LS))
      SFB(LS)=SEZ*COS(SY(LS))
      SDB(LS)=SSB(LS)-SSB0*(1.0-SLS/10.0)
      SY2=SY(LS)*SY(LS)
      SY3=SY2*SY(LS)
      SZ2=SZ(LS)*SZ(LS)
      SZ3=SZ2*SZ(LS)
      SYZ=SZ(LS)*SZ(LS)
      SLOG=0.31831*ALOG(1.781*SQRT(SY2+SZ2))
```

```
      STAN=0.5-0.31831*ATAN(SZ(LS)/SY(LS))
      SSA(LS)=SSB(LS)*SLOG-SPB(LS)*STAN-SY(LS)*(1.0+0.91667*SZ2)
      SSA(LS)=SSA(LS)+SY3*(0.30556+0.01903*(10.0*SZ2-SY2))
      SSA(LS)=SSA(LS)+SYZ*(1.5-0.09514*SZ3+0.34722*(SZ2-SY2))
      SPA(LS)=SPB(LS)*SLOG+SSB(LS)*STAN+SZ(LS)*(1.0-0.91667*SY2)
      SPA(LS)=SPA(LS)+SZ3*(0.30556-0.08681*SZ(LS)+0.01903*(SZ2-10.*SY2))
      SPA(LS)=SPA(LS)+SYZ*(0.09514*SY3)-0.75*SZ2
      SPA(LS)=SPA(LS)+SY2*(0.75-0.08681*SY2+0.52083*SZ2)
      SDA(LS)=SSA(LS)-SSA0*(1.0-SLS/10.0)
      SQ = - SQ
      SFM=((1.0+SA)*SNSL+3.0*SB*SN3SL)*(0.15708+SQ)
      SFQ1=SFQ1+SPB(LS)*SFM
      SFP1=SFP1+SPA(LS)*SFM
      SWF=SWF+SFM/EXP(SZ(LS)*SFRPB/SFRPA)
      SLWN = SFM*SEZ/(6.28318+40.0*SQ)
      SLW(LS)=SLWM+SLWN
      SLWM=SLW(LS)+SLWN
 8004 CONTINUE
      DO 8010 LS=1,9
      SLS=LS
 8010 SLW(LS)=SLW(10)*SLS/10.0-SLW(LS)
      SFQ1=SFQ1-0.50*SPB(10)*SFM
      SFP1=SFP1-0.5*SPA(10)*SFM
      SWF=(SWF-0.50*SFM/EXP(SZ(10)*SFRPB/SFRPA))/(1.0+SA+SB)
      EPA(1,1)=SSA0
      EQA(1,1)=SSB0
      EPC(1)=SLW(10)
      SQ=-0.05236
      DO 8005 KS=2,5
      EPA(KS,1)=0.0
      EQA(KS,1)=0.0
      EPC(KS)=0.0
      SK=(KS-1)*2
```

```
      SR=-0.05236
      DO 8005 MS=1,9
      SQ=-SQ
      SM = MS
      SMSIN=1.27324*(0.15708+SQ)*SIN(SK*SM*0.15708)
      EPA(KS,1)=EPA(KS,1)+SDA(MS)*SMSIN
      EQA(KS,1)=EQA(KS,1)+SDB(MS)*SMSIN
      EPC(KS)=EPC(KS)+SLW(MS)*SMSIN
 8005 CONTINUE
      SAA = SA*SA+3.0*SB
      SAAA=SA*SAA+3.0*SA*SB
      EPA(1,2)=-SW
      EPA(2,2)=-1.0-0.21221*SW
      EPA(3,2)=-SA-0.02122*SW
      EPA(4,2)=-SAA-0.00606*SW
      EPA(5,2)=-SAAA-0.00253*SW
      EPA(1,3)=-0.33333*SW
      EPA(2,3)=0.38197*SW
      EPA(3,3)=-1.0-0.13642*SW
      EPA(4,3)=-SA-0.02358*SW
      EPA(5,3)=-SAA-0.00868*SW
      EPA(1,4)=-0.20*SW
      EPA(2,4)=0.15158*SW
      EPA(3,4)=0.17684*SW
      EPA(4,4)=-1.0-0.09646*SW
      EPA(5,4)=-SA-0.02040*SW
      EPA(1,5)=-0.1429*SW
      EPA(2,5)=0.09903*SW
      EPA(3,5)=0.06752*SW
      EPA(4,5)=0.11427*SW
      EPA(5,5)=-1.0-0.07428*SW
      EPB(1)=1.0+SA+SB
      EPB(2)=0.666667*(0.33333*(1.0+SA)-1.80*SB)
```

```
      EPB(3)=0.31831*(0.06667+0.0667*SA+1.28571*SB)
      EPB(4)=0.63662*(0.00952+0.00952*SA+0.11111*SB)
      EPB(5)=0.31831*(0.00793+0.00793*SA+0.08182*SB)
      DO 8006 KS=1,5
      DO 8006 LS=2,5
 8006 EQA(KS,LS)=0.0
      NEQ=5
 9903 IEPR=7070
      NEP=NEQ+1
      DO 9935 IEQ=1,NEQ
      DO 9948 LEQ=1,NEQ
      EPA(LEQ,NEP)=0.0
 9948 EQA(LEQ,NEP)=0.0
      EPA(IEQ,NEP)=1.0
      IEQY=1
      IF(EPA(IEQ,1))9934,9931,9934
 9931 IF(EQA(IEQ,1))9934,9910,9934
 9934 EQP=EPA(IEQ,1)**2 + EQA(IEQ,1)**2
      EPT1=EPA(IEQ,1)
      EQT1=EQA(IEQ,1)
      DO 9935 JEQ=1,NEP
      EPT=(EPA(IEQ,JEQ)*EPT1+EQA(IEQ,JEQ)*EQT1)/EQP
      EQT=(EQA(IEQ,JEQ)*EPT1-EPA(IEQ,JEQ)*EQT1)/EQP
      EPA(IEQ,JEQ)=EPT
 9935 EQA(IEQ,JEQ)=EQT
      IEQX=0
      IEQY=2
      IF(IEQ-NEQ)9937,9938,9910
 9938 MEQX=IEQ-1
      MEQY=1
      GO TO 9939
 9937 MEQY=IEQ+1
      MEQX=NEQ
```

```
9937 DO 9940 LEQ=NEQY,NEQX
     IEQX=IEQX+1
     EQP=EPA(LEQ,1)
     EPQ=EQA(LEQ,1)
     DO 9940 JEQ=1,NEP
     EPT=EPA(IEQ,JEQ)*EQP-EQA(IEQ,JEQ)*EPQ
     EQT=EPA(IEQ,JEQ)*EPQ+EQA(IEQ,JEQ)*EQP
     EPA(LEQ,JEQ)=EPA(LEQ,JEQ)-EPT
9940 EQA(LEQ,JEQ)=EQA(LEQ,JEQ)-EQT
     IEQY=3
     IF(IEQ-1)9910,9944,9945
9945 IF((NEQ-1)-IEQX)9910,9944,9938
9944 DO 9946 LEQ=1,NEQ
     DO 9946 JEQ=1,NEQ
     NEQU=JEQ+1
     EPA(LEQ,JEQ)=EPA(LEQ,NEQU)
9946 EQA(LEQ,JEQ)=EQA(LEQ,NEQU)
9933 CONTINUE
9952 DO 9953 IEQ=1,NEQ
     EPX(IEQ)=0.0
     EQX(IEQ)=0.0
     EPY(IEQ)=0.0
     EQY(IEQ)=0.0
     DO 9953 JEQ=1,NEQ
     EPX(IEQ)=EPX(IEQ)+EPA(IEQ,JEQ)*EPB(JEQ)
     EQX(IEQ)=EQX(IEQ)+EQA(IEQ,JEQ)*EPB(JEQ)
     EPY(IEQ)=EPY(IEQ)+EPA(IEQ,JEQ)*EPC(JEQ)
     EQY(IEQ)=EQY(IEQ)+EQA(IEQ,JEQ)*EPC(JEQ)
9953 CONTINUE
     GO TO 8009
9910 CONTINUE
     WRITE(6,9906) IEQY
9906 FORMAT(' ROMBFO QUIT WITH IEQY =',I4)
```

```
      GO TO 7499
8009  SF10=9.0*SB*(0.2-0.14286*SA-0.03704*SAA-0.01818*SAAA)
      SF10=SF10-((1.0+SA)*(0.3333+0.06667*SA+0.02857*SAA+0.01587*SAAA))
      SF1=SF10-SW*(1.0+SA)*0.78540
      SF20=-(1.0+SA)*(0.06667+0.02857*SA+0.01587*SAA)
      SF20=SF20-9.0*SB*(0.14286+0.03704*SA+0.01818*SAA)
      SF2=SF20-SW*0.78540*SB
      SF3=-(1.0+SA)*(0.02857+0.01587*SA)-9.0*SB*(0.03704+0.01818*SA)
      SF4=-(1.0+SA)*0.01587-9.0*SB*0.01818
      SFF=EPX(1)*SFF1-EQX(1)*SFQ1+EPX(2)*SF1+EPX(3)*SF2+EPX(4)*SF3
      SFF=SFF+EPX(5)*SF4
      SC=SFF/(0.7854*(1.0+SA+SB)**2)
      SAR=PI*SW*SQRT(EPX(1)**2+EQX(1)**2)
      QUANT(I) = SC*PI*BSTAR(I)**2*RHOG/8.
9999  ABAR(I)=SAR
7499  CONTINUE
      RETURN
      END
      SUBROUTINE COEF(N)
      COMMON G,NSEC,B(21),QUANT(21),ABAR(21),SECOE(21),DRAFT(21),RHOG,
     1 SECL(21),W,KX,CZ,CTHETA,BG,RG,DEPTH,ISHIF,XCG(3),OG,CY,CPSI,ZETA,
     2ZCB(21),GMT,TPHI,KY,KPSI,RGZ
      DIMENSION AT22(21),BDY(21),AT42(21) ,AT44(21)
      COMMON/BLK1/NFREQ,FREMIN,FREMAX,OMEGA(80),K(80),BETA
     1,WNXX(80),WNYY(80)
      COMMON/BLK3/X,Z,THETA,Y,PSI,PHI
      COMMON/BLK4/WC
      COMPLEX A11,A13,A22,A23,A33,B11,B13,B22,
     1 B23, B33, XW, ZW, TOKO, X(3,80),
     2 Z(3,80), THETA(3,80), F0,F1,Z9,DET,FCZERO,FCONE,A44,A45,A46,
     3A55,A54,A56,A64,A65,A66,B44, B45, B46, B55
     4 ,B56, B66, F4, F5, F6, Y(3,80),
     5 PSI(3,80),PHI(3,80)
```

```
      DIMENSION A1(22)
      REAL K,KX,FY,KPSI
      F0(AA,BB) = (0.0,-1.0)/WNX*(CEXP(CMPLX(0.0,WNX*BB)) -
     1 CEXP(CMPLX(0.0,WNX*AA)))
      F1(AA,BB) = -1.0/WNX/WNX*(CEXP(CMPLX(0.0,WNX*BB))*CMPLX(-1.0,
     1 WNX*BB)-CEXP(CMPLX(0.0,WNX*AA))*CMPLX(-1.0,WNX*AA))
      SINH(X) = .5*(EXP(X) - EXP(-X))
      COSH(X) = .5*(EXP(X) + EXP(-X))
      PI = 3.14159
      WN = K(N)
      DO 20 J=1,NSEC
      GAM = 2.*DRAFT(J)/B(J)
      E0 = 4.0/(3.*(1.+GAM)-SQRT(9.*(1.+GAM)**2 - 8.0*(1.+GAM+GAM**2)
     1-32.*GAM*SECOE(J)/PI))
      E1 = E0/2.*(1.-GAM)
      E3 = E0/2.*(1.+GAM) - 1.0
      GSQ =(GAM*E0)**2
      Q1 = ((1.-E1)**2 + 3.*E3**2)/GSQ
      GSQ = GSQ*GAM*E0
      Q2 = 1./GSQ*(1.-E1)**2*(1.-E1/3.-.6*E3)
      Q3 = 1./GSQ*E3**2*(.2-E1/7.-E3/3.)
      Q4 = 2./GSQ*E3*(1.-E1)*(1./3.-E1/5.-3.*E3/7.)
      F1 = -16./PI/GSQ*(E1/3.*(1.-E1) + E3/15.*(4.+4.*E1-5.*E1**2)
     1- E3**2/35.*(20.-7.*E1))
      GSQ = GSQ*GAM*E0
      F2 = -1./PI/GSQ*(E1+E1*E3-4.*E3)*(PI**2*(1.-E1) - (8.-PI/2.)*
     1(E3+E1*(1.-E1)) + 16./9.*E3*(4.*E1-3.) + 56./15.*E3**2)
      F3 = -E3/PI/GSQ*(5.*F1**2*(1.-E1) - 2.*(160./9.-PI**2)*(E3+E1*
     1(1.-E1)) +(128./9.-PI**2/2.)*E3*(4.*E1-3.) + 1030.4/525.*E3**2)
      AT22(J) = PI/2.*DRAFT(J)**2*(Q1+4.*DRAFT(J)*WN/PI*(Q2+Q3-Q4))
      BDY(J) = B(J)**4*(PI*(1.-E1)/(1.+E1+E3)**2)**2
      ATP42 = PI/2.*DRAFT(J)**3*F1
      AT12(J) = ATP12 + DRAFT(J)**4*(F2+F3)*WN
```

```
      AT44(J) = B(J)**4/PI/E0*(E1**2*(1.+E3)**2 + 8./9.*E1*E3*(1.+E3)
     1 + 16./9.*E3**2)/E0**3
  20  CONTINUE
      A0=0.0
      A1=0.0
      A2=0.0
      H0=0.0
      H1=0.0
      H2=0.0
      D0=0.0
      D1=0.0
      D2=0.0
      S220=S221=S222=0.0
      S420=S421=S422=0.0
      SBDY0=SBDY1=SBDY2=0.0
      U = OMEGA(N)**2/G
      WNX = WNXX(N)
      WNY = WNYY(N)
      XI(1) = -XCG(1)
      DO 30 J=1,NSEC
  30  XI(J+1) = XI(J) + SECL(J)
      DO 50 J=1,NSEC
      X1=XI(J+1)-XI(J)
      X2=.5*(XI(J+1)**2-XI(J)**2)
      X3=(XI(J+1)**3-XI(J)**3)/3.
      A0 = A0 + QUANT(J)*X1
      A1= A1 + QUANT(J)*X2
      A2 = A2 + QUANT(J)*X3
      H0 = H0 + B(J)*X1
      H1 = H1 + B(J)*X2
      H2 = H2 + B(J)*X3
      D0 = D0 + ABAR(J)**2*X1
      D1 = D1 + ABAR(J)**2*X2
```

```
      D2 = D2 + ABAR(J)**2*X3
      S220 = S220 + AT22(J)*X1
      S221 = S221 + AT22(J)*X2
      S222 = S222 + AT22(J)*X3
      S420 = S420 + AT42(J)*X1
      S421 = S421 + AT42(J)*X2
      S422 = S422 + AT42(J)*X3
      SBDY0 = SBDY0 + BDY(J)*X1
      SBDY1 = SBDY1 + BDY(J)*X2
      SBDY2 = SBDY2 + BDY(J)*X3
50    CONTINUE
      QQ = U*RHOG
      S220 = QQ*S220
      UU = RHOG/16.*U**3
      S221 = QQ*S221
      S222 = QQ*S222
      S420 = QQ*S420
      S421 = QQ*S421
      S422 = QQ*S422
      SBDY0 = UU*SBDY0
      SBDY1 = UU*SBDY1
      SBDY2 = UU*SBDY2
      A11 = CMPLX(-W*U+KX,-CZ*RHOG*D0/28./U)
      A13 = W*BG*U*(1.0,0.0)
      A22 = CMPLX(-.W+A0)*U+RHOG*H0,-CZ*RHOG*D0/U)
      A23 = CMPLX(U*A1-RHOG*H1,+RHOG*D1/U)
      R2 = RG**2
      A33 = CMPLX(-(W*R2+A2)*U+RHOG*H2,-RHOG*CTHETA*D2/U)
      B11 = A11 - CMPLX(KX,0.0)
      B13 = A13
      B22 = A22
      B23 = A23
      B33 = A33
```

```
      B44 = CMPLX(-W*U-S220,-C7*SBDY0)
      B45 = -CMPLX(S221,.5*(CY+CPSI)*SBDY1)
      B46 = -CMPLX(S420+OG*S220,BG*SBDY0)
      B55 = -CMPLX(U*W*RGZ**2+S222,CPSI*SBDY2)
      B56 = -CMPLX(S421+OG*S221,BG*SBDY1)
      B66 = CMPLX(-U*G*W*GMT*TPHI**2/(2.*PI)**2 + W*GMT,
     1 -OMEGA(N)*ZETA*W*GMT*TPHI/PI)
      XW = (0.0,0.0)
      ZW = (0.0,0.0)
      TORQ =(0.0,0.0)
      F4 = (0.0,0.0)
      F5 = (0.0,0.0)
      F6 = (0.0,0.0)
      DO 100 J=1,NSEC
      AA = XI(J)
      BB= XI(J+1)
      ZBAR = -.5*DRAFT(J)
      S= SECOE(J)*B(J)*DRAFT(J)
      S = S*W/WC
      CDC = COSH(WN*ZBAR) + SINH(WN*ZBAR)*TANH(WN*DEPTH)
      SDC = SINH(WN*ZBAR) + COSH(WN*ZBAR)*TANH(WN*DEPTH)
      FCY = 1.0
      IF(WNY.NE.0.0) FCY = SIN(B(J)*WNY/2.)/(B(J)*WNY/2.)
      IF(WNX.EQ.0.0) GO TO 70
      FCZERO = F0(AA,BB)*FCY
      FCONE = F1(AA,BB)*FCY
      GO TO 75
   70 FCZERO = FCY*(BB-AA)
      FCONE = .5*(BB*BB - AA*AA)*FCY
   75 CONTINUE
      XW = XW -CDC*WNX     *RHOG*FCZERO    *CMPLX(
     1        - ABAR(J) ** 2 * CZ / 28.0 / U / U , S)
      ZW = ZW + CMPLX((RHOG*S+QUANT(J))*(-WN)*SDC +
```

```
     1 RHOG*B(J),-RHOG*WN*SDC/U/U*CZ*ABAR(J)**2)*FCZERO
      TORQ=TORQ
     1                                + CMPLX((RHOG*S+QUANT(J))*(-WN)*SDC +
     2 RHOG*B(J),-RHOG*WN*SDC/U/U*CZ*ABAR(J)**2)*(-1.0)*FCONE
      BDY(J) = BDY(J)/16.
      F4 = F4 +CMPLX(BDY(J)*U*U,-S-AT22(J)-AT42(J)*WN)
     1*WN*SIN(BETA)*CDC*FCZERO*RHOG
      F5 = F5 +CMPLX(BDY(J)*U*U,-S-AT22(J)-AT42(J)*WN)
     1*WN*SIN(BETA)*CDC*FCONE*RHOG
      F6 = F6 - RHOG*WN*SIN(BETA)*CDC*FCZERO*
     1 CMPLX(0.0,AT42(J)+S*ZCBM(J)-B(J)**3/12.0+WN*AT44(J))
100   CONTINUE
      F6 = F6 + OG*F4
      GO TO 150
      ENTRY SOLVE
      A11 = B11 + CMPLX(KX,0.0)
      A22 = B22
      A13 = B13
      A23 = B23
      A33 = B33
150   CONTINUE
      DET = A11*(A22*A33-A23**2) + A13*(-A22*A13)
      X(ISHIP,N) = (XW*(A22*A33-A23**2) + A13*(ZW
     1 *A23 - A22*TORQ))/DET
      Z (ISHIP,N) = (A11*(ZW*A33 - A23*TORQ) +
     1 A13*(XW*A23 - A13*ZW))/DET
      THETA(ISHIP,N) = (A11*(A22*TORQ-ZW*A23) +
     1 XW*(-A13*A22))/DET
      A44 = B44 + KY
      A45 = B45
      A54 = A45
      A46 = B46
      A64 = A46
      A55 = B55 + KPSI
      A56 = B56
```

```
      A65 = A56
      A66 = B66
      DET = A44*(A55*A66-A56*A65) - A45*(A54*A66-A56*A64)
     1 + A46*(A54*A65-A55*A64)
      Y(ISHIP,N) = (F4*(A55*A66-A56*A65) - F5*
     1(A45*A66-A46*A65) + F6*(A45*A56-A55*A46))/DET
      PSI(ISHIP,N) = (A44*(F5*A66-F6*A56) - A54*
     1(F4*A66-F6*A46) + A64*(F4*A56
     2-F5*A46))/DET
      PHI(ISHIP,N) = (F4*(A54*A65-A64*A55) - F5*(A44
     1*A65-A64*A45)+F6*(A44*A55-A54*A45))/DET
      RETURN
      END
      SUBROUTINE FREQ(H, BETAD)
      COMMON/BLK1/NFREQ,FREMIN,FREMAX,OMEGA(80),K(80),BETA
     1,WNXX(80),WNYY(80)
      REAL K
      DEL = (FREMAX-FREMIN)/FLOAT(NFREQ-1)
      OMEGA(1) = FREMIN
      DO 25 N = 2, NFREQ
25    OMEGA(N) = OMEGA(N-1) + DEL
      DO 100 N=1,NFREQ
      U = OMEGA(N)**2/32.2
      X0 = U
      DO 90 L = 1, 200
      T = TANH(X0*H)
      X1 = X0 + ((U -X0 * T) / H ) / (X0 - U * T + T / H)
      IF(ABS(X1-X0),LT,1,E-6*ABS(X0))GO TO 99
      X0 = X1
90    CONTINUE
99    K(N) = X1
      WNXX(N) = K(N)*COS(BETA)
100   WNYY(N) = K(N)*SIN(BETA)
      RETURN
      END
```


ATE
LME